Genes that link the insulin/IGF-like signaling pathway to stress response

By

Wei-Chung Chiang

A dissertation submitted in partial fulfillment
of the requirements for the degree of
Doctor of Philosophy
(Molecular and Integrative Physiology)
in the University of Michigan
2013

Doctoral Committee:

Associate Professor, Ao-Lin Hsu, Chair
Professor Christin Carter-Su
Assistant Professor David Lombard
Associate Professor Scott Pletcher

2013

DEDICATION

This thesis is dedicated to my beloved parents, younger sister and her family, who consistently support and encourage me to pursue my interest in biological sciences over these years. This is a long journey and I will not be able to see the end of it without you.

ACKNOWLEDGEMENTS

I would like to thank members of the Hsu Lab for support, and especially my advisor Allen, without whom this project never would have reached its potential.

I would also like to thank my dissertation committee members, Dr. Christin Carter-Su, Dr. David Lombard, and Dr. Scott Pletcher for their helpful insight and time.

With regard to these two projects, specific thanks go to Dr. Tsui-Ting Ching, Dr. Hee-Chul Lee, Dr. Daniel Tishkoff, Dr. Bo Yang, and Dr. Joshua Wilson-Grady for their collaboration; Dr. Shawn Xu for his assistance in characterization of DDL-2 expression pattern; Dr. David Lombard and Dr. Raymond Yung for providing essential equipments. I am also grateful to Carol Mousigian, Travis Mazer and Dr. Xiaokun Yu for their excellent technical assistance; Carol Mousigian and Tarey Reilly for valuable comments on the manuscript.

Several strains were obtained from the Caenorhabditis Genetics Center (CGC), *C. elegans* Gene Knockout Consortium, National Biosource Project of Japan, and H. Robert Horvitz laboratory.

W-C.C. was supported by 2012 Rackham Predoctoral Fellowship (University of Michigan). This work was supported by grants from NIA (A-L.H.), the Ellison Medical Foundation (A-L.H.), NIGMS (D.B.L.), and the American Federation for Aging Research (D.B.L.)

TABLE OF CONTENTS

LIST OF FIGURES

LIST OF TABLES

LIST OF ABBREVIATIONS

AKT-1/2	Protein kinase B 1/2
BiFC	BImolecular Fluorescence Complementation
CBP	CREB-Binding Protein
CCDC53	Coiled-Coil Domain Containing protein 53
DAF-2	abnormal DAuer Formation 2
DAF-16	abnormal DAuer Formation 16
DDL-1	Daf-16 Dependent Longevity 1
DDL-2	Daf-16 Dependent Longevity 2
DHIC	DDL-1-containing HSF-1 Inhibitory Complex
EMSA	Electro-Mobility Shift Assay
FoxO	Forkhead box O
GFP	Green Fluorescent Protein
HSE	Heat Shock Element
HSF	Heat Shock Factor
HSP	Heat Shock Protein
HSB-1	Heat-Shock protein Binding protein 1
IGF-1	Insulin-like Growth Factor 1
$NADH/NAD^+$	Nicotinamide adenine dinucleotide
PTMs	Post-Translational Modifications
RT-PCR	Real-Time Polymerase Chain Reaction
SGK-1	Serum- and Glucocorticoid- inducible Kinase
SIRT 1-7	SIRTuin 1-7
SIR-2.1	SIRtuin 2.1
SIR-2.4	SIRtuin 2.4
SUMO	Small Ubiquitin-like MOdifier
unc-54	UNCoordinated 54

ABSTRACT

The insulin/IGF-like signaling cascade and stress response pathways are conserved throughout the animal kingdom and known to modulate a wide-range of biological processes to cope with environmental cues or stress. Previous studies have suggested that the insulin/IGF-like signaling and stress response are functionally linked and may play an integral role in controlling aging and longevity. However, our understanding regarding the underlying molecular mechanisms of the cross-talks between the insulin/IGF-like signaling and stress response pathways are incomplete. Thus, in this study, we aimed to further elucidate the cross-talks between these evolutionally conserved biological pathways by studying novel regulators of these pathways.

We demonstrated two potential mechanisms that mediate the cross-talk between insulin/IGF-like signaling and stress response. (1) We found that the activity of HSF-1 is regulated by insulin/IGF-like signaling pathway via two novel HSF-1 regulators, DDL-1 and DDL-2. DDL-1 and -2 negatively regulate HSF-1 activity by forming a protein complex with HSF-1, and the formation of this complex (DHIC) is modulated by the activity of insulin/IGF-like signaling. These data suggested a role for DDL-1 and DDL-2 in insulin/IGF-like signaling-mediated HSF-1 regulation. (2) We also demonstrated that *C. elegans* SIR-2.4 is required for the cellular responses to multiple stressors and promotes stress-induced DAF-16 (FoxO transcription factor) activation. Although SIR-2.4 is a member of the sirtuin deacetylase family, the catalytic activity of SIR-2.4 is dispensable for modulating DAF-16 nuclear translocation. We found that SIR-2.4 regulates DAF-16 function by preventing CBP-1-mediated acetylation, possibly via protein-protein interaction. Overall, our work presented in this study has provided a broader

understanding of potential mechanisms that the link insulin/IGF-like signaling pathway and stress response together at the molecular level.

Chapter 1. Introduction

1-1 Aging

In most advanced countries, the increasing costs of a growing elderly population on a health care system have challenged the society. For example, in the U.S., the older population (65 years or older) was 39.6 million in 2009. In 2030, this number is projected to be 72.1 million, twice as many as in 2009. The health care of senior citizens has gradually become a serious social concern.

Aging is a fundamental biological process defined as gradual changes made to cells and tissues that eventually lead to biological impairment. These changes have a direct impact on the function of organs, biological systems, and ultimately, the organism. These changes adversely affect the vitality and increase the mortality rate as a function of time. Age-related deterioration in an organism was previously considered as simply wear-and-tear on tissues and organs. Aging was not thought to be an actively regulated biological process until the past decade. Recent studies have pointed out that similar to many other biological processes, aging is subjected to regulation by evolutionally conserved genes and signaling pathways. Understanding the biology of aging is an important first step toward developing future pharmacological interventions that could ameliorate various age-related disorders, delay the normal aging process, and promote health span in human populations.

1-2 *C. elegans* as an aging model organism

Aging has always been one of the biological phenomena of greatest interest to mankind. The recent advancement of genetic, molecular biological, and biochemical tools allow us to explore in detail the underlying mechanisms of many biological processes. However, the study of longevity in humans remains difficult because a longitudinal study of longevity of a human population would take more than one generation to complete. Moreover, the genetic background among the human population is highly heterogeneous, making it difficult to assess the genetic interactions of longevity genes. Thus, using model organisms to study aging is an excellent alternative.

Complex biological phenomena, such as aging, disease and behavior, appear only in multi-cellular life forms. Therefore, to study the biological process of aging, an ideal model organism has to be complex enough to address higher-order questions that are relevant to human physiology, but simple enough to manipulate. *Caenorhabditis elegans* is a free-living, soil-dwelling nematode naturally found in nutrient or bacterial-rich environments, where they feed on rotting organic matter as well as on a variety of microbes including bacteria and fungus. *C. elegans* has emerged as an ideal model organism for studying molecular genetics of aging because of its transparency, well-defined anatomy, short lifespan (~20 days), and ease of genetic manipulation. Experimentally, the manipulation of worms is far simpler than many other systems such as primates, rodents, zebrafish, and even mammalian cells: The maintenance of *C. elegans* culture does not require specialized techniques or equipments; worms can easily grow at room temperature in unmodified air; manipulation of *C. elegans* does not require an extensively sterilized environment; and the contamination of worm culture can

be easily removed.

C. elegans is genetically tractable. The genome is fully sequenced and the knockdown of any gene can be easily accomplished by feeding *E. coli* expressing double-strand RNA on the gene of interest. It is the first model organism found in which lifespan can be altered by a single gene mutation. Many fundamental biological processes found in worms and mammals are homologous [5,6]. Moreover, *C. elegans* shares similar characteristics of aging with mammals, including sarcopenia, lipofucin accumulation, reduced cuticle elasticity, and susceptibility to infection [7-9]. As such, studying the biological process of aging in worms could provide invaluable insights into mammalian aging, as well as many age-related diseases, such as macular degeneration, cataracts, Alzheimer's disease, and Parkinson's disease.

1-3 The role of the insulin/IGF-like signaling pathway in longevity regulation

Genetic analysis in *C. elegans* has revealed many longevity genes and pathways. The best-characterized longevity signaling pathway is the insulin/IGF-like signaling cascade. The insulin/IGF-like signaling pathway is conserved throughout the animal kingdom and has been shown to regulate lifespan in a wide range of species [10]. Mutations of insulin/IGF-like signaling components are known to affect longevity. For instance, mutation of *daf-2*, an insulin/IGF-like receptor, was found to double the lifespan of animals [11,12]. In flies, a mutation of the insulin/IGF-1 receptor also increases lifespan by ~80% [10]. Additionally, a mutation of *chico*, an insulin receptor substrate (IRS)-like gene, has also been shown to extend lifespan by ~40% [13,14]. In mice, an adipocyte-specific insulin receptor knock-out (FIRKO) increases lifespan by 18% [15].

Furthermore, IGF-1 heterozygous knock-out female animals live 30% longer than wild-types, while male animals live 16% longer [16]. In addition, mutations of upstream genes that regulate insulin/IGF-1 production also extend lifespan. Mice with a growth hormone receptor deletion or pituitary defect, which results in a severe decrease in insulin and IGF-1 levels, are also long-lived [17,18]. In humans, centenarians were found to have IGF-1 receptor mutations and reduced IGF-1 signaling, suggesting a potential role for the insulin/IGF-like signaling in modulation of human lifespan [19]. An Ecuadorian cohort with GHR deficiency (GHRD), which results in IGF-1 deficiency, was reported to have low incidence of age-related pathologies such as cancer and diabetes. [20]. Taken together, these lines of evidence show that the regulation of lifespan through the insulin/IGF-like signaling pathway is an evolutionally conserved biological process from yeast to humans (Figure 1).

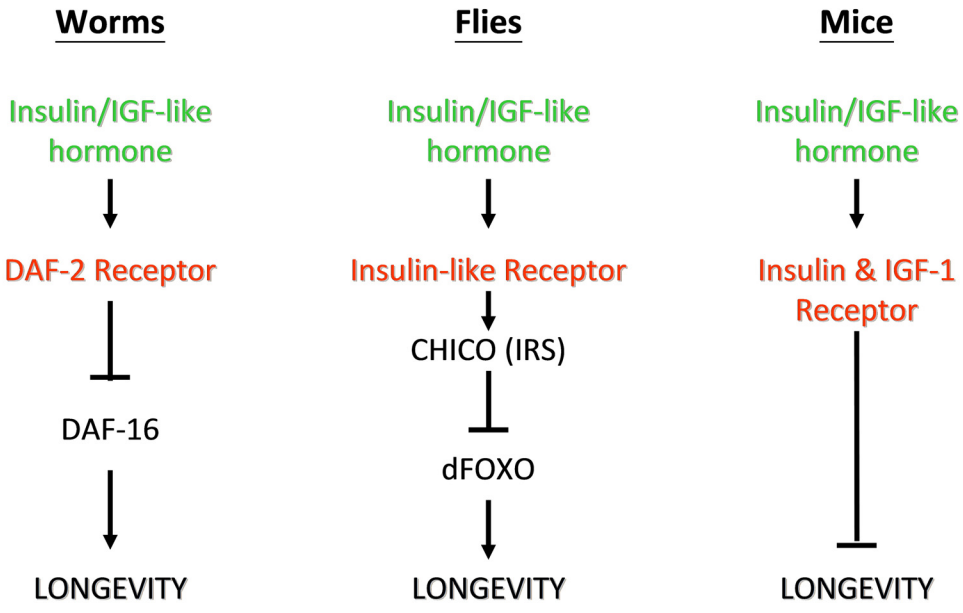

Figure 1. The insulin/IGF-like signaling is conserved among species.

The components of the insulin/IGF-like signaling in *C. elegans* are very similar to those in higher organisms (Figure 2). This signaling pathway is initiated by the binding of putative insulin-like ligands to DAF-2, a homolog of mammalian insulin/IGF-like receptor [11,12]. In *C. elegans*, at least forty putative insulin-like peptides are encoded in the genome [21,22]. Only a few insulin-like peptides have been characterized in detail. Worm insulin-like peptides are expressed primarily in neurons, although a few are also expressed in the intestine [21-24]. These peptides act as either DAF-2 agonists (such as *ins-7* and *daf-28*) or antagonists (*ins-1* and *ins-18*). DAF-2 activates a signaling cascade almost identical to mammalian PI-3 kinase-AKT pathway [25-29] and promotes the phosphorylation of downstream protein DAF-16, a member of the FoxO (Forkhead box O) transcription factor family. Phosphorylated DAF-16 is prevented from entering the nucleus and therefore is unable to activate the expression of its target genes [30,31]. On the contrary, when the insulin/IGF-like signaling is reduced, DAF-16 becomes hypophosphorylated and translocates into the nucleus. Thus, insulin/IGF-like signaling negatively regulates DAF-16/FoxO, at least in part, by modulating its intracellular localization. FoxO transcription factors are present in all eukaryotes and are known to regulate many biological processes. In mammals, there are four FoxO isoforms, including FoxO1, FoxO3A, FoxO4, and FoxO6. In general, all FoxO isoforms have similar organismal functions, including apoptosis, cell cycle arrest, oxidative defense, DNA repair, metabolism, differentiation, stem cell function, and tumor suppression [32]. FoxO transcription factors display distinct but overlapping expression pattern during adulthood and development [33-36]. During mouse development, FoxO1 is primarily expressed in adipose tissues, FoxO3A is present in liver, FoxO4 can be detected in skeletal muscle, and FoxO6 is found in the central nervous system. In adult mice, FoxO1

is present in many tissues at a lower level, but highly expressed in adipose tissues, uterus and ovaries. FoxO3A is ubiquitously expressed; however, higher expression levels can be found in the heart, ovaries, spleen, and brain. FoxO4 is found primarily in adipose tissue, skeletal muscle, and cardiac muscle. FoxO6 is present almost exclusively in brain tissue [37]. Overall, these observations indicate that the activity of FoxOs may be differentially regulated in specific tissue, and the expression pattern of FoxOs may specify their biological functions.

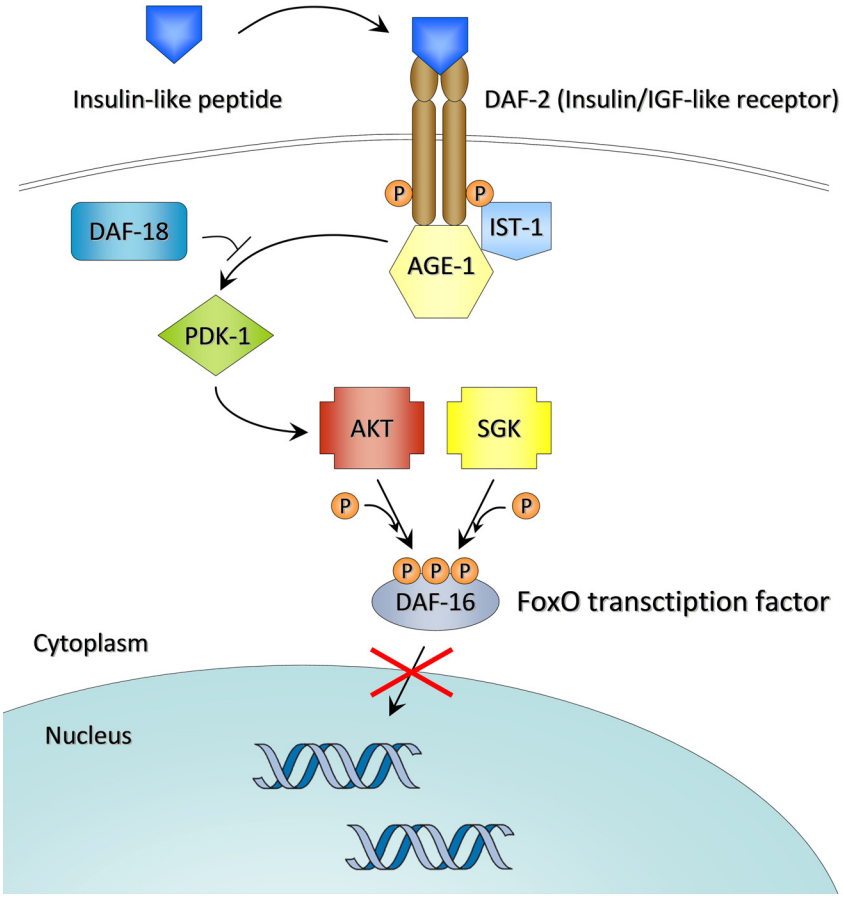

Figure 2. The insulin/IGF-like signaling in *C. elegans*.
DAF-2 encodes the only member of the insulin/IGF-like receptor, which is activated upon binding of insulin-like peptide agonist. DAF-2 initiates a signaling cascade analogous to mammalian PI3-kinase-AKT signaling that leads to inhibitory phosphorylation on DAF-16, thereby attenuating DAF-16 dependent downstream gene expression

In *C. elegans* and flies, an increase in FoxO activity promotes longevity, fat storage, immunity, and stress resistance [32,38]. DAF-16 directs the transcription program that controls energy metabolism, innate immunity, and stress resistance in worms [39,40]. DAF-16 is required for reduction-of-function mutations of genes in the insulin/IGF-like signaling to extend lifespan [30,31]. In mammals, it is not clear whether FoxO is required for the insulin/IGF-like signaling to influence longevity, but it has been shown that FoxO functions via insulin/IGF-like signaling to regulate metabolism and stress resistance in some long-lived mice [41].

1-4 FoxOs are regulated by many types of post-translational modification

FoxOs are tightly controlled by the insulin/IGF-like signaling pathway, a major pathway that influences longevity. Insulin/IGF-like signaling promotes FoxO phosphorylation and cytoplasmic sequestration in a complex with 14-3-3 chaperones. Conversely, stress stimuli promote nuclear translocation of FoxO by mechanisms including activation of stress kinases that phosphorylate FoxO proteins on residues distinct from those phosphorylated in the insulin/IGF-like signaling [38]. In response to oxidative stress, mammalian FoxO proteins are acetylated [42-45], mono-ubiquitylated [46], phosphorylated [47-50] or methylated [51]. These post-translational modifications modulate FoxO activity in response to various stimuli to promote stress responses, cell death, or metabolism.

1-5 Sirtuins

Sirtuins were originally identified in yeast as *Sir2* (*Silent Information Regulator 2*), a multifunctional protein that mediates telomeric gene expression, homologous end joining,

and gene silencing in specific genomic regions. Sirtuins are evolutionally conserved proteins that possess NAD^+-dependent histone deacetylase activity. In mammals, the sirtuin family is comprised of seven members (SIRT1-7) that share a common sirtuin core domain but vary in tissue expression pattern, subcellular localization, substrate specificity and enzyme activity [4] (Figure 3). The regulation of protein function by acetylation has emerged as a significant post-translational regulatory mechanism. Similar to protein phosphorylation, acetylation status can affect many protein functions such as DNA binding, transcriptional activity, protein stability, localization, and enzyme activity [52]. Certain isoforms of sirtuins are known to catalyze the removal of acetyl groups from lysine residues. Unlike many other histone deacetylases, the activity of sirtuins requires NAD^+, a substrate whose concentration is determined by the energy state of the cell. The dependence on NAD^+ has been shown to link sirtuin activity to the ratio of NAD^+/NADH, which controls adaptive response to energy state by modulating the activity of sirtuin and consequently their downstream effectors [53]. The NAD^+ dependence of sirtuins may be important for their ability to link caloric or dietary restriction to longevity. Overall, this class of protein is known to regulate transcription factors, cofactors, histones and many other chromatin proteins. Sirtuins are implicated in many biological process including longevity, stress response, metabolism, and cancer [54].

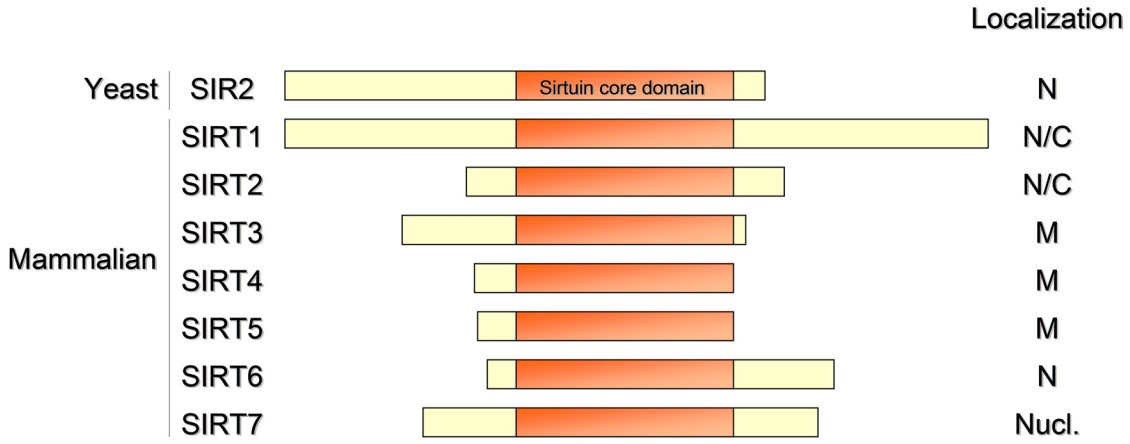

Figure 3. Mammalian sirtuins.
Mammals possess seven sirtuins (SIRT1-7) that share a core sirtuin core domain (in red) and are shown to occupy different subcellular compartments such as nucleus (N), cytoplasm (C), the mitochondria (M) and nucleolus (Nucl.).

1-6 Sirtuins modulate FoxO activity

It has been reported that an increase of sirtuin gene dosage may promote longevity in yeast, flies, worms, and mice [55-58], although the role of sirtuins in lifespan regulation in worms and flies is controversial [59]. In mammals, SIRT1 is shown to directly deacetylate FoxO in response to oxidative stress [60]. SIRT2 also deacetylates FoxO to promote adipocyte differentiation and regulates the level of reactive oxygen species [61,62]. Deacetylation of FoxO by SIRT1 and SIRT2 promotes FoxO nuclear translocation [43,61]. Acetylation of FoxO1 has been reported to attenuate DNA binding, promote AKT-mediated FoxO1 phosphorylation, and direct FoxO1 to nuclear PML (promyelocytic leukemia) bodies [45,63]. The mitochondrial SIRT3 has been proposed to modulate FoxO function [64,65].

1-7 Heat-shock transcription factor (HSF) is a key factor that regulates aging

DAF-16/FoxO is required for the insulin/IGF-like signaling pathway to modulate longevity.

However, very little is known about the contributions of other transcription factors in insulin/IGF-like signaling-dependent longevity. One of the transcription factors recently shown to promote longevity in worms is heat shock factor (HSF), a leucine-zipper transcription factor previously known to function in the cellular response against various stresses [66,67]. Overexpression of HSF-1 in *C. elegans* is reported to promote longevity, whereas knockdown of *hsf-1* shortens lifespan [2,68]. Four HSF isoforms have been identified in vertebrates: HSF1, HSF2 and HSF4 are ubiquitously expressed, whereas HSF3 is only found in avian species [69]. Across species, HSFs share a conservative N-terminal helix-turn-helix domain [70-72], an internal hydrophobic domain required for oligomerization, [73-75] and a carboxyl terminal transactivation domain (Figure 4) [76-79]. Interestingly, mammalian HSF4 lacks carboxyl terminal transactivation domain, suggesting that HSF4 may be involved in the negative regulation of DNA binding activity of other HSF isoforms.

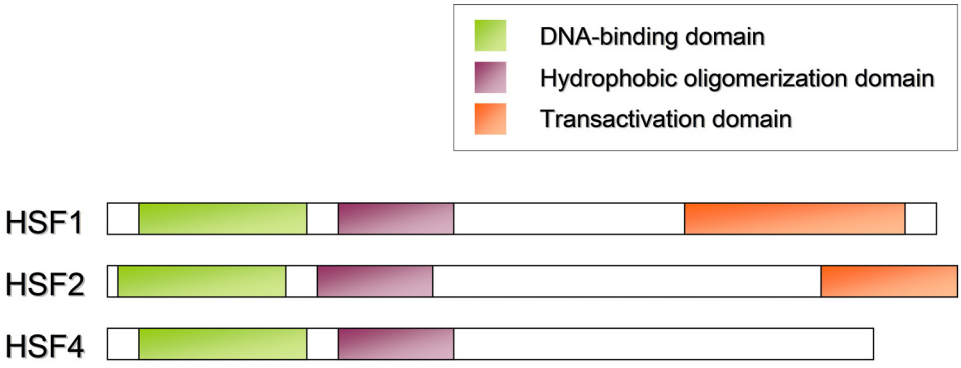

Figure 4. Mammalian HSFs
Mammals possess three heat shock factor isoforms (HSF1, 2, 4)

HSF regulates the expression of a group of heat-shock proteins in response to various stress or pathological conditions. Upon activation, HSF oligomerizes, translocates into the nucleus, binds to a pentanucleotide DNA motif (5'-nGAAn-3') known as heat-shock

element (HSE), and drives the expression of target genes, including molecular chaperone heat-shock protein 70 and 90 (*hsp70* and *hsp90*) and a subset of small heat-shock proteins (*shsps*), to maintain protein homeostasis [80]. Under normal conditions, HSF is repressed in an inert monomeric state by forming an inhibitory complex associated with HSP40/70 and HSP90/p23. Upon heat stress, HSP40/70 and HSP90/p23 interact with aberrant aggregates and unfolded proteins, thereby relieving HSF from the inhibitory complex. Once a sufficient amount of HSPs are produced to act upon unfolded or misfolded proteins, excessive HSP40/70 and HSP90/p23 will again interact with the active HSF and revert it to an inactive, monomeric state (Figure 5).

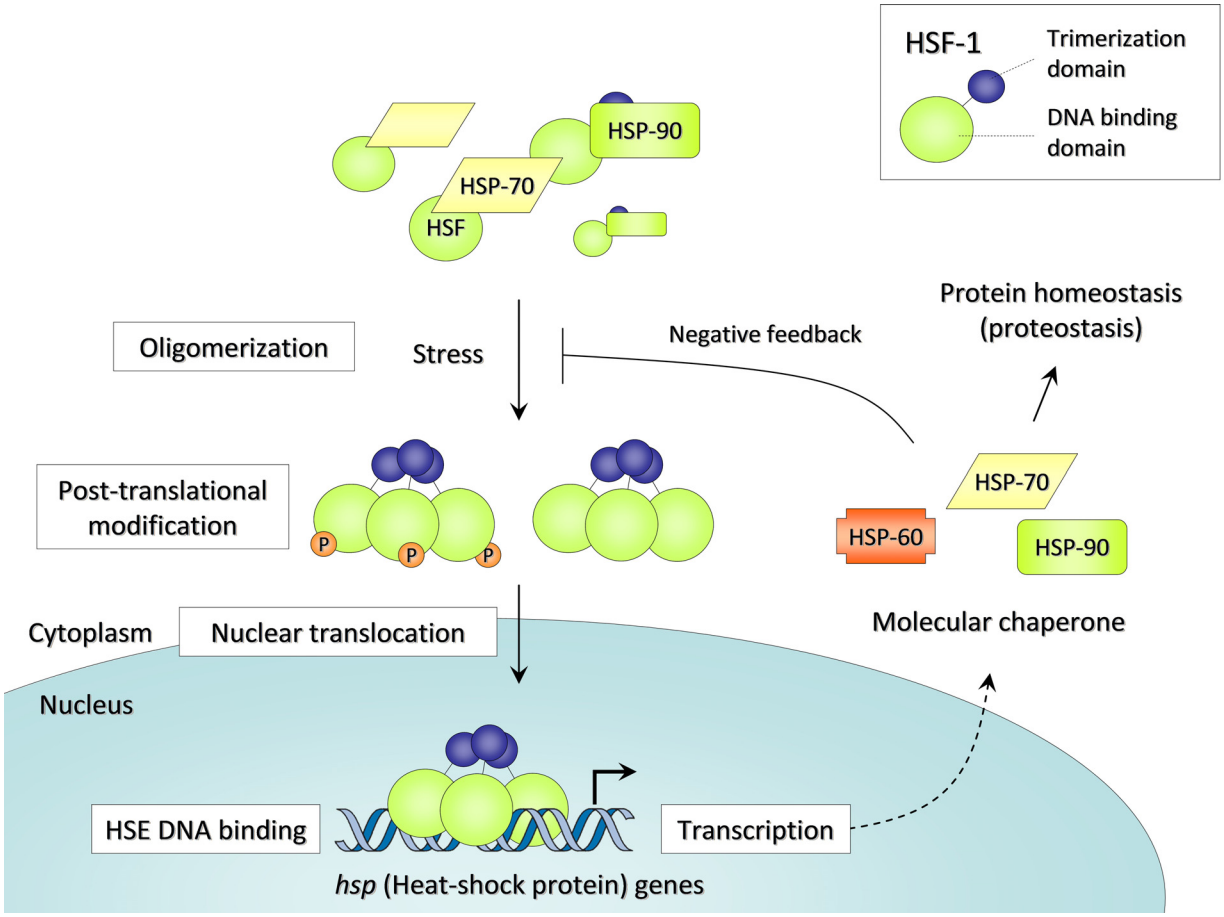

Figure 5. Multi-step activation of heat-shock factor in the mammalian system

Additional mechanisms are known to mediate stress-induced HSF activation. Several genes were reported to positively or negatively regulate HSF activity through a stress-dependent manner, including eEF1A (translation elongation factor), HSR1 (heat shock RNA 1), DAXX (death domain associated protein 6), CHIP (C-terminus of HSP70-interacting protein), and HSBP1 (heat-shock factor binding protein 1) (Figure 6). Translation elongation factor eEF1A was shown to collaborate with HSR1 to activate HSF1 in a stress-dependent manner. Interestingly, in addition to its canonical role in mRNA translation, eEF1A is also a key component of actin cytoskeleton organization. It has been speculated that the collapse of cytoskeleton and the shutdown of protein synthesis during heat stress may release eEF1A, thereby promoting HSF1 activation [81]. HSR1 encodes a highly conserved non-coding RNA required for heat-shock response. It has been hypothesized that HSR1 may function as a cellular RNA thermometer that alters its secondary structure in a temperature-dependent manner [81]. DAXX, a protein formerly known as a modulator of apoptosis and a repressor of basal

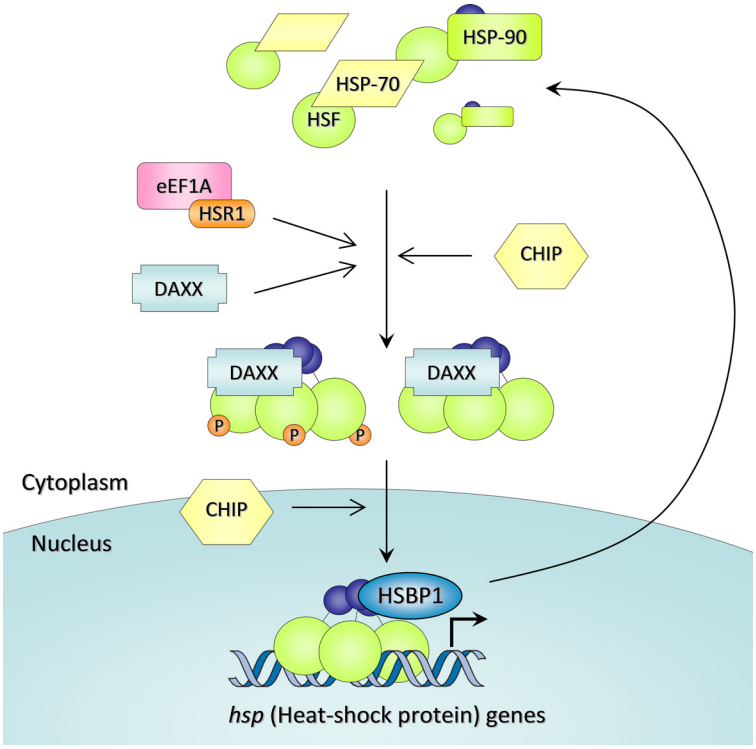

Figure 6. Known positive and negative regulators of HSF

transcription, is found to interact with trimeric HSF1 upon stress and enhance HSF1 transactivation competence. It has been suggested that DAXX may promote HSF transactivation through relieving HSF1 from multi-chaperone complex [82]. Moreover, a co-chaperone has been shown to be important for HSF activation. CHIP (C-terminus of HSP70-interacting protein) was shown to promote HSF1 oligomerization and nuclear import [83]. Animals lacking CHIP are temperature-sensitive and develop apoptosis in multiple organs, indicating that CHIP plays a crucial role in heat-shock response. Finally, HSF1 activity is subject to negative regulation by HSBP1 (heat-shock factor binding protein 1). HSBP1 negatively affects HSF1 DNA binding activity and was shown to play a role in HSF1 attenuation after heat-shock [84]. Overall, these findings indicate that the activity of HSF is controlled at different steps of HSF activation by multiple regulators.

1-8 Modulation HSF activity by post-translational modification

Various types of post-translational modifications (PTMs) are known to promote or attenuate transactivation potential of HSF, thereby fine-tuning the expression of many stress-responsive genes. So far, twenty-one serine/threonine phosphorylation sites were identified on human HSF1. Most of these phosphorylation sites are heat-inducible [85]. It has been reported that some of these residues modulate different levels of HSF activation, including nuclear translocation, DNA binding activity, or transcriptional activity.

In humans, phosphorylation on S307 by ERK inhibits HSF1 activity and prevents HSF1 oligomerization [86]. S307 phosphorylation leads to a subsequent inhibitory phosphorylation on S303 by glycogen synthase kinase 3 (GSK3). S303 is required for the binding of HSF1 to signaling protein 14-3-3 epsilon to achieve transcriptional

repression and cytoplasmic sequestration of HSF1 after heat-shock [87]. S230 phosphorylation promotes HSF1 transcriptional activity and is controlled by calcium/calmodulin-dependent protein kinase II (CaMKII) [88]. Phosphorylation of HSF1 by mitogen-activated protein kinase (MAPK)-activated protein kinase 2 on serine 121 inhibits HSF1 transcriptional activity and promotes HSP90 binding [89]. It has been suggested that T142 phosphorylation by kinase CK2 is involved in promoting transcriptional activity and DNA binding activity of HSF1 [90]. Acetylation status was implicated in regulating HSF activity. Overexpression of SIRT1, a histone deacetylase, promotes HSF1 DNA binding by maintaining HSF1 in a deacetylated form. Acetylation on lysine 80 has been shown to negatively regulate HSF1 DNA binding activity [91]. Stress-dependent modification by the ubiquitin-like protein SUMO-1 on lysine 298 has been reported to activate HSF1 to a DNA-binding form [92] (Figure 7).

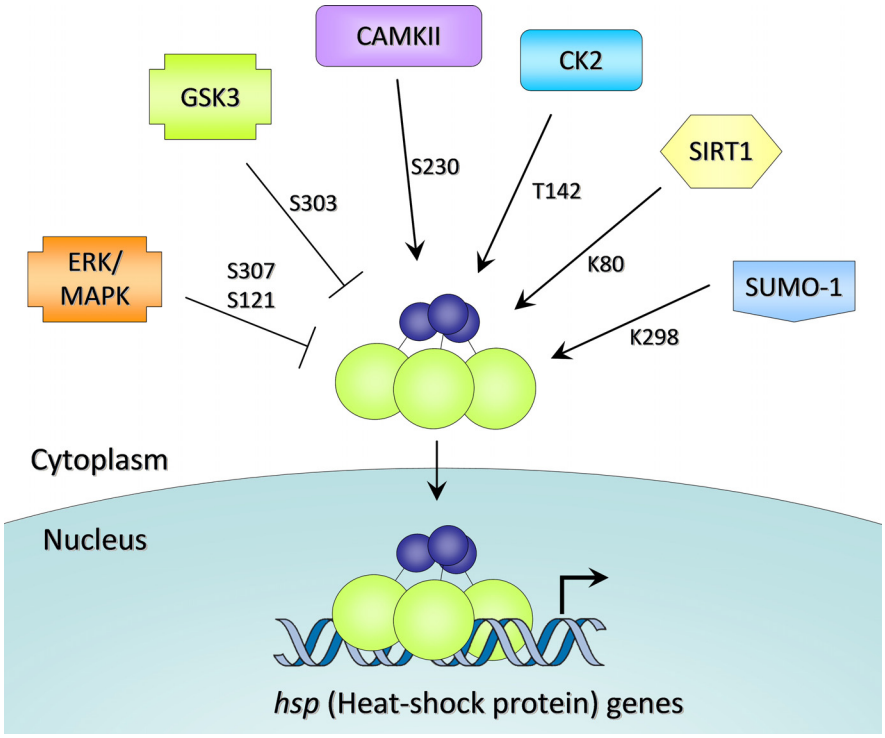

Figure 7. Examples of known stress-dependent regulation of HSF

1-9 Interaction between insulin/IGF-like signaling and stress response pathways

Reduction of insulin/IGF-like signaling occurs in response to unfavorable and adverse environmental conditions. It shifts physiological balance to a status that promotes cell maintenance and survival by activating the expression of many stress response genes, including heat shock proteins, innate immunity genes, and detoxifying genes. In addition to the role as a major downstream effector of the DAF-2 pathway, DAF-16 activity is also subject to regulation by many parallel mechanisms. Several stress-related signaling pathways have been shown to regulate stress-induced FoxO/DAF-16 activation (Figure 8) [47,49,93]. For instance, c-Jun N-terminal kinase (JNK) is a positive regulator of DAF-16 upon stress induction [49]. It has been previously reported that oxidative stress

activates protein kinase MST1, which in turn phosphorylates FoxO, disrupts the interaction with 14-3-3, and promotes FoxO nuclear translocation [47]. Under stress conditions, B55α regulatory subunit of protein phosphatase 2A (PP2A) dephosphorylates FoxO1 and promotes FoxO1 nuclear import. [93]. FoxO can also be modulated by other stress-induced PTMs including acetylation [42-45], mono-ubiquitylation [46], and methylation [51,94]. However, our understanding on how stress-induced FoxO/DAF-16 activation occurs is relatively unclear.

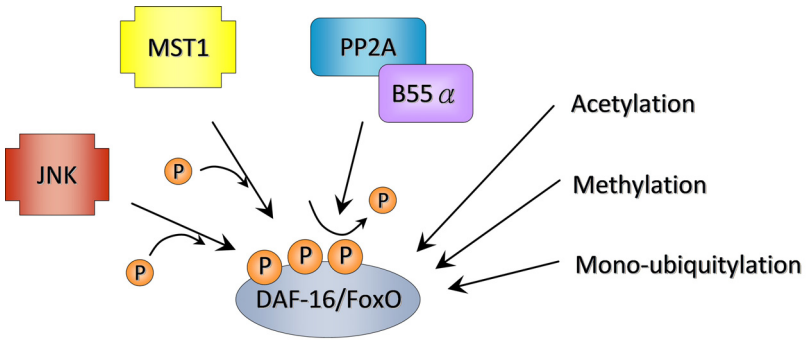

Figure 8. Examples of stress-dependent regulation of DAF-16/FoxO

Activation of HSF-1 promotes thermotolerance and longevity in *C. elegans* in a *daf-16*-dependent manner. Similar to *daf-16*, *hsf-1* is also required for the insulin/IGF-like signaling-mediated lifespan extension [2]. Gene expression analysis has shown that the proper expression of a subset of longevity genes in the DAF-2 pathway requires both HSF-1 and DAF-16. Moreover, potential DAF-16 and HSF-1 binding sites have been found to be located upstream of these genes [2]. This points to the possibility that both transcription factors may function together downstream of the insulin/IGF-like signaling pathway to promote longevity. However, the cross-talk between HSF-1 and the insulin/IGF-like signaling pathway is largely unclear, and the underlying mechanism by

which the insulin/IGF-like signaling cascade regulates HSF-1 has not been established.

The insulin/IGF-like signaling and stress response pathways are functionally linked; however, the interaction between these pathways is not well understood. Therefore, in this thesis, we aim to further explore the interaction between the insulin/IGF-like signaling and stress response pathways by examining the roles of genes that mediate the cross-talk between the insulin/IGF-like signaling and stress response pathways (Figure 9). This study will provide deeper understanding of the potential molecular mechanisms that link these pathways.

Despite the fact that the insulin/IGF signaling and stress response pathways have been found to intertwined, the physiological significance of the cross-talk at organismal level remains elusive. *C. elegans* is a unique and powerful tool to study the functional role and systemic regulation of longevity and stress resistance, as similar studies in mammals can be laborious and extremely expensive. Since the components of many key biological processes (including insulin/IGF-like signaling and heat-shock response) in mammals and *C. elegans* are largely homologous, the cross-talks between these pathways may be important for coordinating proper downstream gene expression in specifying optimum longevity and stress resistance in higher organisms. Thus, findings obtained in *C. elegans* would provide important insights into how insulin/IGF-like signaling and stress response pathways coordinately regulate longevity in humans. Our study presented here will shed light on the mechanisms by which the aging process and stress response are controlled. It may identify potential future targets for therapeutic intervention to increase healthy lifespan among human populations.

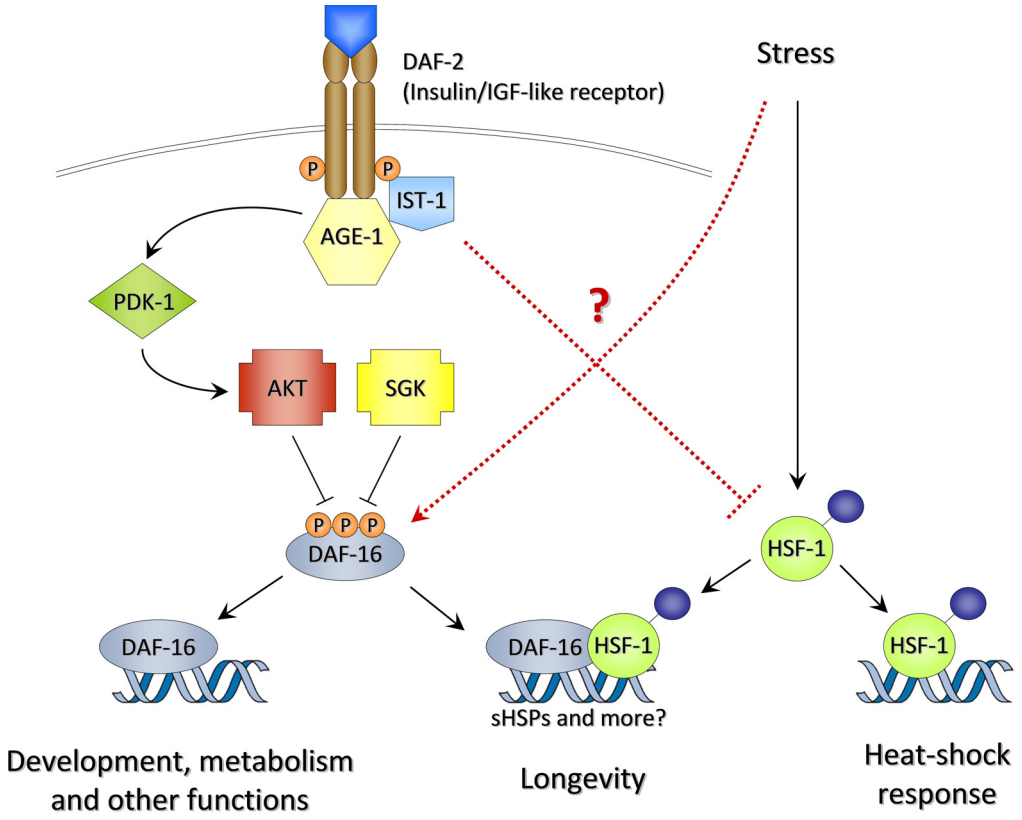

Figure 9. Potential cross-talk between insulin/IGF-like signaling and stress response pathways. (Modified from [2])

Chapter 2. HSF-1 regulators DDL-1/2 link insulin-like signaling to heat-shock responses and modulation of longevity.*

2-1 Abstract

The most prominent longevity signaling pathway in *C. elegans* is the insulin/IGF-like signaling pathway. A reduction in the insulin/IGF-like signaling pathway extends lifespan in *C. elegans*. DAF-16, a member of the FoxO (Forkhead box O) transcription factor family, is required for the reduction-of-function mutations in the insulin/IGF-like signaling pathway to promote longevity and stress resistance. However, very little is known about the contributions of other transcription factors in the context of insulin/IGF-like signaling-mediated longevity.

One of the transcription factor that regulates longevity is heat shock factor-1 (HSF-1), a protein previously known to be involved in cellular survival against various stresses. An elevated level of HSF-1 increases thermotolerance and longevity in *C. elegans*. HSF-1 is also known to be required for the insulin/IGF-like signaling-mediated longevity in worms. Additionally, gene expression analysis showed that the expression of several longevity genes requires both HSF-1 and DAF-16. This evidence points to the possibility that both transcription factors function together downstream of *daf-2* (insulin/IGF-like receptor) to promote longevity. Our data showed that the reduction of insulin/IGF-like signaling leads

* The data from this chapter has been published in: Chiang et. al., HSF-1 regulators DDL-1/2 link insulin-like signaling to heat-shock responses and modulation of longevity. Cell 148: 322-334.

to an increase in HSF-1 oligomerization, post-translational modification, nuclear accumulation, and HSF-1 dependent gene expression, suggesting that HSF is directly regulated by insulin/IGF-like signaling.

In this study, we demonstrated that two novel genes, *ddl-1* and *ddl-2,* influence lifespan and thermotolerance in *C. elegans* in an *hsf-1* dependent manner. DDL-1 and DDL-2 may negatively regulate HSF-1 activity by forming a protein complex with HSF-1. Our data suggested that insulin/IGF-like signaling may regulate HSF-1 through modulating the formation of this DDL-1 containing HSF-1 inhibitory complex (DHIC). Together, DDL-1 and DDL-2 may be an important regulatory link between HSF-1 and insulin/IGF-like signaling.

2-2 Introduction

HSF-1 is a key factor that regulates aging in *C. elegans*. Previous studies have shown that HSF-1 and its downstream targets, including a group of small heat-shock proteins, may act in concert in insulin/IGF-like signaling to regulate longevity in *C. elegans*. Similar to *daf-16*, it has been shown that *hsf-1* is required for *daf-2* mutation to extend lifespan, as the lifespan extension by *daf-2* inactivation is abolished by *hsf-1* mutation [2]. Moreover, it has been shown that the expression of a subset of heat-shock protein is increased in *daf-2* mutants and is partially required for DAF-2-mediated longevity phenotypes [2]. These observations imply that the insulin/IGF-like signaling pathway might, at least in part, influence longevity by modulating HSF-1 activity.

The activation of HSF-1 is a multi-step process in *C. elegans*

In *C. elegans*, HSF-1 is a key transcription factor that regulates cellular responses to various proteotoxic stresses. Previous studies in mammals demonstrated that HSF1 is constitutively present in cells and is activated upon the encounter of proteotoxic stresses. It has been demonstrated in many systems that the activation of HSF1 is tightly controlled. The regulation of HSF appears to be a multi-step process involving oligomerization, post-translational modification, nuclear translocation, acquisition of DNA binding activity and transcriptional activity [95,96]. The multi-step activation of HSF is very well studied in mammals. However, in *C. elegans*, whether the activation of HSF-1 shares common mechanisms with its mammalian homologs is not known; moreover, the activation of *C. elegans* HSF-1 has not been studied in detail. Recent results from our lab done by Dr. Tsui-Ting Ching and Dr. Hee Chul Lee have demonstrated that *C .elegans* HSF-1 responds to heat stress, and the activation of HSF-1 is also a multi-step process.

As observed in other systems, we found that oligomerization of HSF-1 occurs upon heat-shock in *C. elegans*. Our analysis also indicates that post-translational modification (PTM) of HSF-1 occurs after heat-shock in a time-dependent manner. This change in PTM may represent a shift from either a non-modified to a modified form of HSF-1, or a shift between two different post-translationally modified forms of HSF-1 in response to heat-shock. Further analysis revealed that phosphorylation(s) may be responsible for the majority of the PTM observed in HSF-1. In humans, there are currently 31 identified Ser/Thr phosphorylation sites on HSF1 [97]. These phosphorylation sites are constitutive or stress-inducible, as their effect on HSF-1 activity can be positive or negative.

Acquiring DNA binding activity to the heat-shock element (HSE), a pentanucleotide DNA motif (5'-nGAAn-3') located in the upstream regulatory region of HSF target genes, is required for HSF to become transcriptionally active. By using electrophoretic mobility shift assay (EMSA) developed in our lab for worm HSF-1, we found that there is an increased level of HSF-1 that forms a protein complex with biotin-labeled HSE probes upon heat stress, indicating that heat-shock leads to an increase in HSF-1 DNA binding activity.

We created a transgenic line that expresses HSF-1::GFP under the control of its own promoter and examined its expression pattern. HSF-1::GFP is expressed in intestinal cells, body wall muscle cells, and hypodermal cells, as well as many head and tail neurons. Under unstressed conditions, HSF-1::GFP is localized to a similar extent in the nucleus and cytoplasm. After heat stress, HSF-1::GFP accumulates in the nuclei of intestinal cells. To examine further whether HSF-1::GFP is biologically functional, we created a transgenic line with the same HSF-1::GFP expressing construct in *hsf-1(sy441)* mutant, an *hsf-1* loss-of-function mutant known to display shortened lifespan, egg-laying defects, and larval arrest at elevated temperature [98]. We found that the overexpression of HSF-1::GFP rescued the longevity defect resulting from *hsf-1(sy441)* mutations as well as produced a significant lifespan extension in a wild-type background, suggesting that the GFP::HSF-1 is biologically functional. Together, our findings suggested that, similar to the activation of HSF in other systems, the activation of HSF-1 in *C. elegans* is also a multi-step process.

DDL-1 and DDL-2 as potential HSF-1 regulators

ddl-1 and *ddl-2* (*ddl*, *daf-16* dependent longevity) were previously identified from a genome-wide RNAi library screen for longevity genes. Inactivation of *ddl-1* and *ddl-2* by RNAi were found to extend lifespan by 20-30%, suggesting potential roles for *ddl-1* and *ddl-2* in longevity regulation. Moreover, previous yeast-two hybrid data suggested that DDL-1 may physically interact with DDL-2 and heat-shock factor binding protein-1 (HSB-1), a HSF-1 negative regulator known to attenuate HSF-1 activity through an inhibitory binding with HSF-1. This evidence indicates a possibility that DDL-1 and DDL-2 regulate longevity through modulating HSF-1 activity. Interestingly, the predicted human ortholog of DDL-1, CCDC53 (coiled-coil containing protein 53) and HSB-1 human ortholog, HSBP-1, were found to interact with each other by yeast-two hybrid [99], implying that the biological function of DDL-1 and DDL-2 may be evolutionally conserved.

2-3 Material and Methods

C. elegans Strains

The following alleles and strains were used in the study:

CH116: *hsb-1*(cg116)IV,

PS3551: *hsf-1(sy441)I,*

VC2193: ddl-1(ok2916)II,

RB2380: ddl-2(ok3235)II,

EQ14: *iqEx5[pAH47(ddl-1p::gfp) + pRF4(rol-6)]*,

EQ64: *iqEx25[pAH47(ddl-1p::ddl-1::gfp) + pRF4(rol-6)]*,

EQ73: *iqIs28[pAH71(hsf-1p::hsf-1::gfp) + pRF4(rol-6)]*,

EQ84: *hsf-1(sy441)I; iqEx34[pAH71(hsf-1p::hsf-1::gfp) + pAH100(myo-3::rfp)]*,

EQ104: *iqEx39[pAH24(ddl-2p::gfp) + pRF4(rol-6)],*

EQ106: *iqEx40[pAH79(ddl-2p::FLAG-ddl-2) + pRF4(rol-6)],*

EQ135: *iqIs45[pAH87(ddl-1p::FLAG-ddl-1) + pAH76(hsf-1p::myc-hsf-1) + pRF4(rol-6)],*

EQ136: *iqIs44[pAH75(ddl-1p::HA-ddl-1) + pRF4(rol-6)],*

EQ140: *iqIs37[pAH76(hsf-1p::myc-hsf-1) + pRF4(rol-6)],*

EQ146: *ddl-1*(ok2916)II; out-crossed 6x to Hsu lab N2,

EQ149: *ddl-2*(ok3235)II; out-crossed 6x to Hsu lab N2,

EQ150: *hsb-1*(cg116)IV; CH116 out-crossed 4x to Hsu lab N2,

EQ155: *iqIs43[pAH75(ddl-1p::HA-ddl-1) + pAH79(ddl-2p::FALG-ddl-2) + pRF4(rol-6)],*

EQ160: *ddl-1(ok2916)II; hsb-1(cg116)IV,*

EQ161: *ddl-2(ok3235)II; hsb-1(cg116)IV,*

EQ163: *ddl-1(ok2916)II; ddl-2(ok3235)II,*

EQ187: *ddl-1(ok2916)II; iqIs44[pAH75(ddl-1p::HA-ddl-1) + pRF4(rol-6)],*

EQ193: *hsb-1(cg116)IV; iqIs44[pAH75(ddl-1p::HA-ddl-1) + pRF4(rol-6)].*

PS3551, CH116, VC2193, RB2380 and wild-type Caenorhabditis elegans (N2) strains were obtained from the Caenorhabditis Genetic Center.

For the generation of transgenic animals, a plasmid DNA mix was microinjected into the gonad of young adult hermaphrodite animals, using the standard method. F1 progeny were selected on the basis of the roller phenotype or GFP expression. Individual F2 progenies were isolated to establish independent lines. Wild-type (N2) animals were microinjected to generate these strains. For the generation of the EQ14 strain, the plasmid DNA mix consisted of 30 ng/µl pAH13 and 80 ng/µl pRF4. For the generation of

the EQ64 strain, the plasmid DNA mix consisted of 15 ng/µl pAH47 and 80 ng/µl pRF4. For the generation of the EQ70 strain, the plasmid DNA mix consisted of 30 ng/µl pAH71 and 80 ng/µl pRF4. For the generation of the EQ104 strain, 100 ng/µl pAH24 plasmid DNA was used. For the generation of the EQ106 strain, the plasmid DNA mix consisted of 15 ng/µl pAH79 and 80 ng/µl pRF4. For the generation of the EQ135 strain, the plasmid DNA mix consisted of 15 ng/µl pAH87, 15 ng/µl pAH76, and 80 ng/µl pRF4. For the generation of the EQ136 strain, the plasmid DNA mix consisted of 5 ng/µl pAH44 and 100 ng/µl pRF4. For the generation of the EQ140 strain, the plasmid DNA mix consisted of 15 ng/µl pAH76 and 15 ng/µl pRF4. For the generation of the EQ155 strain, the plasmid DNA mix consisted of 15 ng/µl pAH75, 15 ng/µl pAH79, and 80 ng/µl pRF4. Microinjecting N2 animals with 100ng/µl pRF4 (*rol-6*) alone did not affect the mean lifespan of N2 animals grown on either OP50, HT115, or RNAi bacteria that were examined in this study.

RNA-interference (RNAi) Experiments

The identity of all RNA interference (RNAi) clones was verified by sequencing the inserts using M13-forward primer. All clones were isolated from Julie Ahringer's RNAi library. HT115 bacteria transformed with RNAi vectors expressing dsRNA of the genes of interest were grown at 37°C in LB with 10 µg/ml tetracycline and 50 µg/ml carbenicillin, then seeded onto NG-carbenicillin plates and supplemented with 100 µl 0.1M IPTG. The bacterial strain containing empty vector L4440 was used as the control.

Lifespan Analysis

Lifespan analysis was conducted at 20°C as previously described unless otherwise

stated [100]. RNAi treatments were carried out by adding synchronized eggs to plates seeded with the RNAi bacteria. Worms were moved to plates with fresh RNAi bacteria every 2 days until reproduction ceased. Worms were then moved to new plates every 5-7 days for the rest of the lifespan analysis. Viability of the worms was scored every 2–3 days.

Preparation of Worm Nuclear Extracts

Frozen worm pellets were homogenized in a Kontes Pellet Pestle® tissue grinder in the presence of an equal volume of 2X NPB buffer (20 mM HEPES, pH 7.6, 20 mM KCl, 3 mM $MgCl_2$, 2 mM EDTA, 0.5 M sucrose, 1 mM dithiothreitol, protease inhibitors, phosphatase inhibitors). Cells were pelleted (4000 g, 5min, 4°C) and then homogenized 20 strokes with pestle A of the Dounce homogenizer. The suspension was then washed three times in NPB buffer containing 0.25% NP-40 and 0.1% Triton X-100. The nuclei were pelleted again and extracted with 4x volume of HEG buffer (20 mM HEPES, pH 7.9, 0.5 mM EDTA, 10% glycerol, 0.42 M NaCl, 1.5 mM $MgCl_2$, and protease inhibitors) at 4°C for 45 min. The nuclear fraction was collected by centrifugation at 14,000 g, 4°C for 15 min. Protein concentrations were determined by Bradford assay.

Electrophoretic Mobility Shift Assay

1 μg of worm nuclear extracts (NE) was incubated with 1 μg/μl Poly (dI·dC) and 1 nM biotin-labeled oligonucleotide containing the HSE sequence for 15 min at room temperature in binding buffer [20 mM HEPES, pH 7.6, 5 mM EDTA, 1 mM dithiothreitol, 150 mM KCl, 50 mM $(NH_4)_2SO_4$, 1% Tween 20 (v/v)]. The biotin-labeled oligonucleotides were synthesized based on the sequence covering the HSE in the promoter region of

hsp-16.1 (detail sequence listed below). Following native 3.5% polyacrylamide gel electrophoresis, HSF-1-HSE DNA complexes were visualized by LightShift Chemiluminscent EMSA kit (Pierce).

HSE-F:

5'-Bio-TTTTGCAAGAAGCAGCTCGAATGTTCTAGAAAAAGGTGGAAATGAGTATA-3'.

HSE-R:

5'-Bio-TATTTATACTCATTTCCACCTTTTTCTAGAACATTCGAGCTGCTTCTTGC-3'.

Oligomerization Assay

Worms were sonicated on ice for a total of 1 min followed by thawing frozen worm pellets in HEG buffer (20 mM HEPES, pH 7.9, 0.5 mM EDTA, 10% glycerol containing 0.42 M NaCl, 1.5 mM $MgCl_2$, and protease inhibitors). Worms were then dispersed by repeated pipetting followed by incubation on ice for 15 min. The samples were centrifuged at 14,000 rpm for 15 min and the supernatants were collected. Whole worm extracts were then incubated with 1 mM EGS [ethylene glycol bis(succinimidyl succinate)]. EGS was added at a final concentration of 1 mM and incubated at room temperature for 30 min. After quenching the cross-linking reactions with excess 1 M Tris-Cl, pH 8.5, samples were resolved by 6% SDS-polyacrylamide gel electrophoresis and analyzed by western blot with anti-HSF1 antibody.

RNA Isolation and Quantitative RT-PCR

Total RNA was isolated from approximately 3,000 worms, and cDNA was made from 4 μg of RNA using Superscript III RT (Invitrogen). TaqMan real-time qPCR experiments were performed for each gene using the Chromo 4 system (MJ Research). Relative

mRNA levels of the genes of interest were calculated and normalized against the internal control (*act-1*, the *β-actin*) and compared to the stated control (= 1).

Stress Assay

For thermotolerance assays, eggs from N2 worms were transferred to plates seeded with either vector only control, *ddl-1* RNAi, or *ddl-2* RNAi bacteria and grown to Day 1 adulthood. Worms were then transferred to plates without any food and heat-shocked at 35°C. Viability of the worms was scored every 2-3 hr. For oxidative stress assays, eggs from N2 worms were transferred to plates seeded with vector only control, *ddl-1* RNAi, or *ddl-2* RNAi bacteria. The worms were transferred every day to separate them from their progenies until Day 5 of adulthood. Worms were then transferred to 24-well plates and soaked in 300 mM of paraquat. Worms were checked every two hours for their viability.

HSF-1 Nuclear Localization Assay

Day 2 adult animals carrying an integrated *hsf-1::gfp* array (EQ73) grown on a vector control (VC) or different RNAi bacteria were either unstressed or heat shocked on 37°C heat block for 30 min. Fluorescence images of the animals were then taken and scored blindly for the nuclear accumulation of HSF-1::GFP protein in the intestinal cells (white arrows). At least 100 animals were scored per RNAi treatment per experiment. Worms were classified into separate groups according to the nuclear/cytosolic (n/c) ratio of GFP intensity in the intestinal cells.

Coimmunoprecipitation in 293T Cells

Twenty-four hours after 293T cells were transfected with various combinations of different plasmids containing HA-*ddl-1*, FLAG-*ddl-1*, FLAG-*ddl-2*, myc-*hsb-1*, or myc-*hsf-1* cDNA cells were washed with PBS and resuspended in L-RIPA buffer [50 mM Tris-HCl, pH 7.5, 150 mM NaCl, 2 mM EGTA, 0.1% Triton X-100 supplemented with Protease Inhibitor Cocktail Complete Mini (Roche) and 1 mM sodium orthovanadate]. The cell suspensions were then placed on ice for 10 min before being subjected to centrifugation at 14,000 × g for 10 min at 4°C. The supernatants were then collected. The protein levels of whole-cell extract (WCE) were quantified by Bradford assay. For each sample, 1,000 µg of total protein was used for the IP experiments. Anti-HA (Convance, #MMS101P), anti-FLAG (Sigma, #F3165), or anti-Myc (Cell Signaling, #2276) antibodies were added to WCE at 1:150, 1:300, and 1:500 dilutions, respectively. Five mg of anti-mouse rabbit polyclonal antibody was then added as a bridge antibody. Reactions were incubated at 4°C with gentle shaking overnight. 30 µl of 50% Protein A agarose beads (Sigma #P7786; preblocked by 10% BSA) were added into the solutions 4–5 hr after the initiation of the incubation. The beads were washed three times with L-RIPA buffer supplemented with 50 µg/ml ABESF and 1 mM sodium orthovanadate before being subjected to western blot analysis.

Coimmunoprecipitation in Worms

About 15,000 synchronized day 1 adult worms grown on either control or RNAi bacteria at 20°C were harvested by washing three times with cold M9 buffer and one more time with HB-high salt buffer (10 mM HEPES, pH 7.9; 10 mM KCl; 1.5 mM $MgCl_2$; 0.1 mM EDTA; 0.5 mM EGTA; 44 mM Sucrose; 100 mM NaCl; 0.5% Triton X-100). Worm pellets were then resuspended in 3× volume of HB-high salt buffer supplemented with Protease

Inhibitor Cocktail Complete Mini (Roche), 2.5 mM sodium pyrophosphate, 20 mM β-glycerolphosphate, and 1 mM sodium orthovanadate. The pellets were immediately frozen and stored in liquid nitrogen for future use. Frozen suspensions were thawed, homogenized with a Dounce homogenizer (30 strokes with a pestle B), and centrifuged at 14,000 × g at 4°C for 20 min. Supernatants were collected and total protein concentrations were quantified by Bradford assay. If necessary, crosslinking was done by incubating worm protein extracts with 1 mM EGS (ethylene glycol bis[succinimidyl succinate]) at 25°C for 30 min. The crosslinking reactions were stopped by adding and incubating with 20 mM Tris-HCl (pH 7.4) for an additional 30 min. For immunoprecipitation, 30 µl of anti-HA agarose beads (Sigma #A2095) were added to 1,500 mg of protein extract and incubated with gentle shaking at 4°C overnight. The beads were then washed three times with HB-high salt buffer supplemented with 50 µg/ml ABESF and 1 mM sodium orthovanadate before being subjected to western blot analysis.

Western Blot Analysis

The samples were subjected to SDS-PAGE and transferred to a PVDF membrane (Millipore). The transblotted membrane was washed three times with TBS containing 0.05% Tween 20 (TBST). After blocking with TBST containing 5% nonfat milk for 60 min, the membrane was incubated with the primary antibody indicated (e.g., anti-HSF1, Calbiochem, #385580) at 4°C for 12 hr and washed three times with TBST. The membrane was then probed with HRP-conjugated secondary antibody for 1 hr at room temperature and washed with TBST three times. Finally, the immunoblots were detected using a chemiluminescent substrate (Pierce) and visualized by autoradiography.

2-4 Results

2-4-1 DAF-2 insulin/IGF-like signaling inhibits HSF-1 activity

As previously suggested, HSF-1 may play an important role in the insulin/IGF-like signaling pathway [2,68]. Assuming that the insulin/IGF-like signaling pathway directly modulates HSF-1 activity, we postulated that the inactivation of DAF-2 would affect the multi-step activation of HSF-1, including nuclear translocation, post-translational modification, DNA binding activity, and downstream gene expression. We first investigated whether the reduction of insulin/IGF-like signaling activity affects HSF-1 nuclear translocation. Our data showed that a reduction of DAF-2 activity caused a significant increase in the level of nuclear HSF-1 under unstressed or heat-shock conditions (Figure 10A). Inactivation of *akt-1*, another component of the insulin/IGF-like signaling, also led to an increase in HSF-1 nuclear translocation (Figure 10A). DAF-2-mediated HSF-1 nuclear translocation seemed to be *daf-16* independent, as knockdown of *daf-16* did not impact *daf-2*-mediated HSF-1 nuclear translocation (Figure 10A).

We have also found that the reduction of DAF-2 activity affects HSF-1 DNA binding activity. As compared to wild-type N2 animals, *daf-2* deficient animals exhibited substantially increased HSF-1 DNA binding activity under both unstressed and heat-shocked conditions, suggesting that the activity of HSF-1 is higher in *daf-2* RNAi-treated animals (Figure 10B and C). An elevated HSF-1 activity may allow a more robust response against heat-shock and would thereby promote stress resistance and longevity in *daf-2* animals. Nuclear accumulation of oligomerized and post-translationally modified HSF-1 (active form of HSF-1) leads to an increase in HSF-1 DNA binding

activity. Indeed, the western blot analysis showed that the level of post-translationally modified HSF-1 is increased in *daf-2* RNAi-treated animals under both stressed and non-stressed conditions (Figure 10D and E), suggesting an increased level of active HSF-1 upon DAF-2 inactivation. Interestingly, we have also observed that the amount of total HSF-1 is increased in response to heat stress or *daf-2* knockdown, whereas the level of unmodified HSF-1 remained largely unaltered (Figure 10E). However, this increase in the amount of HSF-1 protein is unlikely to be a result of a change in *hsf-1* mRNA expression, as *hsf-1* mRNA levels did not appear to be increased in *daf-2* RNAi animals compared to control animals (Figure 11A). It is possible that post-transcriptionally modified and DNA-bound HSF-1 proteins may be less prone to degradation.

Finally, to examine whether increased HSF-1 DNA binding activity leads to an increase in HSF-1 transcriptional activity, we measured the expression of known HSF-1 downstream target genes, including two small hsps (i.e. *hsp-16.2* and *sip-1*) and two *hsp-70s* (i.e. *F44E5.5* and *C12C8.1*), by quantitative RT-PCR. Indeed, we found that the expression levels of these target genes were increased in *daf-2* RNAi-treated animals under both stressed and unstressed conditions (Figure 11B-E). Taken together, these results indicated that HSF-1 activity, including its multi-step activation process, is subject to negative regulation by the insulin/IGF-like signaling pathway.

Overall, our findings strongly suggested that HSF-1 activity is regulated by the DAF-2 pathway. To further understand how HSF-1 is controlled by insulin/IGF-like signaling, we next attempted to elucidate the mechanism underlying this regulation. In the following

sections, I will focus on *ddl-1* and *ddl-2*, two novel *daf-16*-dependent longevity (*ddl*) genes, and their potential role in HSF-1 regulation in the context of insulin/IGF-like signaling.

2-4-2 *ddl-1*, *ddl-2* and *hsb-1* negatively regulate stress resistance and longevity

Since DDL-1 and DDL-2 were previously suggested to play a role in longevity [101], we first tested whether these two genes also play a role in stress resistance. We found that *ddl-1* and *ddl-2* RNAi animals are more resistant to both heat and oxidative stress, indicating that DDL-1 and DDL-2 may modulate stress response (Figure 12A and B). Moreover, since previous study showed that the depletion of *ddl-1* and *ddl-2* by RNAi extends lifespan in *C. elegans* [101], we also attempted to verify this observation with deletion mutants. The lifespans of *ddl-1* and *ddl-2* deletion and overexpressing animals were tested. Our results showed that animals with *ddl-1(ok2916)* and *ddl-2(ok3235)* deletion alleles displayed significantly extended lifespans, by about 20-30% (Figure 12C). In addition, DDL-1 and DDL-2 have been suggested to interact with HSB-1, a known HSF-1 inhibitor; we thus examined the longevity phenotype of *hsb-1* deletion mutants. Similarly, *hsb-1(cg116)* null mutants are long-lived (about 50% increased longevity), consistent with the phenotype of *ddl-1* and *ddl-2* animals (Figure 12C). Together, these results may indicate that DDL-1, DDL-2 and HSB-1 have similar biological function.

Interestingly, overexpression of DDL-1 and/or DDL-2 in wild-type background was not sufficient to alter lifespan (Figure 12D and E). However, we did observe that the overexpression of DDL-1 reversed the long-lived phenotype of *ddl-1(ok2916)* mutant animals, suggesting that the DDL-1 transgene is functional (Figure 12F). It is possible

that the amount of DDL-1 and DDL-2 is not the limiting factor for longevity regulation. DDL-1 and DDL-2 may have to collaborate with other proteins to modulate longevity and stress resistance; thus the overexpression of one protein may not be sufficient to produce significant longevity phenotype.

2-4-3 *ddl-1* and *ddl-2* are negative regulators of HSF-1

To determine the potential role of DDL-1 and DDL-2 as negative regulators of HSF-1, we examined whether *ddl-1* and *ddl-2* inactivation affect HSF-1 activation. In collaboration with Dr. Hee Chul Lee and Tsui-Ting Ching in our lab, we examined the effect of *ddl-1* or *ddl-2* inactivation on HSF-1 transcriptional activity by quantitative RT-PCR. Inhibition of *ddl-1 or ddl-2* led to increases in mRNA transcription of all four HSF-1 targets, *hsp-16.2*, *hsp-70s* and s*ip-1* upon heat shock (Figure 13). However, under unstressed conditions, inhibition of *ddl-1 or ddl-2* did not significantly elevate the mRNA level of *hsf-1* targets, except for *hsp-16.2* and *sip-1* in *ddl-1* RNAi animals. We found that there was a significantly higher level of nuclear localized HSF-1 in *ddl-1* RNAi animals under both stressed and unstressed conditions and in *ddl-2* RNAi animals under stressed conditions (Figure 14). Inhibition of *ddl-1* appeared to increase DNA binding activity of HSF-1 both before and after heat shock (Figure 14B and C). There was also a significant increase in DNA binding activity of HSF-1 in *ddl-2* RNAi animals under stressed conditions, whereas inhibiting *ddl-2* under unstressed conditions produced no significant effect (Figure 14B and C). We also found an increased level of post-translationally modified HSF-1 in *ddl-1* RNAi animals under stressed and unstressed conditions (Figure 14D and E). Curiously, the level of HSF-1 PTM was slightly reduced in *ddl-2* RNAi animals, suggesting that DDL-1 and DDL-2 may regulate

HSF-1 activity via both overlapping and distinct mechanisms. Together, these findings strongly suggested that HSB-1, DDL-1, and DDL-2 function as negative regulators of HSF-1 in *C. elegans*.

2-4-4 *hsf-1* is required for *ddl-1*, *ddl-2* and *hsb-1* to promote longevity

We hypothesized that DDL-1, DDL-2 and HSB-1 regulate HSF-1 activity through the formation of an inhibitory complex. To test this model, we first asked whether *hsf-1* is required for *ddl-1*, *ddl-2* and *hsb-1*-mediated longevity. We utilized *hsf-1* mutant animals carrying *hsf-1(sy441)*, an *hsf-1* loss-of-function allele. The *hsf-1(sy441)* animals displayed decreased lifespans, egg-laying defects, and larval arrest at elevated temperatures [98]. This allele completely abolished lifespan extension by *ddl-1* and *ddl-2* RNAi, showing that *hsf-1* is required for *ddl-1* and *ddl-2* inactivation to extend lifespan (Figure 17A and B). Similarly, the inactivation of *hsf-1* by RNAi abolished lifespan extension by *hsb-1(cg116)* deletion (Figure 17C). Our genetic epistasis analysis clearly showed the requirement of *hsf-1* for *ddl-1*, *ddl-2* and *hsb-1* mutation to extend lifespan, in agreement with our model that DDL-1, DDL-2 and HSB-1 regulate HSF-1 to influence longevity.

2-4-5 *ddl-1*, *ddl-2* and *hsb-1* might function in the same pathway

A previous yeast-two hybrid interactome study in *C. elegans* suggested that DDL-1 may interact with HSB-1 and DDL-2 [99], implying that they may function in the same molecular pathway. To test whether these genes share a common mechanism to influence HSF-1 activity, we created combinations of *ddl-1*, *ddl-2* or *hsb-1* compound mutants and measured their lifespan. Either *ddl-1(ok2916)* or *ddl-2(ok3235)* mutations

did not lead to further extensions of lifespan in long-lived *hsb-1(cg116)* (Figure 17E and F). We also found that *ddl-1(ok2916)*; *ddl-2(ok3235)* double mutant animals did not live longer than *ddl-1(ok2916)* or *ddl-2(ok3235)* single mutants (Figure 17D). Our RNAi experiments showed similar result, as *ddl-1* and *ddl-2* double RNAi did not lead to a longer lifespan extension than *ddl-1* or *ddl-2* RNAi alone (Table 1). Overall, these data indicated that the inactivation of *ddl-1*, *ddl-2* and *hsb-1* have no additive effect on longevity, strongly suggesting that these genes may genetically function in the same pathway and share a common mechanism to modulate HSF-1 activity.

2-4-6 Physical interaction among HSF-1, HSB-1, DDL-1 and DDL-2

We next attempted to elucidate how HSF-1 may be regulated by DDL-1 and DDL-2. Given that DDL-1 and DDL-2 are negative regulators of HSF-1 and may share a common mechanism with HSB-1 to modulate *hsf-1*-dependent longevity, we hypothesized that DDL-1, DDL-2 and HSB-1 may form an inhibitory complex that binds to HSF-1. To test our model, we first attempted to confirm previously reported DDL-1-HSB-1 and DDL-1-DDL-2 interaction by co-immunoprecipitation in cell culture. Epitope tagged HA-DDL-1 and FLAG-DDL-2 were co-expressed in 293T cells and immunoprecipitated by anti-HA antibody. We were able to detect FLAG-DDL-2, as we immunoprecipitated HA-DDL-1 (Figure 18A, left). Conversely, when we pulled down FLAG-DDL-2, we were able to detect HA-DDL-1 (Figure 18A, right). Similarly, to assess the interaction between DDL-1 and HSB-1, we co-expressed HA-DDL-1 and Myc-HSB-1 and pulled down DDL-1 with anti-HA antibody. The result showed that Myc-HSB-1 can be co-immunoprecipitated with HA-DDL-1, and vice versa (Figure 18B). We were not able to detect the interaction between DDL-2 and HSB-1, even with the co-expression of

DDL-1. DDL-2 and HSB-1 may not directly interact; thus, it is possible that the binding between DDL-1 & HSB-1 or DDL-1 & DDL-2 is obscured by our experimental conditions, including the duration of washing as well as the composition of our buffers. Nonetheless, our findings suggested that DDL-1 may physically interact with HSB-1 and DDL-2 and may be present in a protein complex containing all three of them.

To ask whether the hypothesized inhibitory protein complex binds to HSF-1, we next tested whether HSF-1 is present in the same complex with DDL-1. Myc-HSF-1 and HA-DDL-1 were expressed in 293T cells and co-immunoprecipitated with anti-Myc or anti-HA antibodies. Indeed, we were able to detect the interaction between HA-DDL-1 and Myc-HSF-1 (Figure 18C). In addition, the physical interaction between HSF-1 and HSB-1 has been previously suggested [84], further supporting our hypothesis that these HSF-1 negative regulators form a protein complex with HSF-1 to modulate its activity.

To find out whether a similar protein complex is also present in *C. elegans*, we assessed the interaction between HSF-1 and DDL-1 by creating stable transgenic worms expressing HA-tagged DDL-1. Whole cell extracts from day 1 adult synchronized culture was prepared and immunoprecipitated by anti-HA antibody. We found that HSF-1 can be co-immunoprecipitated with HA-DDL-1 (Figure 18D). We also co-expressed HA-DDL-1 and FLAG-DDL-2 in worms and successfully confirmed the interaction between DDL-1 and DDL-2 (Figure 18E). Notably, the HSF-1-DDL-1 interaction appeared to be diminished in an *hsb-1(cg116)* null mutant background (Figure 18D, EQ193), indicating that the interaction between DDL-1 and HSF-1 largely depends on HSB-1. In other words, HSB-1 may play an important role in DDL-1-HSF-1 interaction.

Overall, this biochemical evidence strongly suggested interactions between DDL-1 and its binding partners. However, we do not know exactly whether these interactions occur *in vivo*. We next investigated the interaction between DDL-1 and its binding partners *in vivo* by using bimolecular fluorescence complementation (BiFC) assay. With this system, we were able to visualize the formation of protein complexes in living animals. BiFC is a well-established method based on the complementation of two non-functional fluorescent protein fragments. These proteins can be fused to a pair of proteins of interest and expressed *in vivo* [102,103]. If the postulated interaction occurs, two fluorescent protein fragments will be brought into proximity, allowing the reformation of native fluorescent molecule and the emission of fluorescence. This approach not only enables the identification of protein-protein interactions, but also reveals the subcellular localization where the interaction occurs. We chose two fragments derived from YFP variant Venus, VN173 (1-173) and VC155 (155-238) as BiFC reporters. To examine the interaction between DDL-1 and HSB-1 *in vivo*, we created transgenic lines expressing both DDL-1::VN173 and HSB-1::VC155 driven by their own promoters (*ddl-1 promoter::ddl-1::VN173; hsb-1 promoter::hsb-1::VC155*). We observed strong fluorescent signal in the cytosolic compartment of the intestine cells, indicating that DDL-1 and HSB-1 indeed physically interact *in vivo* (Figure 19).

Taken together, based on these *in vitro* and *in vivo* analyses, we confirmed the previously reported protein-protein interaction and demonstrated the molecular interaction among HSF-1, HSB-1, DDL-1 and DDL-2. Overall, these findings support our hypothesis that these proteins form a complex called DDL-1 containing HSF-1 inhibitory

complex (DHIC) and that the formation of DHIC prevents HSF-1 oligomerization and subsequent activation.

2-4-7 Tissue expression of *ddl-1* and *ddl-2*

Investigating the tissue expression of *ddl-1* and *ddl-2* will provide valuable insights into their site of action; therefore, we created transgenic animals carrying *ddl-1 promoter::ddl-1::gfp* and *ddl-2 promoter::ddl-2::gfp* extrachromosomal arrays to determine DDL-1/2 tissue expression pattern as well as cellular localization. DDL-1::GFP is mainly expressed in the cytosolic compartment in the intestine as well as several neurons (Figure 15). The cytosolic localization of DDL-1 is in agreement with our BiFC result and our hypothesis that DDL-1, DDL-2 and HSB-1 form a complex that inhibits HSF-1 by cytosolic sequestration. However, we were unable to obtain stable *ddl-2::gfp* transgenic lines, presumably due to the instability of the fusion protein or the toxicity caused by overexpression. Instead, we generated animals carrying *ddl-2* transcriptional fusion (*ddl-2 promoter::gfp*) that expresses GFP under *ddl-2* promoter. Interestingly, unlike DDL-1, DDL-2 is largely expressed in a certain group of neurons in the head (particularily around the nerve ring) and tail (Figure 16). Further characterization revealed that DDL-2 is expressed not only in a subset of neurons, but also in some structure cells (hypodermal and ganglia cells), body wall muscle and a small number of adult intestinal cells. We do not know whether the expression of *ddl-2* in these neurons is critical in determining HSF-1 activity and longevity at this point.

2-4-8 DDL-1 threonine phosphorylation is negatively regulated by insulin/IGF-like signaling

As we overexpressed DDL-1 in mammalian cells, western blot analysis showed two bands at the expected size of DDL-1, suggesting possible post-translational modifications (PTMs) on DDL-1 (Figure 20A and B). Since phosphorylation is the most common type of PTM, we first tested whether phosphorylation is responsible for the observed mobility shift on DDL-1. Upon incubation with CIP (calf intestine alkaline phosphatase), the top band completely disappeared (Figure 20A), suggesting that DDL-1 is phosphorylated. Subsequent western blot analysis with anti-phospho-threonine antibody revealed that the modification(s) includes phosphorylation on at least one threonine residue (Figure 20B, left lane).

We next attempted to examine whether DDL-1 phospho-threonine modification is also present in worms. Whole cell extracts of HA-DDL-1 expressing transgenic animals were prepared, immunprecipitated by anti-phospho-threonine antibody, and western blotted by anti-HA antibody. We were able to detect threonine phosphorylation on DDL-1 (Figure 20C). Moreover, our result showed that inactivation of DAF-2 (insulin/IGF-like receptor) by RNAi leads to a significant increase of DDL-1 threonine phosphorylation (Figure 20C), indicating that DDL-1 phosphorylation status is subject to regulation by the insulin/IGF-like signaling.

2-4-9 The insulin/IGF signaling pathway modulates formation of the DHIC complex

Since protein phosphorylation represents a common mechanism for cellular signaling

and is known to exert its effect by the modulation of protein-protein interaction, our findings pointed to a possibility that the interaction between DDL-1 and its binding partners may be subject to regulation by the insulin/IGF-like signaling cascade. To test this hypothesis, we prepared synchronized cultures of *HA-ddl-1* transgenic worms grown on control or *daf-2* RNAi bacteria, and harvested at day 1 during the adulthood. Whole cell extracts were prepared, immunoprecipitated by anti-HA antibody, and analyzed by HSF-1 western blot. Our data showed that inactivation of *daf-2* by RNAi disrupted the binding between HSF-1 and DDL-1 (Figure 20D and Figure 21A). Similarly, we observed that *akt-1* inactivation led to a modest decrease in HSF-1-DDL-1 binding. These data strongly indicated that the activity of insulin/IGF signaling might affect the formation of the DHIC complex. In addition, we also observed that the interaction between HSF-1 and DDL-1 is not affected by heat stress, implying that the formation of DHIC may be heat-insensitive (Figure 21B).

2-4-10 DDL-1 phosphorylation status may be important for DHIC complex formation

As we demonstrated, the insulin/IGF-like signaling modulates DHIC complex formation and the level of DDL-1 threonine phosphorylation. To ask whether DDL-1 phosphorylation plays a role in modulation of DHIC complex formation, we next used *in-silico* tools to predict phosphorylation on DDL-1. With ScanSite (http://scansite.mit.edu/) and PredPhospho (http://pred.ngri.re.kr/PredPhospho.htm), we were able to find five putative serine/threonine phosphorylation sites (T24, T84, T108, S181 and T182) on DDL-1.

Given that DDL-1 is threonine phosphorylated in both mammalian cells and worms, it is likely that DDL-1 phosphorylation is a common mechanism shared by both organisms. Thus, we looked for conserved motifs present in worms (DDL-1) and mammals (CCDC53), and focused on putative phosphorylation sites located within these motifs. Sequence analysis showed high homology at the C-terminal of DDL-1 and CCDC53, a mammalian DDL-1 ortholog. In close proximity to this evolutionally conserved region, two residues on DDL-1, S181 and T182 are predicted to be phosphorylated by GSK3/CK1 kinase family. Notably, CCDC53 T181, the homologous site for DDL-1 T182, was also a predicted phospho-threonine site.

To verify the prediction result, we utilized serine/threonine dephosphorylation mimetic mutant. DDL-1 mutants that carry threonine-to-alanine mutation on putative phosphorylation sites were created by site-directed mutagenesis and expressed in mammalian cells. Western blot analysis showed that T182A (threonine-to-alanine) mutation completely eliminated threonine phosphorylation on DDL-1, indicating that T182 might be the only threonine phosphorylation site on DDL-1 (Figure 20B). Moreover, our western blot analysis showed that wild-type DDL-1 consistently appears as two bands, while T182A mutation partially eliminated the top band, suggesting that T182 might not be the only PTM on DDL-1 (Figure 20B, top).

Our attempt to examine S181, another putative phosphorylation site located in proximity to the conserved motif, was not successful. We were unable to confirm the phosphorylation status of S181, since the level of serine phosphorylation is not detectable with anti-phospho-serine antibody. It is known that the specificity and affinity

of pan-phospho-antibody depends on the sequence context. Thus, whether S181 is phosphorylated remains uncertain. However, our analysis showed that S181A/T182A double mutation completely eliminates the DDL-1 top band, suggesting that the phosphorylation on S181 remains possible (data not shown).

As we demonstrated, T182 is the only confirmed phosphorylated residue located in conserved motifs of DDL-1. To examine the potential role of T182 in HSF-1 regulation, we tested whether the T182 phosphorylation is crucial for the formation of DHIC. To this end, we created T182A (threonine-to-alanine) mutant to evaluate the impact of dephosphorylation on the interaction between DDL-1 and its binding partners. Wild-type and mutant HA-tagged DDL-1 were expressed in 293T cells and co-immunoprecipitated by anti-HA antibody. We found that T182A mutation enhanced the interaction between HSF-1 and DDL-1 (Figure 20E). This result suggested that dephosphorylated DDL-1 may favor the formation of DHIC, and consequently inhibit HSF-1 oligomerization and subsequent activation. This finding may indicate that the phosphorylation of DDL-1 is likely to play a role in modulating the formation of DHIC. We did not formally evaluate whether T182 phosphorylation impacts the interaction among all DHIC components. However, we did observe that T182A mutation does not affect the binding between DDL-1 and DDL-2, suggesting that at least T182 phosphorylation status does not play a role in modulating DDL-1-DDL-2 interaction (Figure 20F).

Since T182 may be important for the insulin/IGF-like signaling to regulate HSF-1 activity, we next attempted to determine whether T182 also play a role in DAF-2 longevity. We created transgenic rescue animals expressing wild-type or T182A DDL-1 mutant in a

ddl-1(ok2916) background, treated with *daf-2* RNAi bacteria and measured their lifespan. Presumably, if T182A is important for DAF-2 longevity, the expression of DDL-1 T182A in *ddl-1* mutants should lead to a stronger suppression of DAF-2 longevity than the expression of wild-type DDL-1 in the same background. We did not observe strong suppression of DAF-2 longevity by T182A rescue mutants (Figure 22). T182A rescued animals appeared to have slightly shorter lifespans than their wild-type counterparts; however, the difference was not statistically significant. It is possible that overexpressing mutant DDL-1 alone is not sufficient to affect DAF-2 longevity. The co-expression of other DHIC components (i.e. DDL-2 and HSB-1) may be necessary. Further, T182 on DDL-1 may only partially contribute to DAF-2-mediated HSF-1 regulation; thus, threonine-to-alanine mutation on T182 minimally impacted DAF-2 longevity. It is possible that the insulin/IGF-like signaling modulates DHIC formation through multiple parallel mechanisms.

It is currently unclear which kinase(s) catalyzes the phosphorylation on T182 of DDL-1. In an attempt to identify DDL-1 kinase(s), we examined whether DDL-1 is the target of the glycogen synthase kinase 3 (GSK3) family, as T182 is predicted to be phosphorylated by a GSK-like kinase. In *C .elegans,* two GSK3-like kinases are present: *gska-3* (GSK3α) and *gsk-3* (GSK3β). We found that the inactivation of both GSKs did not alter the level of phospho-threonine on DDL-1 (Figure 23). Moreover, the knockdown of *akt-1* did not lead to a decrease in DDL-1 phospho-threonine level; on the contrary, AKT inhibition promoted DDL-1 threonine phosphorylation. These data clearly showed that neither GSKs nor AKT phosphorylates DDL-1. Further investigations are required to identify DDL-1 kinase(s).

2-5 Discussion

2-5-1 The insulin/IGF-like signaling modulates HSF-1 activity

Although the roles of HSF-1 and heat-shock responsive genes in regulating stress response and longevity have been previously described in *C. elegans*, the molecular mechanism by which HSF-1 activity is modulated in response to different environmental or hormonal cues remains largely unclear. Our work presented here provides evidence for a mechanism underlying the regulation of HSF-1 activation by the insulin/IGF-like signaling pathway, one of the major regulatory pathways for longevity. Our model suggested that DDL-1, DDL-2 and HSB-1 negatively regulate HSF-1 activity by forming a protein complex with HSF-1 and consequently reduces the amount of HSF-1 susceptible to heat stress-induced activation. We believe that the insulin/IGF-like signaling controls HSF-1 activity, at least in part, by regulating the formation of DDL-1-containing HSF-1 inhibitory complex (DHIC), possibly by modulating threonine phosphorylation on DDL-1.

2-5-2 Formation of DHIC

It has been previously demonstrated that in mammals, HSF1 activity is tightly regulated by repressive interaction with multiple chaperone complexes containing proteins such as HSP40, HSP70 and HSP90 [96]. These proteins form an inhibitory complex with HSF1, thereby preventing oligomerization and subsequent activation of HSF1. Analogously, we found that DDL-1, DDL-2 and HSB-1, a previously reported HSF negative regulator, may regulate HSF-1 activity through the formation of an inhibitory complex with HSF-1.

The previous yeast-two hybrid interactome data have provided preliminary evidence for

the interactions among DHIC components. Several lines of evidence in our study suggested that these protein interactions are likely to occur *in vivo*. First, our biochemical assay has confirmed the pair-wise interactions between DDL-1-DDL-2, DDL-1-HSB-1 and DDL-1-HSF-1 in cell culture (Figure 18A-C). We have also showed that the interactions between DDL-1-HSF-1 and DDL-1-DDL-2 are present in *C. elegans*. Second, the protein-protein interaction between DDL-1 and HSF-1 can be disrupted by genetic manipulations, such as *daf-2* RNAi knockdown, without affecting the overall protein levels of DDL-1 (Figure 20D). Third, our *in vivo* BiFC assay clearly showed that DDL-1 and HSB-1 interact in cytosolic compartment of the intestinal cells (Figure 19). Moreover, human orthologs of DDL-1, DDL-2, and HSB-1 (CCDC53, WASH2 and HSBP1, respectively) have been reported to either interact with each other or coexist in the same protein complex [104,105], suggesting that the formation of DHIC may be an evolutionally-conserved process.

Although our BiFC assay clearly showed direct interaction *in vivo* between DDL-1 and HSB-1 (Figure 19), our attempt to examine the interaction between DDL-1 and HSF-1 with BiFC was not successful, as HSF-1::VC155/DDL-1::VN173 produced a signal at level similar to its negative control. There are several possibilities. First, fluorescent fusion protein (HSF-1::VC155) may not fold properly to produce functional fluorophore. Second, VN173 or VC155 may sterically hinder the interaction between HSF-1 and DDL-1. Most importantly, the reconstitution of BiFC fluorophore usually occurs at a relatively short distance (~7nm) [106]. If the interaction between HSF-1 and DDL-1 is distant and indirect, fluorescence complementation will not occur efficiently and thus result in low signal. Indeed, our co-immunoprecipitation data showed that the absence of

HSB-1 greatly diminished the interaction between HSF-1 and DDL-1 (Figure 18D), indicating that DDL-1-HSF-1 interaction may be indirect and largely depend on the presence of HSB-1. Thus, an optimized design for BiFC assay will be necessary for studying the detail of DHIC formation in the future.

The expression pattern of HSF-1, DDL-1 and HSB-1 suggested that these proteins may co-localize in the same cell types. HSF-1 is expressed in almost all cell types, as observed in our *hsf-1::gfp* transgenic lines; whereas DDL-1 is mainly expressed in pharynx, intestine, body wall muscle, and a subset of head and tail neurons (Figure 15). HSB-1 has been reported to be expressed in a variety of tissues such as pharynx, intestine, muscles, and tail neurons [107]. The overlapping expression pattern among HSF-1, HSB-1, and DDL-1 supports the idea that these proteins interact with each other *in vivo*. DDL-2, on the contrary, is mainly expressed in a subset of neurons, larval body wall muscles, and a small number of adult intestinal cells (Figure 16). However, it is not clear whether the expression of DDL-2 in those neurons is critical in regulating HSF-1 activity and longevity. Further studies will be required to address these questions.

2-5-3 Direct regulation of HSF-1 activity by insulin/IGF-like signaling through DHIC

It has been shown that HSF-1 plays an important role in promoting many beneficial effects such as thermotolerance and longevity in the insulin/IGF-like signaling pathway [2,68,108]. Similar to DAF-16, lifespan extension results from reduced DAF-2 activity is also HSF-1 dependent. HSF-1 is shown to be required for proper expression of many downstream genes, including a group of small heat-shock proteins, in the context of

DAF-2-mediated longevity [2]. Indeed, our data showed that the inactivation of the DAF-2 pathway leads to an overall increase in HSF-1 activity, as observed in the multi-step activation, including nuclear translocation, oligomerization, post-translational modification, DNA binding activity, and HSF-1 target gene expression (Figure 10 and Figure 11). These results support the idea that HSF-1 is subject to direct control by insulin/IGF-like signaling.

Our study on the regulation of DHIC complex formation strongly suggested that DHIC might be, at least in part, responsible for HSF-1 regulation by insulin/IGF-like signaling. First, we observed that the formation of DHIC is reduced upon DAF-2 inactivation, indicating that insulin/IGF-like signaling may modulate protein-protein interaction among DHIC components (Figure 20D). Moreover, our data pointed out a possibility that DAF-2 activity may modulate the formation of DHIC through affecting the phosphorylation on DDL-1. The phosphorylation of DDL-1 T182 may attenuate the interaction between HSF-1 and DDL-1 (i.e. formation of DHIC), whereas the dephosphorylation of DDL-1 T182 promotes the formation of DHIC. We concluded that T182 may play a role in the insulin/IGF-like signaling regulated HSF-1 activation.

2-5-4 Multiple Layers of Regulation of HSF-1 Activity

The activation of HSF-1 in response to heat or other types of stressors is well-established in many systems. Our study suggested that HSF-1 activity is not only controlled by stress induction, but also subject to direct regulation by the insulin/IGF-like signaling. Comparing the effects of stress stimulation, which acts in a transient and dramatic fashion, hormonal stimulation usually involves in long-term regulation. As

observed in our co-immunoprecipitation experiment, the modulation of DHIC formation by insulin/IGF-like signaling do not seemed to be affected by heat stress (Figure 21B), suggesting that the DAF-2 pathway regulates DHIC in a molecular mechanism independent of canonical heat-shock-induced HSF activation pathway. Although it remains possible that chronic stress may indirectly modulate HSF-1 activity through affecting hormonal pathways including the insulin/IGF-like signaling, we concluded that the insulin/IGF-like signaling/DHIC-mediated HSF-1 regulation is unlikely to be responsible for immediate, acute stress-induced HSF-1 activation. We believe that insulin/IGF-like signaling may act as a modulatory pathway that regulates the level of stress-susceptible (inducible) HSF-1, thereby fine-tuning stress response.

2-5-5 Model of HSF-1 Activation Regulated by insulin/IGF-like signaling in *C. elegans*

In *C. elegans*, modulation of the insulin/IGF-like signaling pathway is a pivotal determinant of the endocrine control of many physiological processes such as growth, reproduction, metabolism, longevity, as well as stress response. HSF is a master transcription factor previously known to be required for stress response and homeostasis, and has been postulated to act downstream of insulin/IGF-like signaling to mediate longevity. In this chapter, we have demonstrated that HSF-1 is subject to direct regulation by insulin/IGF-like signaling, and this regulation occurs via the modulation of the formation of DHIC, an HSF-1 inhibitory complex.

Upon heat stress stimulation, HSF-1 undergoes oligomerization, posttranslational modification, and nuclear translocation in an undefined order before acquiring DNA

binding and transcriptional activity. The formation of a DDL-1-containing HSF-1 inhibitory complex (DHIC), consisting of HSF-1, HSB-1, DDL-1, and DDL-2, reduces the pool of HSF-1 susceptible to heat stress stimulation. We proposed that increased insulin/IGF-like signaling promotes the formation of DHIC, whereas reducing insulin/IGF-like signaling activity promotes DDL-1 phosphorylation, disrupts DHIC formation, and consequently increases HSF-1 activity. (Figure 24)

2-6 Figures

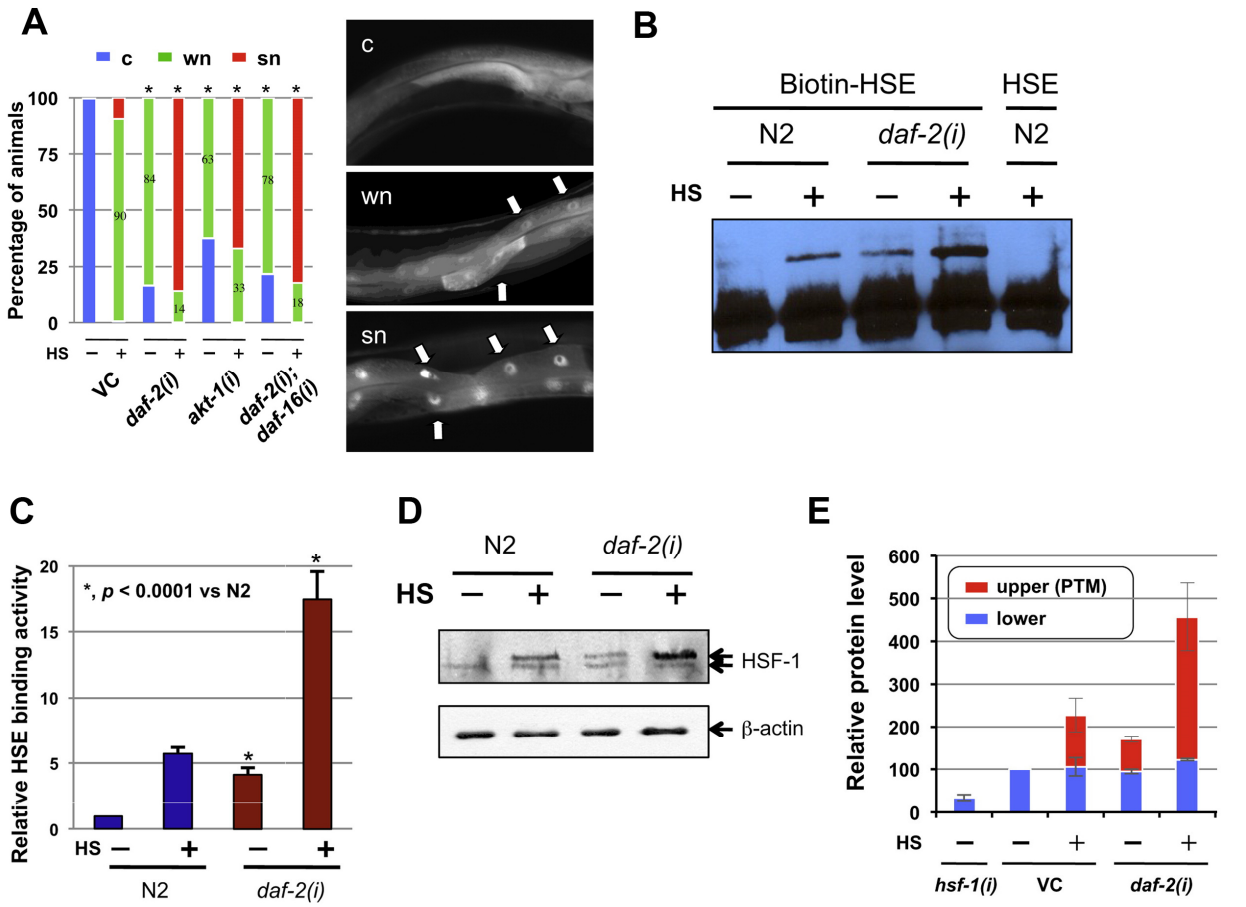

Figure 10. Inactivation of DAF-2 positively regulates HSF-1 activity and heat-shock response [3] **(A)** Nuclear accumulation of HSF-1 in response to insulin/IGF-like signaling inactivation. EQ73 animals (*hsf-1::gfp)* grown on vector control (VC) or different RNAi bacteria were unstressed or heat shocked for 30 min (HS) before being classified into three groups according to the nuclear/cytosolic (n/c) ratio of GFP intensity in the intestinal cells (right). "c," "wn," and "sn" are animals with n/c ratio < 1.2, 1.2~2.0, and > 2.0, respectively. The means of three independent experiments were pooled and shown (left). $^{*}p < 0.0001$ versus VC under same conditions (chi^2 test). n ≥ 300. **(B)** The result of a representative experiment of DNA binding activity of HSF-1 in *daf-2(e1370)* mutants in response to 90 min of heat shock (HS). **(C)** The mean ± SD of three independent experiments in (B) (mean ± SD), normalized to the control (N2 with unlabeled HSE). **(D and E)** N2 or *daf-2* RNAi animals were unstressed or heat shocked for 90 min (HS). Worm whole-cell extracts (WCE) of these animals were subjected to immunoblot analysis using anti-HSF-1 (top) or anti-β-actin (bottom) antibodies. Detailed quantification is shown in (E).

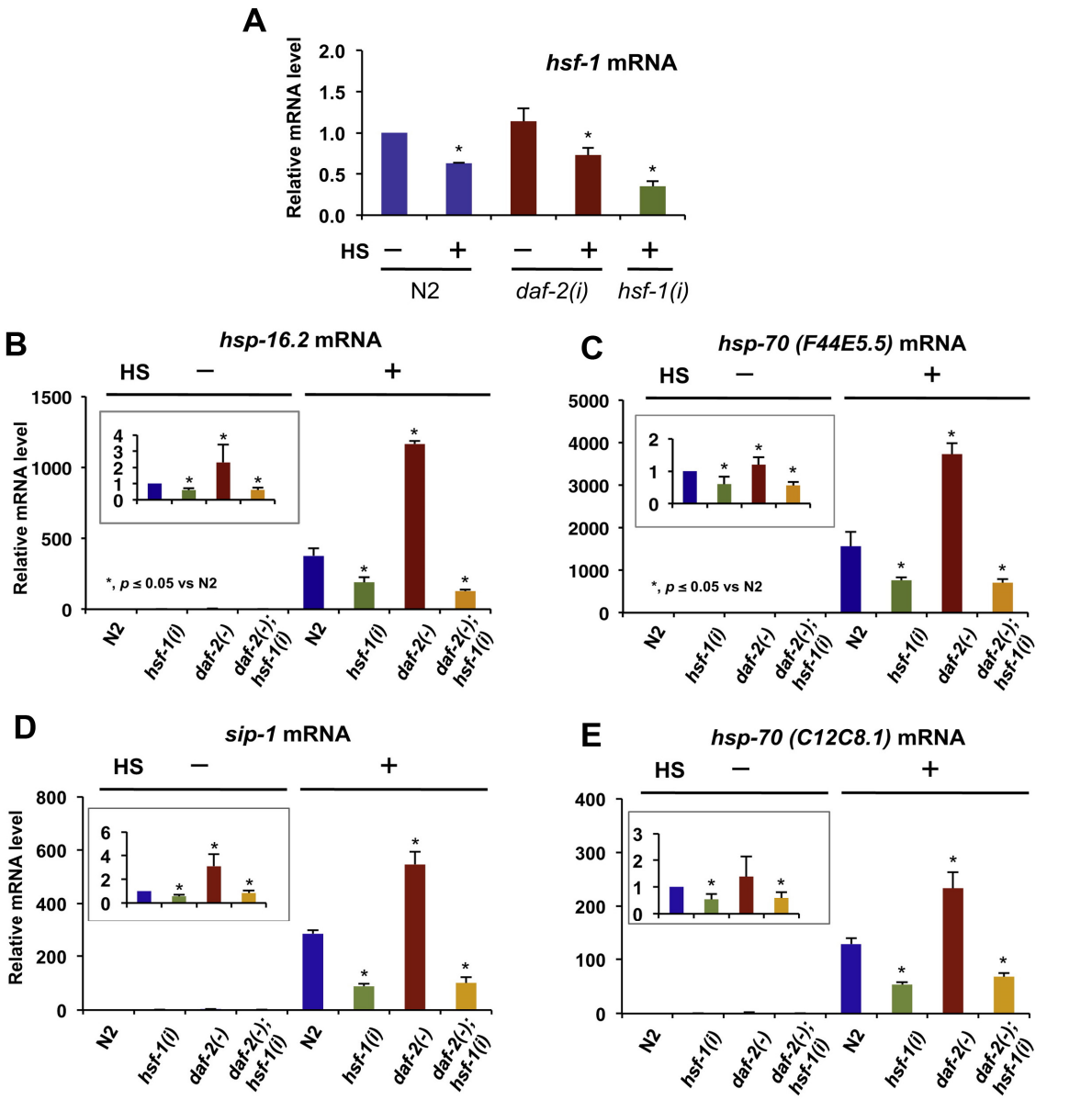

Figure 11. Quantitative RT-PCR analysis of *hsf-1*, *hsp-16.2*, *sip-1*, and *hsp-70s* expression [3]
(A) The mRNA level of *hsf-1* is not affected by *daf-2* knockdown. Relative abundance of *hsf-1* mRNA in animals fed with vector control, *daf-2* or *hsf-1* RNAi bacteria with or without heat-shock. The mRNA levels were measured by quantitative RT-PCR. "HS" indicates that the animals were shifted to 37°C for 90 minutes before they were collected. In all cases, the relative mRNA levels were normalized against the internal control *act-1* (β -actin) and compared to the unstressed vector control (= 1). The data for at least three independent experiments were pooled, and the mean ± SD of each treatment is shown. $^{*}p < 0.05$ when compared to the unstressed vector control. The differences in *hsf-1* mRNA level between control and *daf-2(RNAi)* animals both under HS conditions were not statistically significant, however. **(B-E)** Relative abundance of (B) *hsp-16.2*, (C) *hsp-70 (F44E5.5)*, (D) *sip-1* and (E) *hsp-70 (C12C8.1)* mRNA in wild-types (N2) or *daf-2(e1370)* mutants fed with control or *hsf-1* RNAi bacteria. The mRNA levels were measured by quantitative RT-PCR. "HS" indicates that the animals were shifted to 37°C for 90 minutes before they were collected. The inset shows the mRNA level under unstressed conditions (without 90 minutes HS). Data were combined from at least three experiments, and the mean ± SD of each treatment is shown.

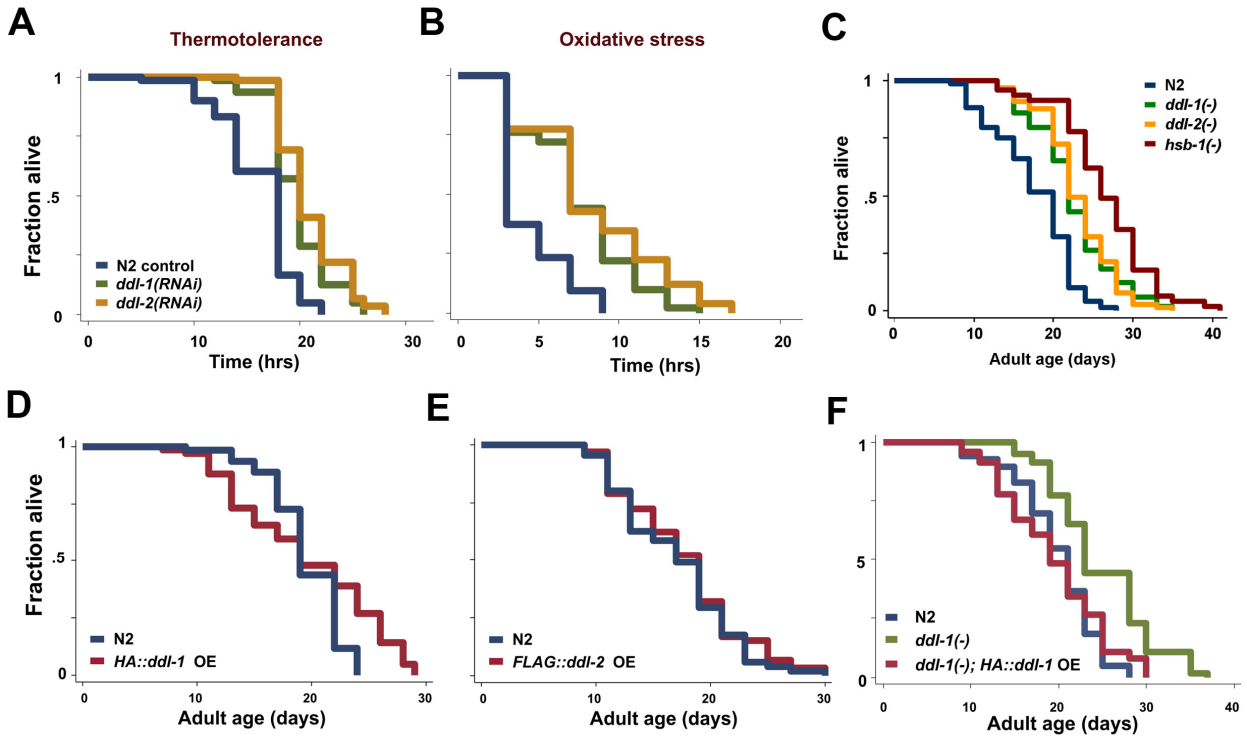

Figure 12. Effects of altering *ddl-1* and *ddl-2* expression on longevity and stress response [3]
(A and B) Reduction of *ddl-1* or *ddl-2* expression results in increased resistance to heat and oxidative stresses. N2 animals grown on vector control (blue), *ddl-1* RNAi (green), or *ddl-2* RNAi (orange) bacteria were exposed to different types of environmental stressors. The viability of these animals was then scored every 2-4 hr. (A) For the thermotolerance analysis, animals were shifted to 35°C. (B) For the oxidative stress analysis, animals were exposed to 300 mM paraquat. **(C)** Lifespan analysis of wild-type (N2), *ddl-1(ok2916)*, *ddl-2(ok3235) and hsb-1(cg116)* mutant animals at 20°C. **(D and E)** Overexpression of *ddl-1* and *ddl-2* failed to produce significant longevity phenotypes.(D) Lifespan analysis of wild-type animals (N2, blue) and animals overexpressing *HA::ddl-1* (EQ136, red) at 20°C.(E) Lifespan analysis of wild-type animals (N2, blue) and animals overexpressing *FLAG::ddl-2* (EQ106, red) at 20°C. **(F)** The lifespan-extending effect of *ddl-1(ok2916)* mutation is abolished by overexpressing HA-tagged DDL-1. Lifespan analysis of N2 animals, *ddl-1(ok2916)* mutants, or transgenic animals overexpressing *hsf-1::gfp* in *ddl-1(ok2916)* background (EQ187) at 20°C. Statistical details were summarized in Table 2 and Table 3.

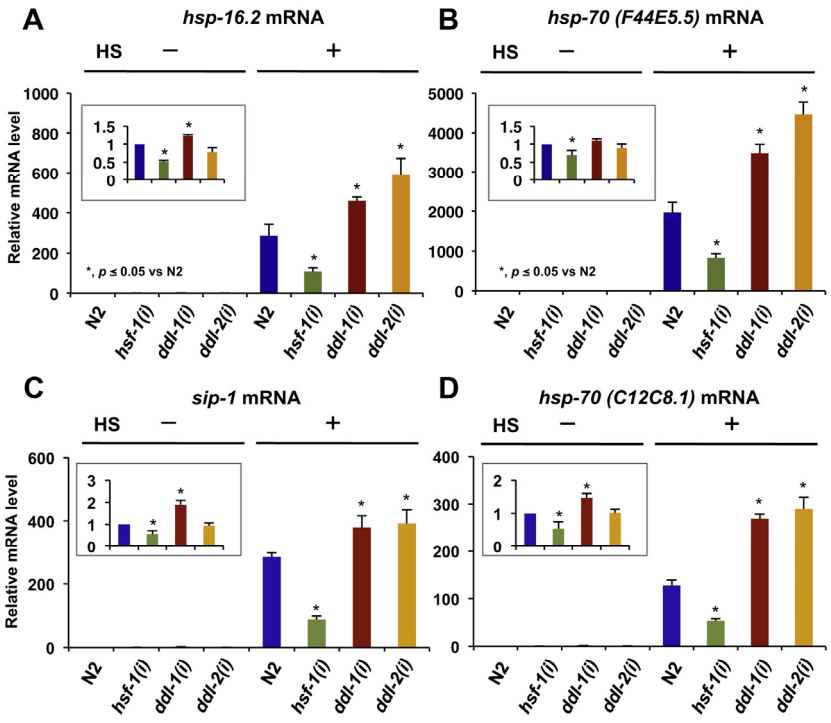

Figure 13. DDL-1 and DDL-2 negatively regulate mRNA expression of HSF-1 downstream targets [3]
Relative abundance of **(A)** *hsp-16.2*, **(B)** *hsp-70* (*F44E5.5*), **(C)** *sip-1* and **(D)** *hsp-70 (C12C8.1)* mRNA in N2, *hsf-1*(RNAi), *ddl-1*(RNAi), or *ddl-2*(RNAI) animals with or without heat shock (90 min). The inset shows the mRNA level under unstressed conditions. The means ± SD of three independent experiments were pooled and shown here.

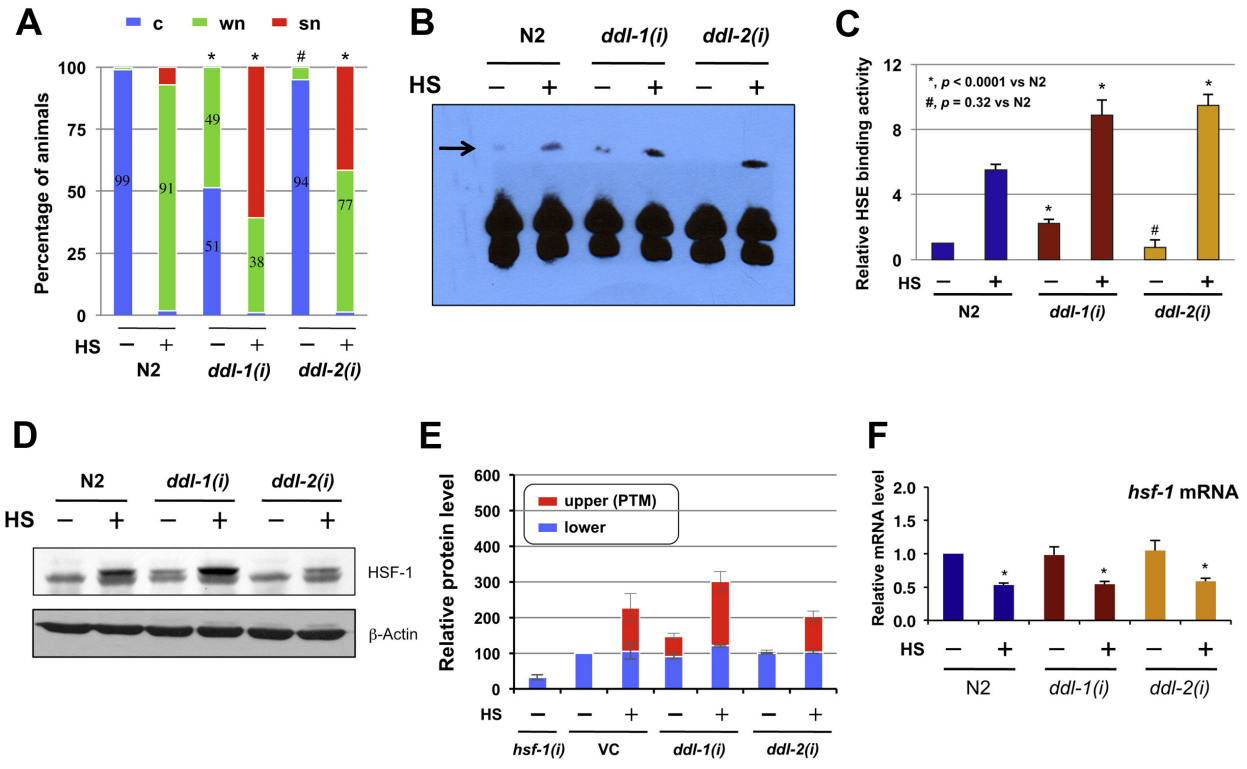

Figure 14. DDL-1 and DDL-2 negatively regulate nuclear translocation, DNA binding, and post-translational modification of HSF-1 [3]
(A) Nuclear accumulation of HSF-1 in response to DDL-1/2 inactivation. EQ73 animals (*hsf-1::gfp)* grown on control, *ddl-1*, or *ddl-2* RNAi bacteria were unstressed or heat shocked for 30 min (HS). The results of three experiments were pooled and shown here. Data are mean, n ≥ 300 per RNAi treatment. $^{*}p <$ 0.0001; $^{\#}p = 0.097$ versus N2 under same conditions (chi^{2}test). **(B and C)** Lowering *ddl-1* or *ddl-2* expression increases HSF-1 DNA binding activity. The DNA binding activity of HSF-1 in N2, *ddl-1(RNAi)*, or *ddl-2(RNAi)* animals was measured by EMSA before or after 90 min of heat shock (HS). A representative experiment is shown in (B). Quantification of three independent experiments (mean ± SD) is presented in (C). **(D and E)** Worm whole-cell extracts (WCE) prepared from N2, *ddl-1(RNAi)*, or *ddl-2*(*RNAi)* animals with or without 90 min of HS were subjected to immunoblot analysis using anti-HSF-1 (top) or anti-β-actin (bottom) antibodies. Detailed quantification is shown in (E). **(F)** The mRNA level of *hsf-1* is not affected by *ddl-1 or ddl-2* RNAi knockdown. Relative abundance of *hsf-1* mRNA in animals fed with vector control, *ddl-1* or *ddl-2* RNAi bacteria with or without heat-shock. $^{*}p < 0.05$ when compared to the unstressed vector control. The differences in *hsf-1* mRNA level between control and *ddl-1(RNAi)* or *ddl-2(RNAi)* animals under stressed conditions are not statistically significant.

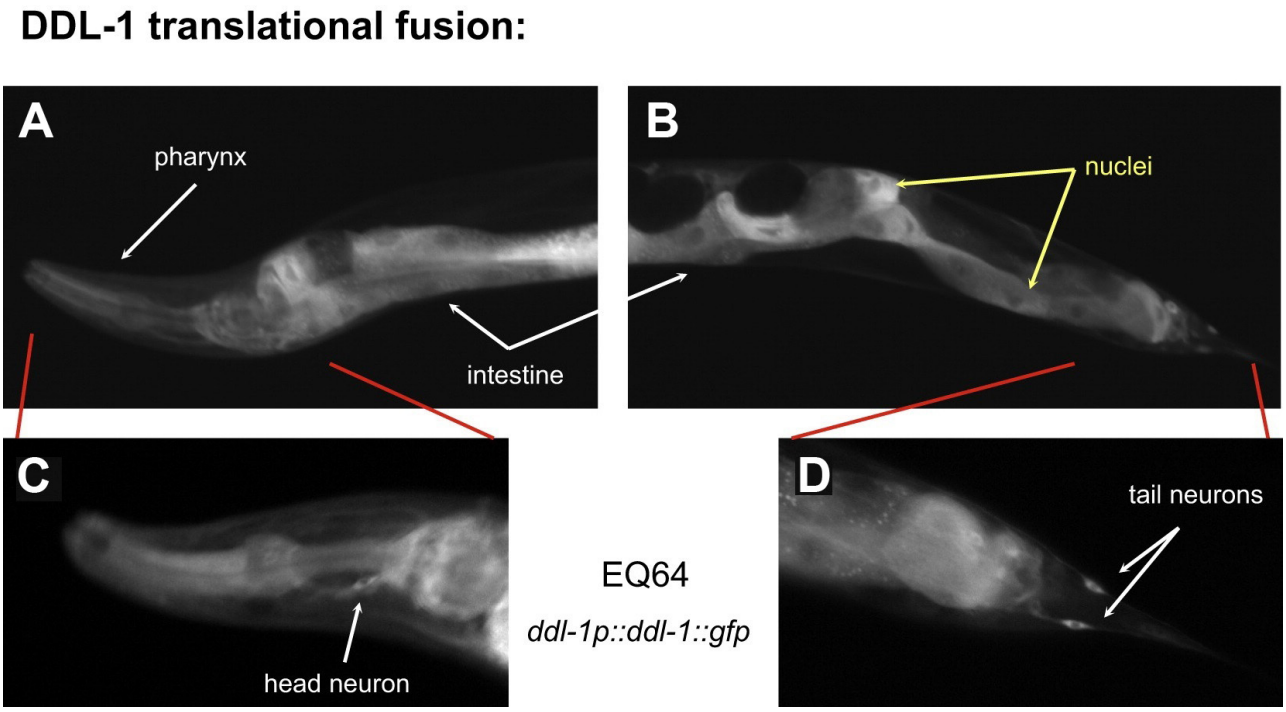

Figure 15. The expression pattern of *ddl-1* in *C. elegans* [3]
Transgenic lines expressing a translational GFP fusion (*ddl-1p::ddl-1::gfp*) of DDL-1 have been utilized to analyze the expression pattern of *ddl-1* in *C. elegans*. **(A–D)** Images of transgenic animals expressing GFP-tagged DDL-1 driven by the endogenous *ddl-1* promoter. DDL-1::GFP expression can be found primarily in the cytoplasm of intestinal cells, pharyngeal cells, and a number of neuronal cells in the head and tail (white arrows). The yellow arrows depict the lack of DDL-1 in the nuclei.

DDL-2 transcriptional fusion:

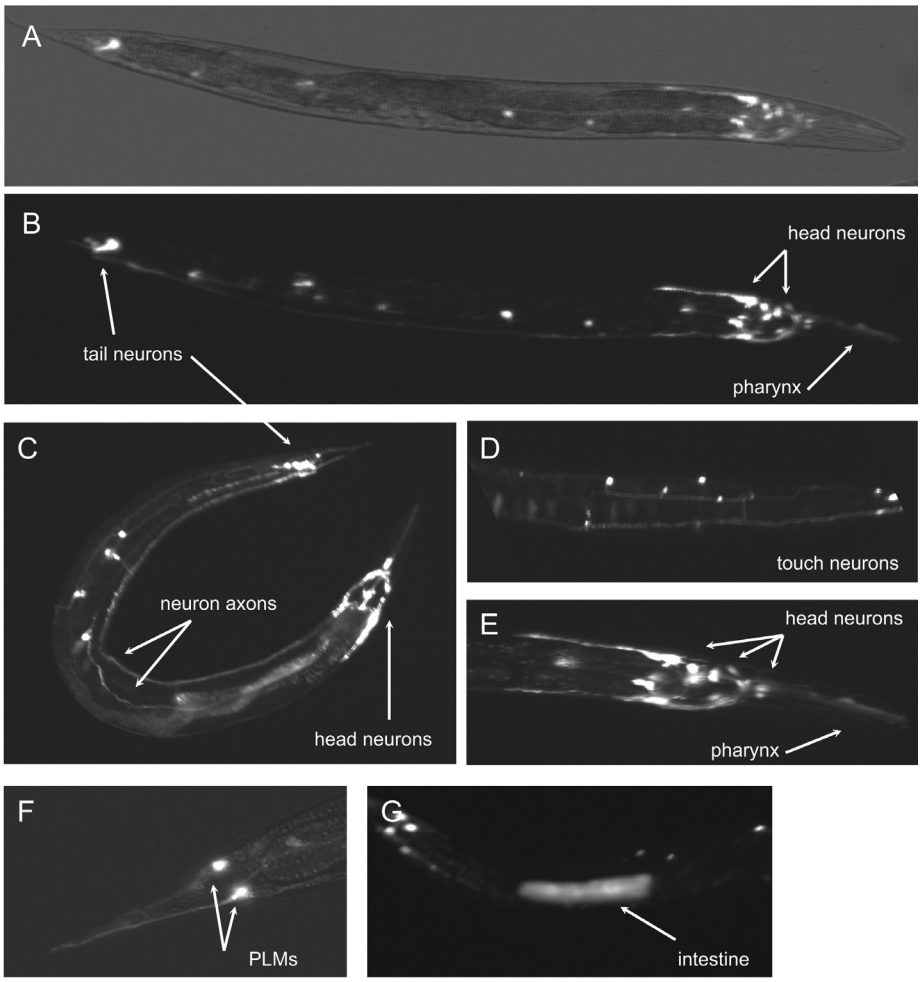

EQ104 *ddl-2p::gfp*

Figure 16. The expression pattern of *ddl-2* in *C. elegans* [3]
Images of transgenic animals (EQ104) carrying a *ddl-2p::ddl-2::gfp* array.(A–F) Expression of DDL-2::GFP is found in several neurons located throughout the body. The neurons that express *ddl-2* might include six touch receptor neurons (AVM, ALM, PVM, PLM), motor neuron HSN, interneuron AVH, and ALA.(G) Occasional expression of DDL-2 in one adult intestinal cell. It is estimated that about 15%–20% of transgenic animals show expression in one or two intestinal cells.

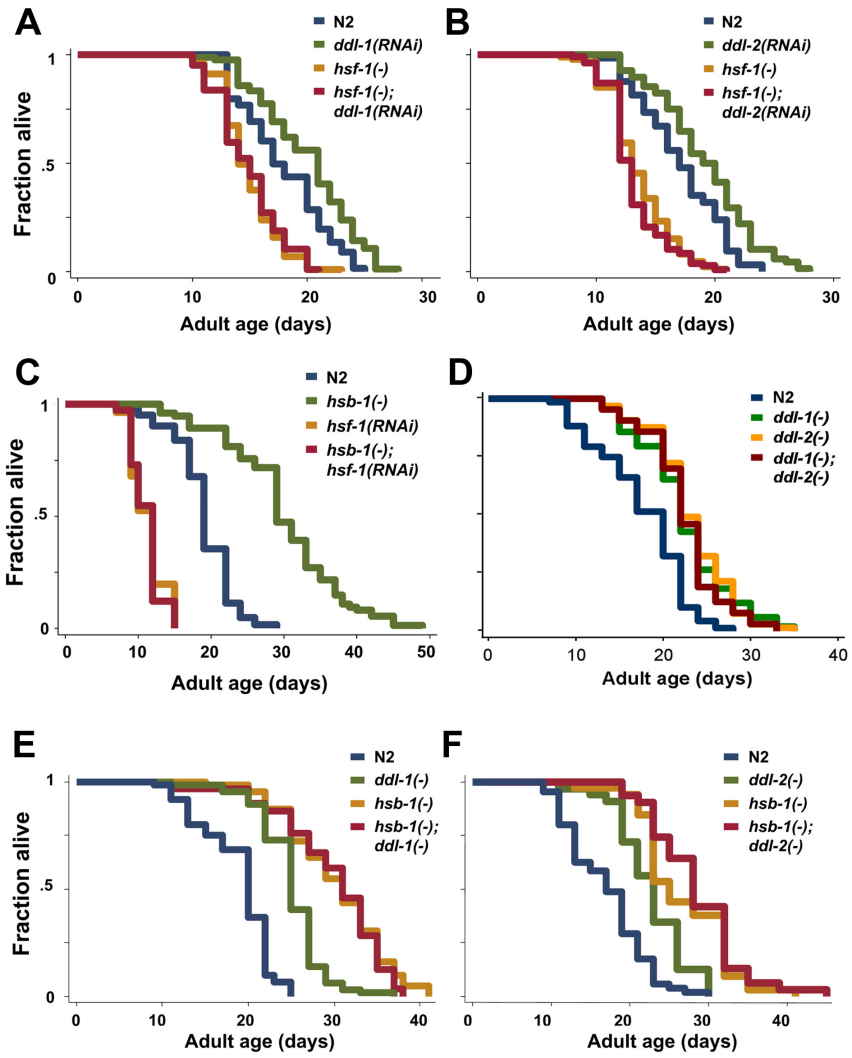

Figure 17. A common *hsf-1*-dependent mechanism mediates the longevity effects of *ddl-1*, *ddl-2*, and *hsb-1* [3]

(A) Lifespan analysis of wild-type (N2) animals or *hsf-1(sy441)* mutants grown on empty vector control or *ddl-1* RNAi bacteria at 20°C. **(B)** Lifespan analysis of N2 animals or *hsf-1(sy441)* mutants grown on control or *ddl-2* RNAi bacteria at 20°C.**(C)** Lifespan analysis of N2 animals or *hsb-1(cg116)* mutants grown on control or *hsf-1* RNAi bacteria at 20°C. **(D)** Lifespan analysis of N2, *ddl-1(ok2916)*, *hsb-1(cg116)*, or *ddl-1(ok2916);hsb-1(cg116)* mutants at 20°C. **(E)** Lifespan analysis of N2, *ddl-2(ok3235)*, *hsb-1(cg116)*, or *ddl-2(ok3235);hsb-1(cg116)* mutants at 20°C. **(F)** Lifespan analysis of N2, *ddl-1(ok2916)*, *ddl-2(ok3235)* or *ddl-1(ok2916)*; *ddl-2(ok3235)* mutants at 20°C. Statistical details are summarized in Table 1 and Table 2.

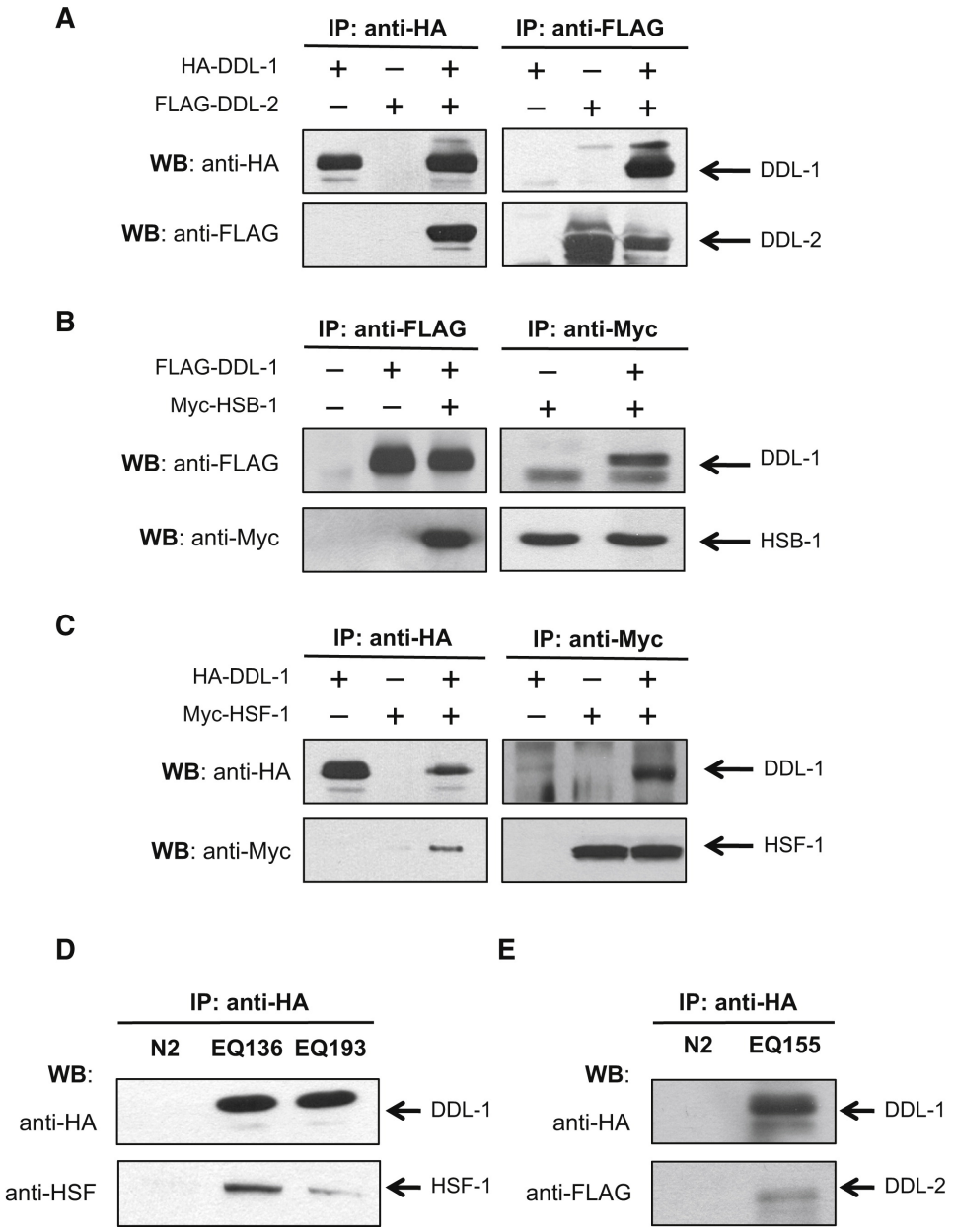

Figure 18. DDL-1 forms a protein complex with HSF-1, HSB-1, and DDL-2 in mammalian cells and *C. elegans* [3]

(A) DDL-1 interacts with DDL-2 in 293T cells. Here and in (B) and (C), 293T cells were transfected with indicated combinations of pCMV-HA-DDL-1, pFLAG-CMV2-DDL-2, pFLAG-CMV2-DDL-1, pCMV-Myc-HSB-1, or pCMV-Myc-HSF-1 plasmids. Whole-cell extracts were then immunoprecipitated (IP) and subsequently western blotted (WB) using indicated antibodies. **(B)** DDL-1 interacts with HSB-1 in 293T cells. **(C)** DDL-1 may form a protein complex with HSF-1 in 293T cells. **(D)** DDL-1 forms a protein complex with HSF-1 in *C. elegans*. Worm whole-cell extracts (WCE) were prepared from N2, EQ136 (*HA-ddl-1* o.e.), or EQ193 [*HA-ddl-1* o.e.; *hsb-1(cg116)*] animals. Samples were immunoprecipitated and subsequently western blotted using indicated antibodies. **(E)** DDL-1 interacts with DDL-2 in *C. elegans*. WCE were prepared from N2 or EQ155 animals expressing both HA-DDL-1 and FLAG-DDL-2 proteins. Samples were immunoprecipitated and western blotted using indicated antibodies.

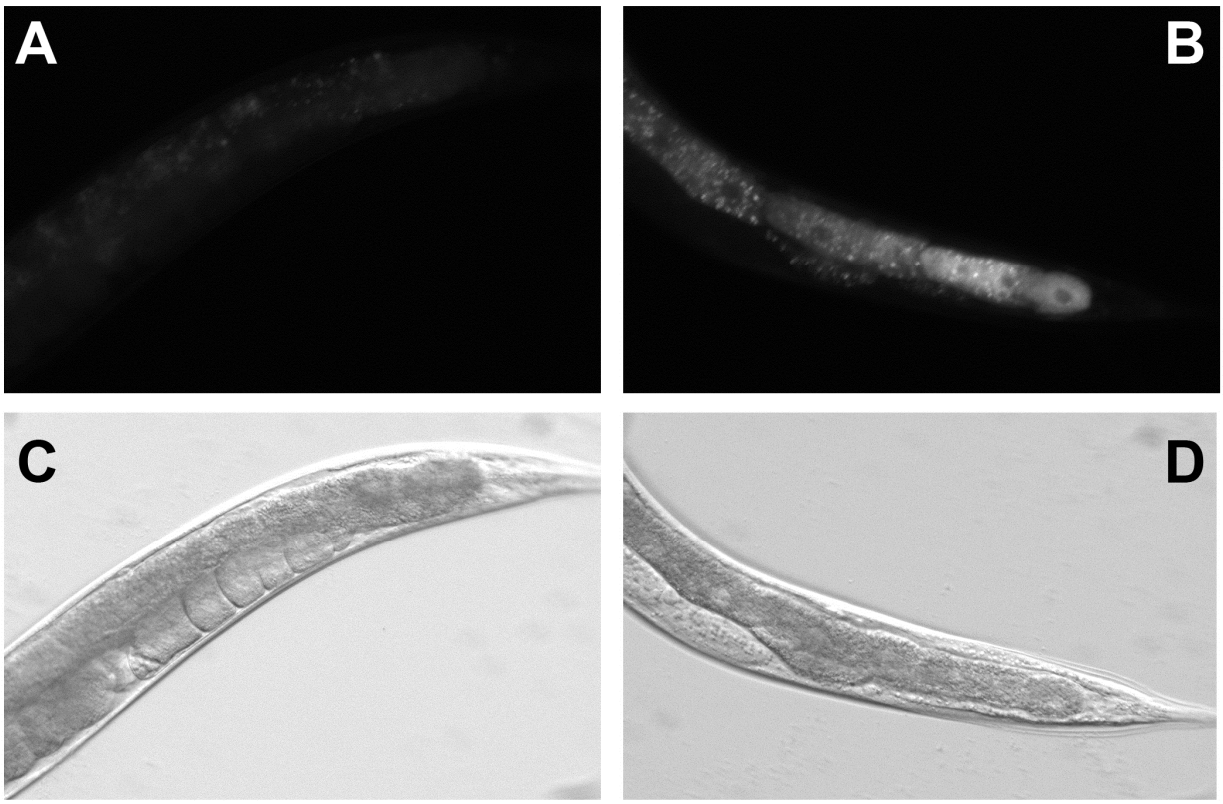

Figure 19. DDL-1/HSB-1 bimolecular fluorescence complementation assay (BiFC)
(A and C) Animals expressing MalE::VN173 and HSB-1::VC155 as negative control. *MalE* encodes a bacterial maltose binding protein that has no known molecular interaction with eukaryotic proteins. These animals produced minimal fluorescence signal. **(B and D)** Animals expressing DDL-1::VN173 and HSB-1::VC155. Strong fluorescence can be observed in the cytosolic compartment of the intestinal cells.

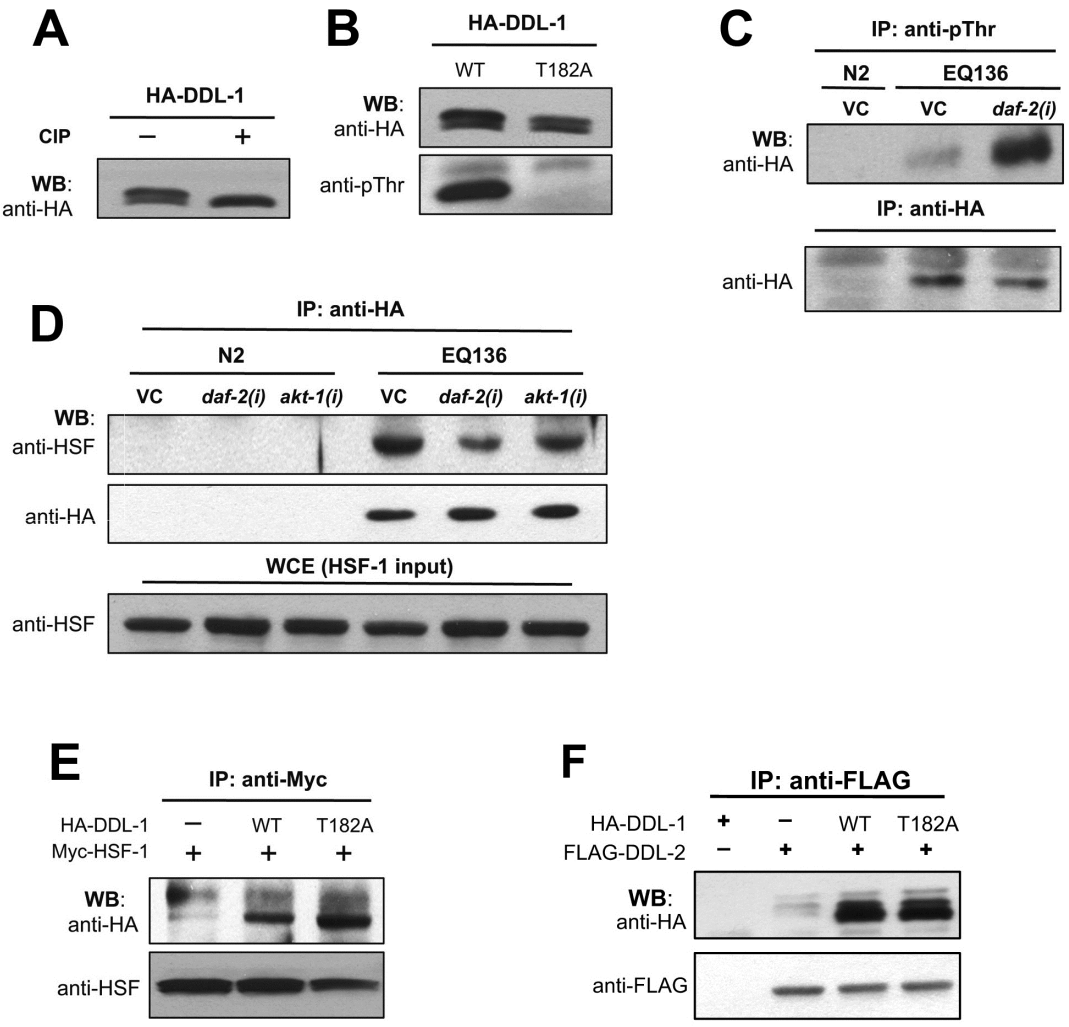

Figure 20. Both the formation of DHIC and the threonine phosphorylation of DDL-1 are regulated by insulin/IGF-like signaling [3]

(**A)** Whole-cell extracts prepared from 293T cells overexpressing HA-DDL-1 were treated with buffer or 1 U/μg protein CIP (calf intestinal alkaline phosphatase) for 1 hr. Samples were then subjected to western blot analysis (WB) with anti-HA antibodies. **(B)** Whole-cell extracts prepared from 293T cells overexpressing HA-tagged wild-type or mutated (T182A) DDL-1 were subjected to western blot analysis (WB) using anti-HA or anti-phosphothreonine antibodies. **(C)** The level of threonine-phosphorylated DDL-1 is elevated in *daf-2* mutants. WCE prepared from N2 or EQ136 worms grown on control or *daf-2* RNAi bacteria were immunoprecipitated and western blotted using indicated antibodies. **(D)** The formation of DHIC is disrupted by insulin/IGF-like signaling inactivation. Worm whole-cell extracts (WCE) prepared from N2 or EQ136 (*HA-ddl-1* o/e) adult animals grown on control, *daf-2*, *akt-1*, or a 1:1 mixture of *daf-2* and *daf-16* RNAi bacteria were subjected to immunoprecipitation (IP) and western blot analysis (WB) with indicated antibodies. The total HSF-1 input of each IP experiment was measured by blotting each WCE sample with anti-HSF1 antibodies. Quantitation is shown in (Figure 21A) **(E)** 293T cells were transfected with indicated combinations of pCMV-driven HA-DDL-1(WT), HA-DDL-1(T182A), or Myc-HSF-1 plasmids. Whole-cell extracts prepared from these cells were immunoprecipitated (IP) and subsequently western blotted (WB) using indicated antibodies. **(F)** Interaction between DDL-1 and DDL-2 is not affected by T182A mutation. 293T cells were transfected with the indicated combinations of HA-DDL-1(WT), HA-DDL-1(T182A) or Flag-DDL-2 plasmids. Protein extracts prepared from these cells were then immunoprecipitated (IP) and subsequently western-blotted (WB) using indicated antibodies.

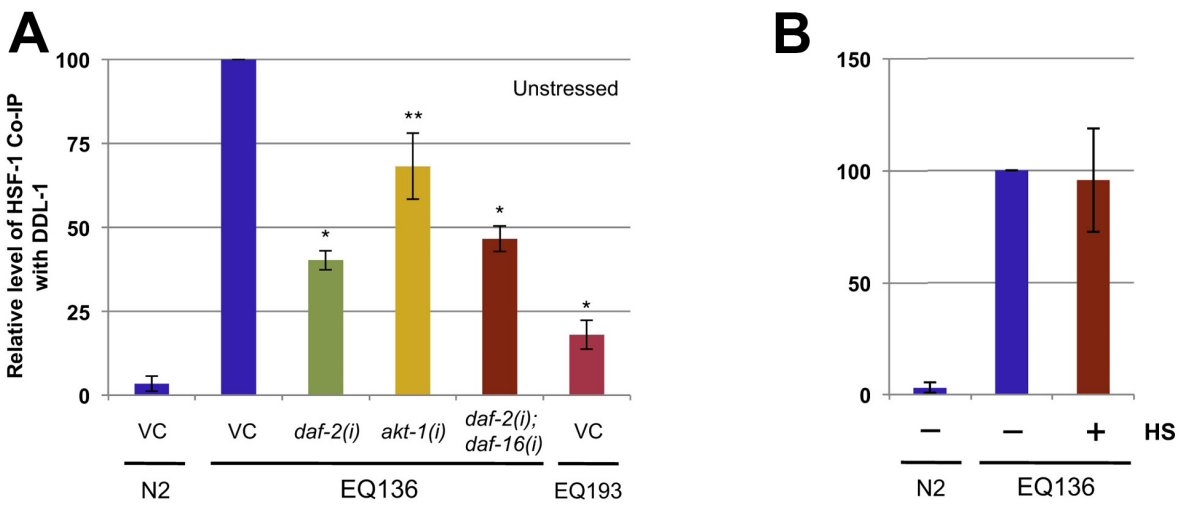

Figure 21. The formation of DHIC is altered by insulin/IGF-like signaling, HSB-1 level, but not heat stress [3]

(A and B) Worm whole cell extracts (WCE) were prepared from synchronized day 1 N2, transgenic EQ136 [*HA-ddl-1* OE], or EQ193 [*HA-ddl-1* OE in *hsb-1(cg116)* background] adult animals grown on vector control, *daf-2, akt-1,* or a 1:1 mixture of *daf-2* and *daf-16* RNAi bacteria. Animals were either unstressed (-) or heat-shocked (+) at 37°C for 90 min (HS) before being harvested. WCE were then subjected to immunoprecipitation with anti-HA antibodies and Western-blotting with anti-HSF antibodies. The total HSF-1 input of each IP experiment was measured by blotting each WCE sample with anti-HSF1 antibodies. At least three independent experiments were performed and representative immunoblots are presented in Figure 20D. Shown here is relative HSF-1 level (mean ± SD) pulled down together with HA-DDL-1. The relative HSF-1 levels were normalized against total HSF-1 input and compared to the EQ136 empty vector control (= 100). $^{*}p < 0.0001$; $^{**}p < 0.005$ when compared to the control under the same stress conditions. The difference between *daf-2(RNAi); daf-16(RNAi)* and *daf-2(RNAi)* treatments is not statistically significant ($p = 0.08$). The difference between stressed (HS) or unstressed animals (right panel) is also not statistically significant ($p = 0.76$).

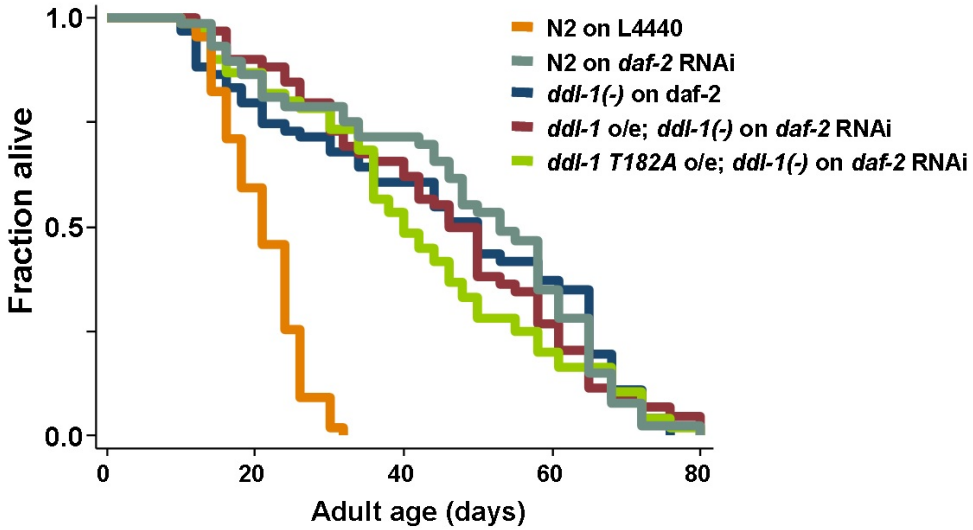

Figure 22. *ddl-1 T182A* mutation minimally impacts DAF-2 longevity

Lifespan analysis of wild-type (N2), *ddl-1(ok2916)* mutant, and *ddl-1* rescue animals grown on empty vector control or *daf-2* RNAi bacteria at 20°C. Statistics are summarized in Table 3.

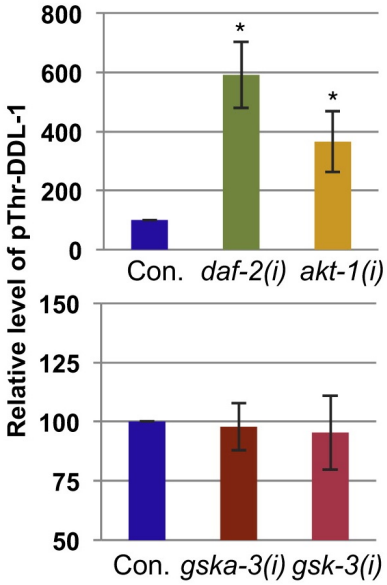

Figure 23. DDL-1 phospho-threonine level is not diminished by *gska-3*, *gsk-3* and *akt-1* inhibition [3]

Quantitation of threonine phosphorylated DDL-1 in *daf-2(RNAi)*, *akt-1(RNAi)*, *gska-3(RNAi)* and *gsk-3(RNAi)* animals. Shown here are relative levels (mean ± SD of at least three independent experiments) of threonine phosphorylated DDL-1 in WCE samples prepared from synchronized day 1 adult EQ136 or EQ97 (HA:*ddl-1*) worms fed with control or the indicated RNAi bacteria. WCE were immunoprecipitated with anti-phospho-threonine antibodies and Western-blotted with anti-HA antibodies. The relative pT182-DDL-1 levels were normalized against total DDL-1 input and compared to the empty vector control (= 100). $^{*}p < 0.01$ when compared to the vector control. $p = 0.72, 0.63$ for *gska-3* and *gsk-3* RNAi, respectively.

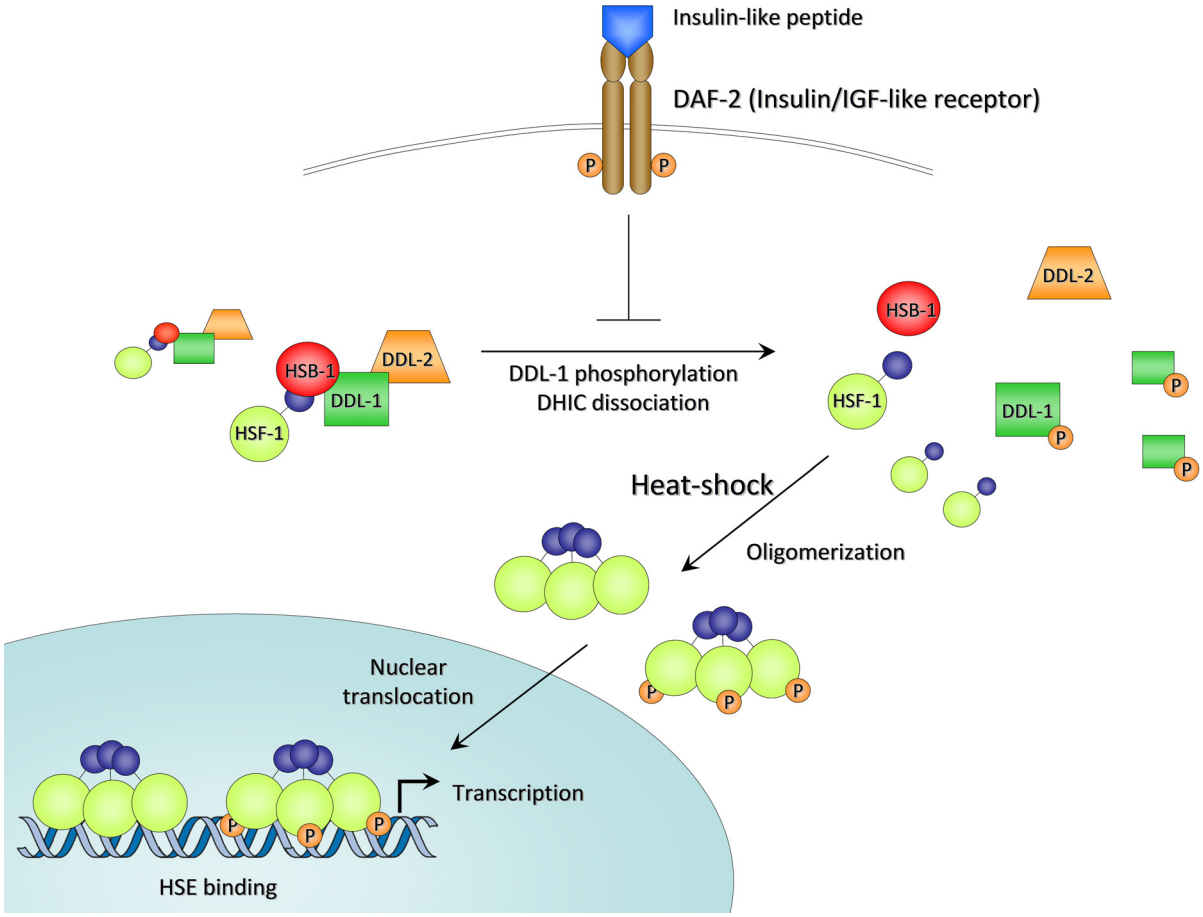

Figure 24. Model of HSF-1 activation regulated by insulin/IGF-like signaling in *C. elegans* [3]

2-7 Tables

Table 1.

Strain	Mean Lifespan ± SEM (Days)	75th Percentile (Days)	*P* Value	n
N2; control (i)	17.2 ± 0.3	21	–	67/90
N2; *ddl-1(RNAi) (i)*	19.1 ± 0.3	22	0.0034[a]	84/90
hsf-1(sy441); control	14.9 ± 0.1	16	<0.0001[a]	101/169
hsf-1(sy441); ddl-1(RNAi)	14.9 ± 0.3	17	<0.0001[a], <0.0001[b], 0.74[c]	96/170
N2; control (ii)	17.2 ± 0.2	20	–	63/82
N2; *ddl-2(RNAi) (ii)*	19.2 ± 0.2	22	0.0008[a]	68/86
hsf-1(sy441); control	13.6 ± 0.2	15	<0.0001[a]	86/156
hsf-1(sy441); ddl-2(RNAi)	13.2 ± 0.1	14	<0.0001[a], <0.0001[b], 0.26[c]	107/156
N2; control (iii)	19.1 ± 0.2	22	–	62/72
N2; *hsf-1(RNAi)*	11.2 ± 0.2	12	<0.0001[a]	46/72
hsb-1(cg116); control	30.0 ± 0.4	35	<0.0001[a]	74/84
hsb-1(cg116); hsf-1(RNAi)	11.1 ± 0.2	12	<0.0001[a], 0.78[b], <0.0001[c]	33/84
N2	17.1 ± 0.5	22	–	68/72
ddl-1(ok2916)	22.6 ± 0.2	26	<0.0001[a]	49/72
ddl-2(ok3235)	23.2 ± 0.3	26	<0.0001[a]	65/72
ddl-1(ok2916); ddl-2(ok3235)	22.5 ± 0.2	24	<0.0001[a], 0.6732[d], 0.3587[f]	63/72
N2 (i)	18.9 ± 0.2	22	–	60/72
ddl-1(ok2916)	25.1 ± 0.3	27	<0.0001[a]	65/72
hsb-1(cg116) (i)	30.3 ± 0.5	35	<0.0001[a]	62/72
hsb-1(cg116); ddl-1(ok2916)	29.9 ± 0.3	35	<0.0001[a], <0.0001[d], 0.51[e]	57/72
N2 (ii)	17.1 ± 0.4	21	–	52/72
ddl-2(ok3235)	22.6 ± 0.3	26	<0.0001[a]	32/72
hsb-1(cg116) (ii)	26.8 ± 0.4	32	<0.0001[a]	32/72

hsb-1(cg116); ddl-2(ok3235)	28.6 ± 0.4	32	<0.0001[a], 0.0026[f], 0.32[e]	31/72
N2; control (RNAi) (iv)	17.2 ± 0.6	23	–	82/90
N2; *ddl-1(RNAi) (iv)*	21.3 ± 0.5	25	0.0006[a]	81/90
N2; *ddl-2(RNAi) (iv)*	21.4 ± 0.6	28	0.0001[a]	81/90
N2; *ddl-1(RNAi); ddl-2(RNAi)*	20.9 ± 0.3	25	<0.0072[a], 0.34[g], 0.26[h]	86/90
N2; control (RNAi) (iv)	16.8 ± 0.4	19	–	61/71
N2; *ddl-1(RNAi) (iv)*	22.3 ± 0.3	25	0.0001[a]	65/75
N2; *ddl-2(RNAi) (iv)*	23.5 ± 0.2	25	0.0001[a]	66/72
N2; *ddl-1(RNAi); ddl-2(RNAi)*	24.0 ± 0.3	27	<0.0072[a], 0.0903[g], 0.63[h]	67/72

Table 1. Effects of *ddl-1*, *ddl-2*, and *hsb-1* mutations on lifespan [3]
Adult mean lifespan ± SEM in days. Lifespan experiments were carried out at 20°C. The 75th percentile is the age at which the fraction of animals alive reaches 0.25. "n" shows the number of observed deaths relative to total number of animals started. The difference between these numbers represents the number of animals censored. Animals that exploded, bagged, or crawled off the plates were censored at the time of the event. The log rank (Mantel-Cox) test was used for statistical analysis (p values).

a *p* values calculated by pairwise comparisons to N2 grown on vector control of the same experiment.
b Compared to N2 grown on the same RNAi bacteria.
c Compared to the same mutants grown on vector control.
d Compared to *ddl-1(ok2916)* mutants.
e Compared to *hsb-1(cg116)* mutants.
f Compared to *ddl-2(ok3235)* mutants.
g Compared to N2 grown on the *ddl-1* RNAi bacteria of the same experiment.
h Compared to N2 grown on the *ddl-2* RNAi bacteria of the same experiment.

Table 2.

Strain	Mean Survival ± SEM (Hours)	75th Percentile (Hours)	*P* Value	n
(i) Thermotolerance				
N2; control (i)	16.2 ± 0.3	18	–	60
N2; *ddl-1(RNAi) (i)*	19.9 ± 0.2	22	<0.0001[a]	63
N2; *ddl-2(RNAi) (i)*	20.9 ± 0.2	22	<0.0001[a]	62
N2; control (i)	16.6 ± 0.2	18	–	90
N2; *ddl-1(RNAi) (i)*	20.6 ± 0.3	24	<0.0001[a]	90
N2; *ddl-2(RNAi) (i)*	21.2 ± 0.3	24	<0.0001[a]	90
hsf-1(sy441); control (i)	14.8 ± 0.4	16	<0.0001[a]	90
hsf-1(sy441); *ddl-1(RNAi) (i)*	14.8 ± 0.3	16	0.38[c]	90
hsf-1(sy441); *ddl-2(RNAi) (i)*	15.2 ± 0.2	17	0.29[c]	90
(ii) Oxidative stress				
N2; control (i)	19.1 ± 0.2	5	–	43
N2; *ddl-1(RNAi) (i)*	11.2 ± 0.2	9	<0.0001[a]	50
N2; *ddl-2(RNAi) (i)*	30.0 ± 0.4	11	<0.0001[a]	49
N2; control (i)	17.1 ± 0.5	6	–	90
N2; *ddl-1(RNAi) (i)*	22.6 ± 0.2	10	<0.0001[a]	90
N2; *ddl-2(RNAi) (i)*	23.2 ± 0.3	8	<0.0001[a]	90

Strain	Mean Lifespan ± SEM (Days)	75th Percentile (Days)	*P* Value	n
N2; *control(RNAi)*	16.5 ± 0.3	20	–	67/81
N2; ddl-1(RNAi)	18.4 ± 0.2	20	<0.0067[a]	71/92
hsf-1(sy441; *control(RNAi)*	13.5 ± 0.2	15	<0.0001[a]	85/106
hsf-1(sy441); ddl-1(RNAi)	13.2 ± 0.2	15	<0.0001[a], <0.0001[b], 0.51[c]	88/111
N2; *control(RNAi)*	17.2 ± 0.1	19	–	68/90
N2; ddl-1(RNAi)	19.5 ± 0.1	21	<0.0001[a]	80/90
hsf-1(sy441; *control(RNAi)*	13.1 ± 0.2	16	<0.0001[a]	94/120

hsf-1(sy441); ddl-1(RNAi)	13.5 ± 0.2	16	<0.0001[a], <0.0001[b], 0.51[c]	88/120
N2; *control(RNAi)*	18 ± 0.3	21	–	67/90
N2; ddl-2(RNAi)	20.2 ± 0.3	23	0.0003[a]	81/95
hsf-1(sy441); *control(RNAi)*	14.9 ± 0.2	16	<0.0001[a]	101/130
hsf-1(sy441); ddl-2(RNAi)	15.4 ± 0.2	17	<0.0001[a], <0.0001[b], 0.19[c]	85/111
N2; *control(RNAi)*	17.2 ± 0.1	19	–	68/90
N2; ddl-2(RNAi)	19.9 ± 0.1	23	<0.0001[a]	85/90
hsf-1(sy441); *control(RNAi)*	13.1 ± 0.2	16	<0.0001[a]	94/120
hsf-1(sy441); ddl-2(RNAi)	13.1 ± 0.2	16	<0.0001[a], <0.0001[b], 0.89[c]	102/120
N2; *control(RNAi)*	18.5 ± 0.2	21	–	73/84
N2; hsf-1(RNAi)	11.2 ± 0.2	14	<0.0001[a]	59/84
hsb-1(cg116); *control(RNAi)*	29.6 ± 0.5	37	<0.0001[a]	75/84
hsb-1(cg116); hsf-1(RNAi)	11.2 ± 0.2	12	<0.0001[a], 0.61[b], <0.0001[c]	52/84
N2; *control(RNAi)*	18.8 ± 0.2	22	–	72/84
N2; hsf-1(RNAi)	10.4 ± 0.2	12	<0.0001[a]	65/84
hsb-1(cg116); *control(RNAi)*	31.1 ± 0.5	37	<0.0001[a]	54/84
hsb-1(cg116); hsf-1(RNAi)	10.8 ± 0.2	12	<0.0001[a], 0.33[b], <0.0001[c]	78/84
N2	19.0 ± 0.5	22	–	68/72
ddl-1(ok2916)	23.4 ± 0.3	26	<0.0001[a]	66/72
hsb-1(cg116)	29.1 ± 0.5	36	<0.0001[a]	57/72
hsb-1(cg116); *ddl-1(ok2916)*	28.1 ± 0.4	32	<0.0001[a], 0.0003[d], 0.68[e]	28/72
N2	18.2 ± 0.3	22	–	74/80
ddl-1(ok2916)	24.1 ± 0.2	26	<0.0001[a]	75/80
hsb-1(cg116)	30.8 ± 0.4	34	<0.0001[a]	73/80
hsb-1(cg116); *ddl-1(ok2916)*	29.2 ± 0.4	32	<0.0001[a], 0.0003[d], 0.51[e]	75/80
N2	19.5 ± 0.4	22	–	71/77

ddl-2(ok3235)	24.0 ± 0.2	25	<0.0001[a]	65/78
hsb-1(cg116)	27.8 ± 0.3	32	<0.0001[a]	58/78
hsb-1(cg116); *ddl-2(ok3235)*	29.2 ± 0.3	32	<0.0001[a], 0.0001[f], 0.078[e]	63/77
N2	17.1 ± 0.5	22	−	71/77
ddl-2(ok3235)	21.8 ± 0.3	25	<0.0001[a]	65/78
hsb-1(cg116)	26.2 ± 0.5	32	<0.0001[a]	58/78
hsb-1(cg116); *ddl-2(ok3235)*	27.9 ± 0.7	32	<0.0001[a], 0.0001[f], 0.078[e]	63/77
N2	16.8 ± 0.4	22	−	71/77
ddl-2(ok3235)	22.3 ± 0.3	25	<0.0001[a]	65/78
hsb-1(cg116)	23.5 ± 0.2	32	<0.0001[a]	58/78
hsb-1(cg116); *ddl-2(ok3235)*	24.0 ± 0.3	32	<0.0001[a], 0.0001[f], 0.078[e]	63/77

Table 2. Effects of *ddl-1*, *ddl-2*, and *hsb-1* mutations on stress resistance and lifespan [3]
For stress resistance analysis (*i-ii*), N2 animals grown on vector control, *ddl-1* RNAi, or *ddl-2* RNAi bacteria were exposed to heat (35°C) or oxidative stress (300 mM paraquat). Mean survival SEM, in hours, observed in the stress analysis was shown in the table. 75th percentile is the time at which the fraction of animals alive reaches 0.25. 'n' indicates the number of animals scored in the each experiment. For lifespan analysis, the experiments were carried out at 20°C. All experiments were repeated 3 times (shown in Table 1 and here). Each set of repetitions was carried out independently and shown here in separate groups. 75th percentile is the age at which the fraction of animals alive reaches 0.25. 'n' shows the number of observed deaths relative to total number of animals started at day 1. The difference between these numbers represents the number of animals censored during the experiment.

a *p*-Values calculated by pair-wise comparisons to N2 grown on vector control of the same experiment.
b *p*-Values calculated by pair-wise comparisons to N2 grown on the same RNAi bacteria.
c *p*-Values calculated by pair-wise comparisons to the same mutants grown on vector control.
d *p*-Values calculated by pair-wise comparisons to *ddl-1(ok2916)* mutants.
e *p*-Values calculated by pair-wise comparisons to *hsb-1(cg116)* mutants.
f *p*-Values calculated by pair-wise comparisons to *ddl-2(ok3235)* mutants.

We used Stata 8 software for statistical analysis and to determine means and percentiles. The logrank (Mantel-Cox) test was used to test the hypothesis that the survival functions among groups were equal.

Table 3.

Strain	Mean Lifespan ± SEM (Days)	75th Percentile (Days)	*P* Value	n
N2	16.2 ± 0.3	19	-	61/71
hsf-1::gfp (OE)	22.1 ± 0.3	25	<0.0001[a]	62/69
myc::hsf-1 (OE)	21.0 ± 0.2	24	<0.0001[a]	63/72
N2	19.6 ± 0.3	22	-	75/80
hsf-1::gfp (OE)	24.5 ± 0.4	29	<0.0001[a]	73/80
myc::hsf-1 (OE)	23.8 ± 0.5	29	<0.0001[a]	76/80
N2	15.9 ± 0.5	21	-	51/58
hsf-1(sy441)	13 ± 0.2	15	0.0001[a]	52/89
hsf-1(sy441);hsf-1::gfp (OE)	19 ± 0.4	23	0.0006[a], <0.0001[b]	79/91
N2	17.4 ± 0.5	21	-	79/83
hsf-1(sy441)	12.5 ± 0.2	15	0.0001[a]	64/83
hsf-1(sy441);hsf-1::gfp (OE)	19.5 ± 0.4	23	0.027[a], <0.0001[b]	71/81
N2	19.6 ± 0.3	22	–	61/72
HA::ddl-1(OE)	19.7 ± 1.0	26	0.028[a]	66/72
N2	17.1 ± 0.6	21	–	52/72
Flag::ddl-2(OE)	17.8 ± 0.6	21	0.47[a]	60/72
N2	18.9 ± 0.4	22	–	60/72
HA::ddl-1(OE);Flag::ddl-2(OE)	16.9 ± 0.6	20	0.059[a]	62/72
N2	21.6 ± 0.5	28	–	56/72
HA::ddl-1(OE)	20.2 ± 0.6	28	0.67[a]	65/72
Flag::ddl-2(OE)	21.2 ± 0.7	28	0.71[a]	62/72
N2	19.8 ± 0.4	22	–	70/90
HA::ddl-1(OE)	19.1 ± 0.5	24	0.71[a]	66/76
Flag::ddl-2(OE)	18.3 ± 0.5	22	0.21[a]	61/75
HA::ddl-1(OE);Flag::ddl-2(OE)	18.2 ± 0.5	22	0.21[a]	59/90
N2	19.9 ± 0.4	23	–	61/73
ddl-1(ok2916)	24.8 ± 0.3	28	<0.0001[a]	57/70
ddl-1(ok2916); HA::ddl-1(OE)	19.5 ± 0.5	25	0.62[a]	65/72
N2	20.0 ± 0.5	24	–	60/72
ddl-1(ok2916)	24.4 ± 0.3	28	<0.0001[a]	63/72

ddl-1(ok2916); HA::ddl-1(OE)	19.5 ± 0.6	24	0.90[a]	64/72
N2; control (RNAi)	21.0 ± 0.5	26	–	58/72
N2; *daf-2*(RNAi)	48.3 ± 1.4	65	<0.0001[a]	47/72
ddl-1(ok2916); *daf-2*(RNAi)	45.1 ± 1.6	65	<0.0001[a]	51/72
ddl-1(ok2916); HA::ddl-1(OE); daf-2 (RNAi)	45.9 ± 1.0	61	<0.0001[a], 0.7836[c]	53/84
ddl-1(ok2916); HA::ddl-1 T182A(OE); daf-2(RNAi)	42.4 ± 1.6	58	<0.0001[a], 0.3765[c], 0.3709[d]	58/84

Table 3. Effects of *ddl-1*, *ddl-2*, and *hsf-1* overexpression on lifespan [3]
Adult mean lifespan SEM, in days, observed in lifespan analysis. Lifespan experiments were carried out at 20°C. 75th percentile is the age at which the fraction of animals alive reaches 0.25. 'n' shows the number of observed deaths relative to total number of animals started at day 1. The difference between these numbers represents the number of animals censored during the experiment. All experiments were repeated at least 2 times. Each set of repetitions was carried out independently and shown here in separate groups.

a *p*-Values calculated by pair-wise comparisons to N2 control of the same experiment.
b *p*-Values calculated by pair-wise comparisons to *hsf-1(sy441)* mutants.
c *p*-Values calculated by pair-wise comparisons to *ddl-1(ok2916); daf-2 RNAi* animals
d *p*-Values calculated by pair-wise comparisons to *ddl-1(ok2916); HA-ddl-1(OE); daf-2 RNAi* animals

We used Stata 8 software for statistical analysis and to determine means and percentiles. The logrank (Mantel-Cox) test was used to test the hypothesis that the survival functions among groups were equal.

2-8 Contributions

Figure 10: All data were performed by Dr. Tsui-Ting Ching.

Figure 11 and Figure 13: RT-PCR experiments were performed by Dr. Hee-Chul Lee.

Figure 14 A-C: HSF-1 nuclear translocation assay are performed by Dr. Ao-Lin Hsu and EMSA were performed by Dr. Tsui-Ting Ching.

Figure 19: Photographs were taken by Dr. Tsui-Ting Ching.

Chapter 3. *C. elegans* SIRT6/7 homolog SIR-2.4 promotes DAF-16 relocalization and function during stress[†].

3-1 Abstract

FoxO transcription factors and sirtuin family deacetylases/ADP-ribosyl-transferases regulate diverse biological processes, including stress responses, metabolism and longevity. We show that the *C. elegans* sirtuin SIR-2.4 – a homolog of the mammalian SIRT6 and SIRT7 proteins – is required for stress responses to heat shock, oxidative insult, and proteotoxicity. It has been previously known that multiple stresses promote nuclear translocation and activation of FoxO transcription factor DAF-16, which directs the transcriptional program controlling metabolism, longevity, and stress resistance. In this study, we found that SIR-2.4 is required for stress-induced DAF-16 nuclear localization and DAF-16 dependent gene expression, indicating that SIR-2.4 may play an important role in modulating DAF-16 function in response to stress.

We investigated the mechanism by which SIR-2.4 regulates DAF-16 activity. Surprisingly, deacetylase/ADP-ribosyltransferase catalytic activity of SIR-2.4 is not required for DAF-16 nuclear accumulation under stress conditions. Our biochemical analysis showed that the level of CBP-dependent DAF-16 acetylation is inhibited by both wild-type and catalytic null SIR-2.4 mutant, indicating that SIR-2.4 modulates DAF-16 indirectly. We

[†] The data from this chapter has been published in: Chiang et. al., *C. elegans* SIRT6/7 homolog SIR-2.4 promotes DAF-16 relocalization and function during stress. PLoS Genet 8: e1002948.

also found evidence to suggest that SIR-2.4 may modulate DAF-16 activity by blocking the CBP-dependent DAF-16 acetylation. Overall, our findings establish an important role for SIR-2.4 in regulating DAF-16 upon stress, and demonstrate a novel mechanism by which SIR-2.4 and CBP modulate DAF-16 activity under stress conditions.

3-2 Introduction

Sirtuins comprise an evolutionally conserved family of proteins that possess histone deacetylase and mono-ribosyltransferase activity. This class of proteins is known to function in the regulation of diverse biological processes including longevity, stress response, metabolism, and cancer. Acetylation is an important way to modulate protein functions. Similar to phosphorylation, acetylation of a protein can alter its function (e.g., DNA binding, transcriptional activity, protein stability, localization, and enzyme activity). Sirtuins are a class of protein deacetylases that catalyze the removal of acetyl groups from lysine residues, although it is recently found that some sirtuins do not act as deacetylase . Unlike many other deacetylases, such as class I, IIA, IIB and IV histone deacetylases (HDACs), sirtuins require NAD^+. The dependence of NAD^+ links sirtuin activity to cellular energy status, via the ratio of NAD^+/NADH. Indeed, recent studies have shown that sirtuins act as key metabolic sensors that directly link nutritional status and environment signals to metabolic homeostasis [109]. Although sirtuins were originally identified as histone deacetylases, the deacetylation of histones is not the only mechanism for sirtuins to modulate cellular functions. Various mammalian transcription factors have been shown to be the substrates of sirtuins. In many cases, deacetylation of a transcription factor is usually associated with transcriptional activation rather than inhibition.

As previously suggested, sirtuin genes are involved in the regulation of longevity in yeast, flies, worms, and likely in mice [55-58], indicating an evolutionally ancient role of sirtuins in longevity assurance. Extension of lifespan by overexpressing sirtuins was first reported in yeast. Soon after, similar effects were also observed in flies and worms. In yeast, the strain carrying duplicated copy of the SIR2 gene showed around a 30% increase in lifespan. In flies, overexpression of dSIR2 leads to lifespan extension up to 57%. In worms, overexpression of *sir-2.1* leads to increased longevity in a *daf-16*-dependent manner. However, some of these findings have recently been challenged [59,110]. It has been found that lifespan extension by sirtuins overexpression in flies and worms was the result of genetic background. Thus, the role of sirtuins in longevity regulation in flies and worms remains controversial.

Recent studies indicate that sirtuin may mediate the beneficial effect of caloric restriction, a dietary regime known to promote longevity in many organisms ranging from yeast to mammals [111-113]. Sirtuins have been linked to the insulin/IGF signaling pathway to regulate FoxO activity in many systems. In mammals, SIRT1 has been shown to activate FoxO during oxidative stress [60]. SIRT2 is known to regulate FoxO activity to inhibit adipocyte differentiation [61,62]. Both SIRT1/2 are known to directly deaceylate FoxO. However, in *C. elegans*, whether DAF-16 is regulated by sirtuins via deacetylation is unknown.

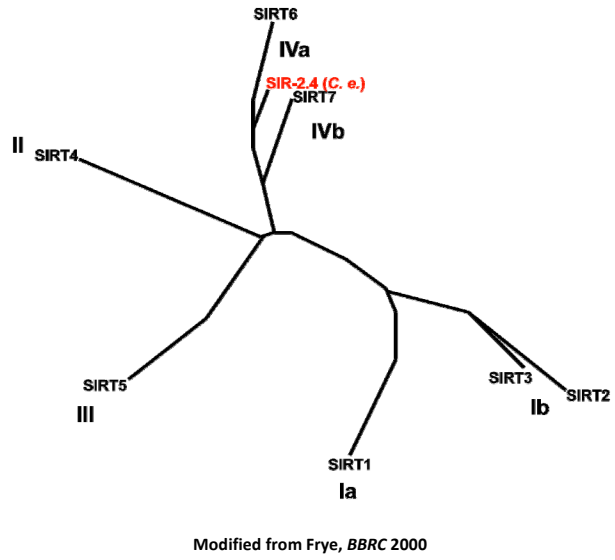

Mammalian	*C. elegans*
SIRT1	SIR-2.1
SIRT2	———
SIRT3	———
SIRT4	SIR-2.2/2.3
SIRT5	———
SIRT6	SIR-2.4
SIRT7	SIR-2.4

Figure 25. Phylogenetic classification of *C. elegans* and mammalian sirtuins [4]

In *C. elegans,* there are four putative sirtuin-like genes, SIR-2.1 to SIR-2.4. SIR-2.1 has been shown to regulate metabolism and stress response. While SIR-2.1 has been extensively studied, very little is known about the biological functions and characteristics of other worm sirtuins. In this study, we attempted to characterize the function of SIR-2.4, a homolog of mammalian SIRT6/7 (Figure 25). SIRT6 has been implicated in DNA repair, metabolism and aging. SIRT6-deficient cells showed increased sensitivity to certain forms of genotoxic damage and increased genome instability. Mice lacking SIRT6 have prominent metabolic defects including hypoglycemia, low insulin, and low IGF1 levels, while possessing degenerative syndrome mimicking models of accelerated aging [114]. In this study, we found that SIR-2.4 plays a key role in promoting resistance against heat, oxidative and proteotoxic stress. SIR-2.4 is required for a proper onset of stress-induced DAF-16 nuclear translocation and activation. The overexpression or inactivation of SIR-2.4 does not alter the lifespan of wild-type animals, and it does not play a significant

role in the insulin/IGF-like signaling-mediated DAF-16 nuclear accumulation, longevity, and dauer formation. Overall, our findings suggested that SIR-2.4 primarily functions in stress response and is largely independent of the DAF-2 pathway. Further analysis showed that SIR-2.4 regulates DAF-16 through blocking CBP (CREB-binding protein)-dependent DAF-16 acetylation through a catalytic activity-independent manner. Together, these findings demonstrated that SIR-2.4 is a critical mediator of stress responses through a DAF-16-dependent pathway, and revealed a novel mechanism by which sirtuins regulate FoxO functions.

3-3 Material and Methods

C. elegans Strains

CF1041: *daf-2(e1370)III,*

TJ356: *zIs356 [daf-16::gfp + rol-6],*

AM140: *rmIs132[unc-54p::Q35::yfp],*

MT18068: *sir-2.4(n5137)I,*

EQ137: *iqEx47 [sir-2.4p::sir-2.4::gfp + rol-6],*

EQ158: *iqEx50 [sir-2.4p::sir-2.4 + myo-3p::rfp],*

EQ200: *sir-2.4(n5137)*I; *zIs356* [*daf-16::gfp* + *rol-6*],

EQ205: *sir-2.4(n5137)I; zIs356 [daf-16::gfp + rol-6]; iqEx59*

[sir-2.4p::sir-2.4NA + myo-3p::rfp],

EQ211: *sir-2.4(n5137)I; zIs356 [daf-16::gfp + rol-6]; iqEx60*

[sir-2.4p::sir-2.4 + myo-3p::rfp].

All strains used were maintained and handled as described previously [115]. TJ356,

AM140 and CF1041 were obtained from the Caenorhabditis Genetic Center. For the generation of transgenic animals, plasmid DNA mixes were injected into the gonad of young adult hermaphrodite animals, using the standard method described previously. F_1 progeny were selected on the basis of the roller phenotype. Individual F_2 progenies were isolated to establish independent lines. For the generation of the EQ137 (SIR-2.4::GFP overexpressor) strain, plasmid DNA containing a mixture of 100 ng/µl of *sir-2.4p::sir-2.4::gfp* and 50 ng/µl of pRF4 (*rol-6*) constructs was injected into N2 animals. For the generation of EQ158 (native SIR-2.4 overexpressor), plasmid DNA containing a mixture of 30 ng/µl of native *sir-2.4* driven by its own promoter and 50 ng/µl of coinjection marker *myo-3p::rfp* was injected into N2 animals. For the generation of EQ211, plasmid DNA containing a mixture of 30 ng/µl of *sir-2.4p::sir-2.4* and 80 ng/µl of *myo-3p::rfp* constructs was injected into TJ356 animals. For the generation of EQ205, plasmid DNA containing a mixture of 30 ng/µl of *sir-2.4p::sir-2.4NA* and 80 ng/µl of *myo-3p::rfp* constructs was injected into TJ356 animals.

RNA-interference (RNAi) Experiments

HT115 bacteria transformed with RNAi vectors (L4440) expressing dsRNA of the genes indicated were grown at 37ºC in LB with 10 mg/ml tetracycline and 50 mg/ml carbenicillin, then seeded onto NG-carbenicillin plates and supplemented with 100 µl 0.1M IPTG. The *sir-2.4* RNAi construct was generated by cloning nucleotides 1-467 of the *sir-2.4* cDNA into the L4440 vector. The identity of all RNAi clones was verified by sequencing the inserts using M13 forward primer. Eggs were added to plates and transferred to new plates every 3-6 days.

sir-2.4 Deletion Mutant Analysis

The deletion in a *sir-2.4* mutant strain (kind gift of the Horvitz laboratory) was mapped by PCR, and found to encompass 1,929 bp of chromosome I (5990775-5992703), which encodes nucleotides 28-879 of the SIR-2.4 (C06A5.11) spliced mRNA.

DAF-16 Nuclear Localization Assay

For quantification of DAF-16::GFP localization, synchronized eggs from TJ356 animals (i.e. transgenic animals expressing DAF-16::GFP) or other strains as indicated were seeded onto either vector control or appropriate RNAi plates. For stress response experiments, day 1 adults were washed with M9 three times and transferred to new 20 plates or and subjected to heat shock (35°C) or oxidative stress (1.5 mM H_2O_2 in M9). GFP localization was then analyzed using an Olympus BX61 fluorescent microscope at 40x or 100x magnification. For time-course analysis, worms were scored for the presence or absence of GFP accumulation within the nuclei of head hypodermis cells (n= 30~50) in a blinded fashion every 5-30 min. An animal was scored as having nuclear GFP if more than one head hypodermic nucleus contained DAF-16::GFP. For single time point experiments, worms were blindly scored for the presence or absence of GFP accumulation within the nuclei of indicated cells (n = 120 or greater). *P* values were calculated by Poisson regression (time-course assays) or chi-square test (single time point assays).

Quantitative RT-PCR Analysis

Total RNA was isolated from approximately 5,000 day 1 adult worms, and cDNA was generated from 5 µg of RNA using Superscript III RT (Invitrogen). Real-time qRT-PCR

experiments were performed using the Power SYBR Green PCR Master mix (Applied Biosystems) and the Chromo 4 system (MJ Research). Relative mRNA level of the genes of interest were calculated and normalized against an internal control (*act-1*; worm β-actin). Primer sequences were (all 5'-3'):

sod-3 (GTTTCAGCGCGACTTCGGTTCCCT, CGTGCTCCCAAACGTCAATTCCAA);

dod-3 (AAAAAGCCATGTTCCCGAAT, GCTGCGAAAAGCAAGAAAAT);

dod-24 (TGTCCAACACAACCTGCATT, TGTGTCCCGAGTAACAACCA);

C32H11.4 (TTACTTCCCATCGCCAAAGT, CAATTCCGGCGATGTATGAT);

hsp-16.1 (GATCAAAAGTTTGCCATAAATCTC, TTCAGTCTTTAATTCTTGTTCTCC);

ins-7 (TCGTTGTGGAAGAAGAATACATTC, TTAAGGACAGCACTGTTTTCG); and

act-1 (CTACGAACTTCCTGACGGACAAG, CCGGCGGACTCCATACC).

Stress Assay

For thermotolerance assays, eggs from N2 worms were transferred to plates seeded with vector control, *daf-16* RNAi, or *sir-2.4* RNAi bacteria and grown to day 1 of adulthood. Worms were then transferred to plates without any food and heat-shocked at 35°C. Viability was determined at the indicated time points; death was determined by the lack of movement after prodding. For oxidative stress assays, eggs from N2 worms were transferred to plates seeded with vector control, *daf-16* RNAi, or *sir-2.4* RNAi bacteria and grown to day 3 of adulthood. Worms were then transferred to 24-well plates and soaked in 1.5 mM H_2O_2 in M9 media. Viability was determined at the indicated timepoints as above. For stress assays, a Kaplan−Meier survival analysis with a log-rank test was performed, and a *P*-value of 0.05 was considered statistically significant.

Paralysis Assay

Synchronized eggs from AM140 animals (i.e. transgenic animals expressing Q35::YFP) were seeded on either vector control or the indicated RNAi bacteria. Animals were scored for polyQ-induced paralysis every other day during adulthood. Paralyzed worms were identified as those failing to make forward or backward movement in response to stimulation by plate-tapping and tail-prodding; these worms still exhibited pharyngeal pumping. For the paralysis assay, a Kaplan−Meier survival analysis with a log-rank test was performed.

Lifespan Analysis

Lifespan analysis were conducted at 20°C as described previously [100,116]. Strains were grown at 20°C for at least two generations without starvation prior to lifespan analysis. At least 72 worms were used for each experiment. In all experiments, the pre-fertile period of adulthood was used as t = 0 for lifespan analysis. Stata 9 software was used for statistical analysis to determine the means and percentiles. In all cases, *P*-values were calculated using the log-rank (Mantel-Cox) method.

Assessment of DAF-16 Acetylation in Worms

~15,000 synchronized day 1 adult worms grown at 20ºC were harvested by washing three times with cold M9 buffer with 0.01% Triton X-100 and once with HB-high salt buffer (10 mM HEPES, pH 7.9; 10 mM KCl; 1.5 mM $MgCl_2$; 0.1 mM EDTA; 0.5 mM EGTA; 44 mM Sucrose; 100 mM NaCl; 0.5 % Triton X-100). Worm pellets were then resuspended in 3X volume of HB-high salt buffer supplemented with Protease Inhibitor Cocktail Complete (Roche), 20 mM β-glycerophosphate, 1 mM sodium orthovanadate, 1

mM nicotinamide and 1 μM trichostatin A. Pellets were immediately frozen and stored in liquid nitrogen. Frozen suspensions were thawed, homogenized with a Dounce homogenizer (30 strokes with pestle B), and centrifuged at 14,000xg at 4 ºC for 20 minutes. Supernatants were collected and total protein concentrations were quantified by Bradford assay. For immunoprecipitation, 30 μl of anti-acetyl-lysine agarose beads (Immunechem; ICP0388) were added to 1 mg of protein extract with 100 μg/ml of ethidium bromide and incubated with gentle shaking at 4ºC overnight. The beads were then washed 3 times with HB-high salt buffer supplemented with 50 mg/ml ABESF, 1 mM sodium orthovanadate, 1 mM nicotinamide and 1 μM trichostatin A. before being subjected to western blot analysis. The samples were subjected to SDS-PAGE and transferred to a PVDF membrane (Millipore). The membrane was washed three times with TBS containing 0.1% Tween 20 (TBST). After blocking with TBST containing 5% nonfat milk for 60 min, the membrane was incubated with the primary antibody indicated (e.g. anti-GFP, Abcam, #AB6556) at 4°C for 12 h and washed three times with TBST. The membrane was then probed with HRP-conjugated secondary antibody for 1 h at room temperature and washed with TBST three times. Finally, the immunoblots were developed using a chemiluminescent substrate (Millipore) and visualized by autoradiography.

Assessment of SIR-2.4/DAF-16 Interaction

10 cm dishes of HEK293T cells were transfected using TransIT-293 (Mirus) with plasmids encoding HA-tagged DAF-16 (1 μg), FLAG-tagged SIR-2.4 (9 μg), both DAF-16 and SIR-2.4 plasmids together, or a plasmid encoding GFP (5 μg), to assess transfection efficiency. Cells were harvested 48 hours post transfection, and were lysed

by rotation at 4°C for 20 minutes in lysis buffer (LB; 150 mM NaCl, 1% Triton X-100, 0.5% NP40, 50 mM Tris pH 7.4, 10% glycerol, with Protease Inhibitor Cocktail Complete-EDTA free (Roche), followed by brief sonication. 1 mg of whole cell extract from each cell line was pre-cleared by slow rotation with 50 μl of protein G conjugated agarose beads. For immunoprecipitation, either 25 μl of M2-agarose beads (Sigma) (anti-FLAG IP) or 25 μl of anti-HA-agarose beads (Roche) (anti-HA IP) was added to pre-cleared WCE, and IPs were incubated overnight by slow rotation at 4°C. After incubation, beads were pelleted and washed three times in LB. FLAG-tagged proteins were eluted in 80 μl of FLAG elution buffer (150 ng/μl 3xFLAG peptide (Sigma), 10 mM Tris-HCl (pH 8.0) and 150 mM NaCl) at 4°C for 4 hours. 40 μl of eluate was loaded on an SDS-PAGE gel. For HA IPs, 80 μl of Laemmli buffer was added to the anti-HA-agarose beads, and beads were boiled at 100°C for 5 minutes; 40 μl was loaded on a gel. DAF-16 and SIR-2.4 interaction was assessed by immunoblot using anti-DAF-16 (Santa Cruz) or anti-HA antibodies.

In vitro DAF-16 Acetylation Assay

3xFLAG tagged DAF-16, CBP or SIR-2.4 were each transfected and expressed in 293T cells. These proteins were then purified with Anti-FLAG M2 Affinity Gel (Sigma, A2220). 0.5 μg of purified DAF-16 was incubated with 0.2 μg of purified CBP with or without 0.5 μg of purified SIR-2.4 in the presence of HAT buffer (50 mM Tris-HCl, pH 8.0, 0.1 mM EDTA, 1 mM dithiothreitol, 10% glycerol) supplemented with 200 μM of acetyl-CoA. The reactions were incubated at 37ºC for 3 hours and analyzed by western blot. Acetylated DAF-16 was queried with anti-acetyl-lysine antibody (Immunechem; ICP0380) and total level of DAF-16 were assessed with anti-FLAG antibody (Sigma, #F3165).

3-4 Results

3-4-1 SIR-2.4 promotes DAF-16 nuclear translocation and function

Previous studies in mammals showed that FoxO activity is subject to regulation by sirtuins. We therefore tested the potential role of SIR-2.4 in DAF-16 subcellular localization and function. We created RNAi construct expressing dsRNA of *sir-2.4* cDNA (generated by Bo Yang in Dr. David Lombard's lab) and tested the effect of SIR-2.4 inactivation in wild-type N2 animals. Under basal conditions, inactivation of SIR-2.4 by RNAi had no obvious effect on DAF-16::GFP localization. However, *sir-2.4* knockdown led to a significant decrease in DAF-16::GFP nuclear translocation upon both oxidative and heat stress (Figure 26A and B), indicating that stress-induced DAF-16 nuclear translocation is impaired by the inactivation of SIR-2.4. We also verified this phenotype with a mutant carrying *sir-2.4(n5137)* allele. This mutant allele contains a deletion that encompasses almost the entire *sir-2.4* open reading frame, leaving only nine N-terminal amino acids of SIR-2.4 open reading frame. This strain is viable and has no distinguishable morphological defects. Similar to *sir-2.4* RNAi knockdown, *sir-2.4* deletion did not alter DAF-16::GFP localization in unstressed conditions, but showed apparent defect in stress-induced DAF-16::GFP translocation (Figure 26C). In addition, we noticed that in either *sir-2.4* RNAi or deletion mutants, DAF-16 did eventually translocate into the nucleus after prolonged stress exposure, indicating that inactivation of SIR-2.4 delays but does not prevent stress-induced DAF-16 translocation.

To verify this observation, we scored for DAF-16::GFP nuclear translocation on *sir-2.4* deletion animals at different time points following stress induction. Time-course

experiments showed that *sir-2.4* deletion resulted in a right-shifted stress response curve upon oxidative stress (Figure 26 D, $p<0.001$ by Poisson regression analysis) and heat shock (Figure 26E, $p<0.001$), confirming that the inactivation of SIR-2.4 delays the onset of stress-induced DAF-16::GFP nuclear translocation. This finding implies that SIR-2.4 may play a crucial role in modulating DAF-16 nuclear translocation, particularly at an early phase of stress response.

DAF-16 is a transcription factor known to regulate the expression of many genes that function in longevity, metabolism, and stress response. To investigate whether SIR-2.4 regulates DAF-16 function, we examined the mRNA expression level of two groups of genes previously identified as DAF-16 targets: class I (positively regulated by DAF-16) and class II (negatively regulated by DAF-16) by quantitative RT-PCR. SIR-2.4 knockdown by RNAi led to a decreased level in mRNA expression of class I genes (*sod-3*, *hsp-16.1* and *dod-3*) under both stress and non-stress conditions (Figure 27, top). Conversely, class II genes (*dod-24*, *C32H11.4* and *ins-7*) showed a significant increase in mRNA expression in *sir-2.4* knockdown animals (Figure 27, bottom) under both conditions. These findings suggested that DAF-16 transcriptional activity is subject to regulation by SIR-2.4.

3-4-2 SIR-2.4 is required for resistance against multiple stressors

DAF-16 is a well-known regulator for stress response [117-119]. The transcriptional targets of DAF-16 includes a large number of genes playing a critical role in cellular response to heat-shock response, oxidative damage, as well as innate immunity against bacterial infection. Thus, we tested whether the inactivation of SIR-2.4 would have any

effect on stress resistance. We challenged *sir-2.4* knockdown or deletion worms with heat-shock (35°C) or oxidative insult (1.5 mM H_2O_2) and monitored their survival. As compared to wild-type animals, *sir-2.4* knockdown or deletion rendered these animals considerably more sensitive to heat or oxidative stress (Figure 28A and B, Table 4). Moreover, simultaneous inhibition of *daf-16* and *sir-2.4* produced stress sensitivity to the extent similar to that of *daf-16* alone (Figure 28A and B), suggesting that DAF-16 and SIR-2.4 may function in the same pathway to modulate stress resistance. Interestingly, neither *sir-2.4* overexpressing nor RNAi knockdown animals showed altered longevity phenotype (Figure 28D and Figure 30A). We concluded that SIR-2.4 is required for stress resistance in a DAF-16-dependent manner but does not play a role in longevity determination.

Progressive accumulation of aggregation-prone proteins and global collapse of the protein homeostasis (proteostasis) network are featured in many late-onset neurodegenerative disorders. In *C. elegans*, the DAF-2/DAF-16 pathway has been shown to play an essential role in maintaining proteostasis and protects animals from aggregation-associated proteotoxicity. Thus, we asked whether SIR-2.4 is required to maintain proper proteostasis. Proteotoxicity induced by a polyglutamine repeat-containing protein was examined by using the worms expressing fluorescent protein-tagged polyQ35 in body wall muscle (*unc-54p::Q35::YFP*). The expression of Q35 in body wall muscle cells led to age-dependent paralysis and an increase in the number of non-soluble aggregates. Consistent to the role of DAF-2/DAF-16 in modulating proteostasis, *daf-2* RNAi animals showed considerably delayed onset of paralysis, whereas *daf-16* RNAi animals showed accelerated progression (Figure 28C).

Similar to *daf-16*, we found that the inactivation of *sir-2.4* by RNAi resulted in an early onset of paralysis. Taken together, all these data suggested that SIR-2.4 is required for proper response against multiple types of stress, including heat-shock, oxidative insult, and proteotoxicity.

3-4-3 Tissue expression pattern of SIR-2.4

To understand whether SIR-2.4 is required in a specific tissue, or whether SIR-2.4 acts in a cell-autonomous fashion, we attempted to determine the expression pattern of SIR-2.4. Transgenic lines overexpressing SIR-2.4 translational fusion (*sir-2.4p::sir-2.4::gfp*) (created by Dr. Bo Yang) were utilized to analyze the expression pattern of SIR-2.4. In general, we found that SIR-2.4 is expressed in most tissues, although the expression level is relatively weak. Higher expression was observed in a subset of head and tail neurons and some somatic gonad (spermathecal-uterine valve) cells (Figure 29).

3-4-4 SIR-2.4 is dispensable for DAF-16 regulation in the context of insulin/IGF-like signaling

In *C. elegans*, insulin/IGF-like signaling is known to modulate longevity and stress response in a DAF-16-dependent fashion. To ask whether SIR-2.4 is important in DAF-16 regulation in the context of reduced insulin/IGF-like signaling, we examined the effect of SIR-2.4 inactivation on longevity, DAF-16 nuclear translocation, and dauer formation in the context of reduced DAF-2 signaling. We found that *sir-2.4* RNAi knockdown had no lifespan phenotype on N2 (wild-type) and did not suppress longevity in *daf-2(e1370)* animals (Figure 30A). The knockdown or deletion of *sir-2.4* minimally impacted DAF-16 nuclear translocation induced by *daf-2* RNAi (Figure 30B and 25C).

We also measured the formation of dauer diapause, a physiological process modulated by insulin/IGF-like signaling. The inactivation of *sir-2.4* minimally impaired dauer formation on *daf-2* RNAi-sensitized animals (Figure 30D). These data clearly indicated that the role of SIR-2.4 in regulating DAF-16 function is largely independent of insulin/IGF-like signaling.

3-4-5 SIR-2.4 regulates DAF-16 acetylation and function independent of its catalytic activity

Other members of the mammalian sirtuin family including SIRT1, SIRT2 and SIRT3 were previously shown to deacetylate FoxO [42,44,61,62,64,120,121]. SIR-2.4 is predicted to possess deacetylase activity; however, whether SIR-2.4 functions as a deacetylase to regulate DAF-16 has never been examined. It has been proposed that the modulation of FoxO acetylation status plays an important role in regulating FoxO function and activity; however, the acetylation of DAF-16 has never been demonstrated. Given the role of SIR-2.4 in regulating DAF-16 localization and function, we next examined whether SIR-2.4 affects the level of DAF-16 acetylation by *in vitro* assays, in collaboration with Dr. Daniel Tishkoff and Dr. Bo Yang.

Our result indicated that DAF-16 is acetylated. The level DAF-16 acetylation is elevated in *sir-2.4* knockdown or deletion animals (Figure 31A and B). Moreover, co-immunoprecipitation experiments indicated an interaction between SIR-2.4 and DAF-16 in mammalian cells (Figure 31D), implying that SIR-2.4 may directly deacetylate DAF-16. To test whether the catalytic activity of SIR-2.4 is required for DAF-16 deacetylation, we performed *in vitro* SIR-2.4 deacetylase assay. Purified wild-type

SIR-2.4 and SIR-2.4 N124A, a predicted catalytic null mutant based on homology, were incubated with pre-acetylated DAF-16 as substrate. We were unable to detect DAF-16 deacetylation by either wild-type SIR-2.4 or SIR-2.4 N124A (data not shown). It is possible that the buffer used is not optimized for SIR-2.4, and SIR-2.4 may require other additional factors to be fully active *in vitro*.

Thus, we tested the requirement of SIR-2.4 catalytic activity directly in *C. elegans* by analyzing stress-induced DAF-16 translocation. The results showed that *sir-2.4* deletion strongly impacted DAF-16 nuclear translocation, whereas the overexpression of SIR-2.4 in *sir-2.4* deletion background rescued mutant defect (Figure 31E, SIR-2.4KO + SIR-2.4). To our surprise, the overexpression of SIR-2.4 N124A, a predicted catalytic-null mutant, rescued this defect as efficiently as wild-type SIR-2.4 (Figure 31E, SIR-2.4KO + SIR-2.4NA), indicating that SIR-2.4 catalytic activity is not required for promoting stress-induced DAF-16 translocation. Unfortunately, we were not able to confirm DAF-16 acetylation level in SIR-2.4 overexpressing animals by biochemical analysis, as the worms carrying chromosomal integrated *daf-16* and *sir-2.4* transgenes are very sick and produce few progeny. Overall, these data led to the conclusion that SIR-2.4 regulates DAF-16 activity independent of its catalytic activity, potentially through a mechanism that recruits other DAF-16 deacetylases or prevents the action of other DAF-16 acetyltransferses.

3-4-6 SIR-2.1 does not play a major role in stress-induced DAF-16 nuclear translocation

Chromatin modifying complex contains multiple enzymes, including histone

deacetylases. These proteins share common enzymatic activity and have been shown to possess redundant function to some extent. Based on this observation, we considered a possibility that SIR-2.4 collaborates with other sirtuins or non-sirtuin deacetylases to modulate DAF-16 localization and function. Given the role of SIR-2.1 in DAF-16 activation suggested previously [122], potential collaboration between SIR-2.1 and SIR-2.4 was tested. We first examined the interaction between SIR-2.1 and SIR-2.4 by co-immunoprecipitation in cell culture. To eliminate potential association through chromatin-associated complexes, cell extracts were co-immunoprecipitated with the presence of ethidium bromide (EtBr), a DNA intercalating agent that disrupts protein-DNA interactions. We observed strong physical interaction between SIR-2.1 and SIR-2.4 (Figure 32A). The presence of EtBr did not disrupt the association, suggesting that the interaction between SIR-2.1 and SIR-2.4 occurs through protein-protein interactions.

We next examined whether SIR-2.1 plays a role in regulating DAF-16 nuclear translocation upon stress. Our data showed that *sir-2.1* knockdown by RNAi had little effect on DAF-16 nuclear translocation upon either oxidative stress (Figure 26D, p=0.72) or heat-shock (Figure 26E, p=0.44). This result indicated that SIR-2.1 does not play a major role in stress-induced DAF-16 nuclear translocation, consistent with previously published data [123]. Moreover, inactivation of *sir-2.1* in *sir-2.4(n5137)* mutant animals did not result in any further delay in stress-induced DAF-16 nuclear translocation (Figure 26D and E). These findings suggested that it is unlikely that SIR-2.1 and SIR-2.4 collaboratively modulate stress-dependent DAF-16 localization and function.

However, our biochemical assays indicated that *sir-2.1* knockdown caused a modest increase in DAF-16 acetylation (Figure 31C), indicating that SIR-2.1 may still deacetylates DAF-16, similar to its mammalian ortholog SIRT1. Simultaneous inactivation of SIR-2.1 and SIR-2.4 resulted in a strong increase in DAF-16 acetylation to an extent similar to SIR-2.4 inactivation alone (Figure 31C), suggesting that SIR-2.1 and SIR-2.4 may impact common DAF-16 acetylation site(s). The fact that SIR-2.1 itself does not possess strong effect on stress-induced DAF-16 nuclear translocation and acetylation raised a possibility that the SIR-2.1-dependent acetylation may not play a significant role in stress-dependent DAF-16 localization and function. Thus, we concluded that despite the fact that SIR-2.1 does physically interact with SIR-2.4, SIR-2.1 does not collaborate with SIR-2.4 to modulate stress-induced DAF-16 function.

3-4-7 CBP-1 and SIR-2.4 acts antagonistically to affect DAF-16 localization

To ask whether SIR-2.4 prevents DAF-16 acetylation by blocking the acetylation site or by preventing the action of an acetyltransferase, we screened for known acetyltransferase(s) that affects DAF-16::GFP localization. We examined five putative *C. elegans* acetyltransferases genes: *cbp-1* (p300/CBP), *pcaf-1* (p300/CBP-associated factor), *mys-1*, *mys-2* and *mys-4* (MYST histone acetyltransferases). Worms fed on *cbp-1* RNAi displayed robust nuclear DAF-16 translocation even under basal conditions (Figure 33A), whereas animals fed on *pcaf-1*, *mys-1*, *mys-2* and *mys-4* RNAi did not show any significant effects under the same condition.

CBP (CREB-binding protein)/p300 is known to play a critical role in development, homeostasis, and transcriptional regulation. It contains intrinsic histone acetyltransferase

activity and has been shown to acetylate histone and non-histone proteins. Although p300/CBP has been shown to regulate FoxOs via acetylation in mammals [124], its *C.elegans* ortholog, CBP-1, has not been well characterized in the context of DAF-16 regulation. Our data indicated that the effect of CBP-1 and SIR-2.4 in regulating DAF-16 localization is largely antagonistic, as *sir-2.4* deletion strongly impaired *cbp-1* RNAi-induced DAF-16 nuclear localization (Figure 33A). Consistent with the idea of CBP-1 as an acetyltransferase for DAF-16, we found that *cbp-1* RNAi knockdown resulted in a modest but detectable reduction in DAF-16 acetylation level (Figure 33B).

In principle, if *cbp-1* RNAi promotes DAF-16 nuclear translocation, we would expect that *cbp-1* RNAi-mediated DAF-16 nuclear accumulation leads to a beneficial effect on longevity and stress resistance. On the contrary, we observed that *cbp-1* knockdown led to hypersensitivity to heat-shock and oxidative stress and a shortened lifespan (Figure 33C and D). Although it seemed contradictory to the role of CBP-1 in modulating DAF-16 localization, this observation is consistent with the previously published results [125]. The inhibition of *cbp-1* might not be beneficial for longevity and stress resistance, as constitutive nuclear accumulation of DAF-16 may be insufficient for proper DAF-16 activation. In addition, since CBP-1 has crucial role in regulating the expression of many genes functioning in diverse biological processes, we do not rule out the possibility that the optimum expression of certain essential genes is greatly perturbed by the inactivation of *cbp-1*.

3-4-8 SIR-2.4 blocks CBP-dependent DAF-16 acetylation

To ask whether SIR-2.4 prevents p300/CBP-dependent DAF-16 acetylation, Dr. Tishkofff

performed the *in vitro* CBP acetylation assay by co-incubating purified DAF-16 and CBP with and without SIR-2.4 protein. The presence of SIR-2.4 greatly diminished the level of CBP-mediated DAF-16 acetylation (Figure 33E). A SIR-2.4 catalytic null mutant (H124Y) appeared to exert a similar effect on DAF-16 (Figure 33E, SIR-2.4NA), suggesting that SIR-2.4 inhibits CBP-dependent DAF-16 acetylation through a mechanism independent of its catalytic activity. This result suggested two possible mechanisms by which SIR-2.4 prevents CBP-dependent DAF-16 acetylation: (1) SIR-2.4 binds to DAF-16 and thereby blocks CBP-1 action; and (2) SIR-2.4 inhibits the enzymatic activity of CBP-1 independent of deacetylase activity.

3-4-9 Identification of DAF-16 acetylation sites

To reveal a potential mechanism by which SIR-2.4 prevents CBP-dependent DAF-16 acetylation, we attempted to identify potential CBP-1 acetylation sites on DAF-16 in collaboration with Dr. Steven Gygi's lab at Harvard University. Recombinant DAF-16 were expressed and acetylated by CBP *in vitro*, and mass-spectrometry analysis was performed. We identified four CBP-1-dependent acetylation sites on DAF-16: K248, K253, K375, and K379. Notably, acetylation on K248 is also present on mammalian FoxO1 (K262) and FoxO3A (K259), implying a potential common mechanism in which CBP regulates FoxO/DAF-16 function. To further examine the functional impact of these acetylation sites on DAF-16, future studies such as creating transgenic animals carrying DAF-16 acetylation deficient or mimetic mutations and assessing their effect on DAF-16 localization and function may need to be conducted.

3-5 Discussion

3-5-1 SIR-2.4 modulates stress-dependent DAF-16 localization and function

In this chapter, we demonstrated a crucial role for SIR-2.4 in the stress response against heat, oxidative and proteotoxic stress (Figure 28A-C). We found that SIR-2.4 affects the kinetics of the DAF-16 nuclear translocation and activation (Figure 26D and E). SIR-2.4 neither affects longevity, nor plays a significant role in insulin/IGF-like signaling-mediated DAF-16 nuclear accumulation, longevity, and dauer formation (Figure 30A-D). Overall, our findings suggested that SIR-2.4 primarily functions in stress resistance and is largely independent of the DAF-2 pathway. Interestingly, we found that the catalytic activity of SIR-2.4 is not required for the regulation of stress-induced DAF-16 nuclear translocation (Figure 31E). Further analysis revealed that SIR-2.4 prevents CBP-dependent DAF-16 acetylation (Figure 33E), likely through a protein-protein interaction. Together, we revealed a novel mechanism by which SIR-2.4 indirectly modulates DAF-16 localization and function in response to stress.

Despite the fact that sirtuins were found to directly deacetylate and modulate FoxO function in mammals, whether this activity is also conserved in *C. elegans* has never been confirmed. In this study, we demonstrated for the first time that DAF-16 is acetylated (Figure 31A-C), and the modulation of DAF-16 acetylation may be critical for proper DAF-16 localization, target gene expression, and organismal survival upon stressful conditions.

3-5-2 SIR-2.1 and SIR-2.4 may play distinct role in regulating DAF-16 function

SIR-2.1 is reported to modulate DAF-16 activity to promote longevity (although this is currently disputed). However, according to our data and previous observations [123], SIR-2.1 seemed to have a much less prominent role in promoting stress-induced DAF-16 nuclear accumulation (Figure 26D and E). On the other hand, SIR-2.4 does not affect longevity (Figure 28D), appears to function largely independently of the insulin/IGF-like signaling pathway (Figure 30A), but plays a crucial role in regulating DAF-16 nuclear translocation and survival in the context of stress (Figure 26D and E). Together, our observations suggested differential physiological functions for SIR-2.1 and SIR-2.4. These two sirtuins may play distinct roles in modulating different aspects of DAF-16 function.

As previously mentioned, our biochemical data showed that SIR-2.1 inactivation modestly increased DAF-16 acetylation, whereas SIR-2.4 inactivation had a much stronger effect (Figure 31C). Simultaneous inactivation of both SIR-2.1 and SIR-2.4 resulted in an increase of DAF-16 acetylation similar to that of SIR-2.4 alone, suggesting that SIR-2.1 and SIR-2.4 may influence common acetylation site(s). Since SIR-2.4 inactivation led to a much stronger increase in DAF-16 acetylation than SIR-2.1, it is conceivable that SIR-2.4 plays a much more prominent role in modulating DAF-16 acetylation. As shown previously, SIR-2.1 and SIR-2.4 mutants displayed distinct phenotypes in longevity and stress response; thus, it is likely that SIR-2.1- and SIR-2.4-dependent acetylation modulate diverse functions of DAF-16. However, whether the individual or combination of these residue(s) contributes to SIR-2.1- or SIR-2.4-mediated DAF-16 regulation and function remains unclear.

3-5-3 Catalytic activity-independent functions of sirtuins

Previous studies have shown that the neuroprotective effect of SIRT1 is achieved through a catalytic-independent mechanism that protects neurons from low-potassium induced apoptosis and promotes cell survival [126]. SIRT1 was also shown to physically interact with DOT1, a histone H3K79 methylase and enhance DOT1 function in repressing α-ENaC (epithelian Na+ channel α-subunit) transcription independent of its deacetylase activity [126]. Similarly, our experiments showed that SIR-2.4 promotes stress-induced DAF-16 nuclear accumulation in a deacetylase-independent fashion (Figure 31E). These findings suggested that the molecular function of SIR-2.4 may include but may not be limited to deacetylation. Other sirtuins might also carry out some of their function through a similar deacetylase-independent mechanism.

3-5-4 Antagonistic function of SIR-2.4 and CBP-1 in DAF-16 regulation

FoxO transcription factors are known to interact with and be acetylated by p300/CBP in mammalian cells [63,124,127]. However in *C .elegans*, whether p300/CBP modulates DAF-16 function has not been reported. Our result showed that CBP-1 inactivation led to strong, constitutive nuclear accumulation under basal conditions (Figure 33A), suggesting a potent role for CBP-1 in promoting DAF-16 nuclear recruitment. Although CBP-1 can acetylate DAF-16 at multiple residues *in vitro*, we were only able to detect a modest decrease in the level of DAF-16 acetylation in *cbp-1* RNAi animals (Figure 33B). We do not rule out the possibility of the presence of CBP-1-independent acetylation site(s), as well as compensations from other acetyltransferase(s) functionally redundant to CBP-1. In addition, since the anti-acetyl-lysine antibody used in western blot does not

well discriminate the number of acetylated lysine on DAF-16, it is possible that the actual difference between control and *cbp-1* RNAi may be obscured by this technical limitation.

Despite the fact that *cbp-1* RNAi animals have constitutive nuclear DAF-16, our observations and previous report showed that these animals are stress sensitive and short lived (Figure 33C) [125]. It has been shown that DAF-16 constitutively localizes in the nucleus in long-lived, stress resistant *daf-2* mutant animals [128-130]; however, nuclear accumulation *per se* may not be sufficient for proper DAF-16 activation, as mutation on AKT phosphorylation sites on DAF-16 leads to constitutive DAF-16 nuclear accumulation but does not promote longevity and dauer formation [25,130]. Therefore, DAF-16 nuclear entry induced by CBP-1-dependent acetylation may be required, but not sufficient for subsequent DAF-16 activation. In *cbp-1* RNAi animals, nuclear accumulation of inactivated (or partially activated) DAF-16 may perturb gene expression by occupying binding sites at promoter regions or interacting with other factors, leading to a deleterious effect on longevity and stress resistance. Moreover, since CBP-1 is a multi-functional protein implicated in the transcriptional regulation of many biological pathways, it is likely that the expression of certain essential genes is greatly perturbed by CBP-1 inactivation. Nevertheless, our findings have demonstrated that CBP-1 plays a crucial role in DAF-16 nuclear accumulation.

The proto-oncogene protein DEK has been shown to exert potent inhibitory effects on p300- and PCAF-mediated histone acetylation via protein-protein interaction [131]. We found that SIR-2.4 may pose its inhibitory effect on CBP-1-mediated DAF-16 acetylation through a similar mechanism. Our *in vitro* assay showed that the presence of SIR-2.4

greatly diminished the level of DAF-16 acetylation by CBP-1 (Figure 33E). The fact that SIR-2.4 prevents CBP-1 action through a catalytic-independent fashion rules out the possibility that SIR-2.4 inhibits CBP-1 activity through deacetylating CBP-1. Since SIR-2.4 and DAF-16 were found to physically interact in our co-immunoprecipitation experiment, it is likely that SIR-2.4 blocks CBP-1-dependent DAF-16 acetylation through a protein-protein interaction.

3-5-5 Possible mechanism by which SIR-2.4/CBP-1 regulates stress-induced DAF-16 function

We hypothesized that, under unstressed conditions, SIR-2.4 does not interact with DAF-16. This allows CBP-1 to directly acetylate DAF-16 and prevent DAF-16 nuclear translocation and function. Upon stress, SIR-2.4 binds to DAF-16, inhibits CBP-1-dependent acetylation, and promotes DAF-16 nuclear accumulation and subsequent activation (Figure 34). Alternatively, SIR-2.4 may directly bind to and inhibit CBP-1 activity. Overall, in order to further test these hypotheses, it will be necessary to examine the interactions among DAF-16, SIR-2.4 and CBP-1 in the context of basal and stress conditions in the future.

We observed a significant reduction in DAF-16 acetylation level under oxidative stress conditions (Figure 32B), indicating that the DAF-16 acetylation status is regulated by stress. Our mass spectrometry analysis has identified four DAF-16 acetylation sites: K248, K253, K375, and K379. K248 is found to be homologous to mammalian FoxO acetylation site K262(FoxO1) and K259(FoxO3A). We do not know whether these sites are responsible for stress-induced DAF-16 acetylation and function. Thus, to further

understand whether these DAF-16 lysine residues regulate stress-induced DAF-16 localization and function, future work will focus on examining whether SIR-2.4 prevents CBP-1-dependent acetylation on these residues, and whether these residues play a role in stress-dependent DAF-16 nuclear accumulation and function. In addition, it will also be interesting to explore the role of these acetylation sites(s) in regulating other divergent physiological functions of DAF-16.

Taken together, we showed that SIR-2.4 plays a crucial role in regulating stress resistance and DAF-16 activity largely independent of insulin/IGF-like signaling pathway. SIR-2.4 is found to regulate DAF-16 acetylation and localization independent of its catalytic activity, indicating that SIR-2.4 may interact with other factor(s) to affect DAF-16 function. Further analysis revealed that SIR-2.4 inhibits DAF-16 acetylation by preventing CBP-1-dependent DAF-16 acetylation, likely through a protein-protein interaction. We hypothesize that SIR-2.4 prevents CBP-1-dependent DAF-16 acetylation in a stress-dependent manner, thereby allowing subsequent DAF-16 nuclear translocation and activation. Although details regarding the proposed mechanism remain unclear and require further investigation, our study presented here provides important insights into how sirtuins may regulate FoxOs activity in a catalytic activity-independent manner.

3-6 Figures

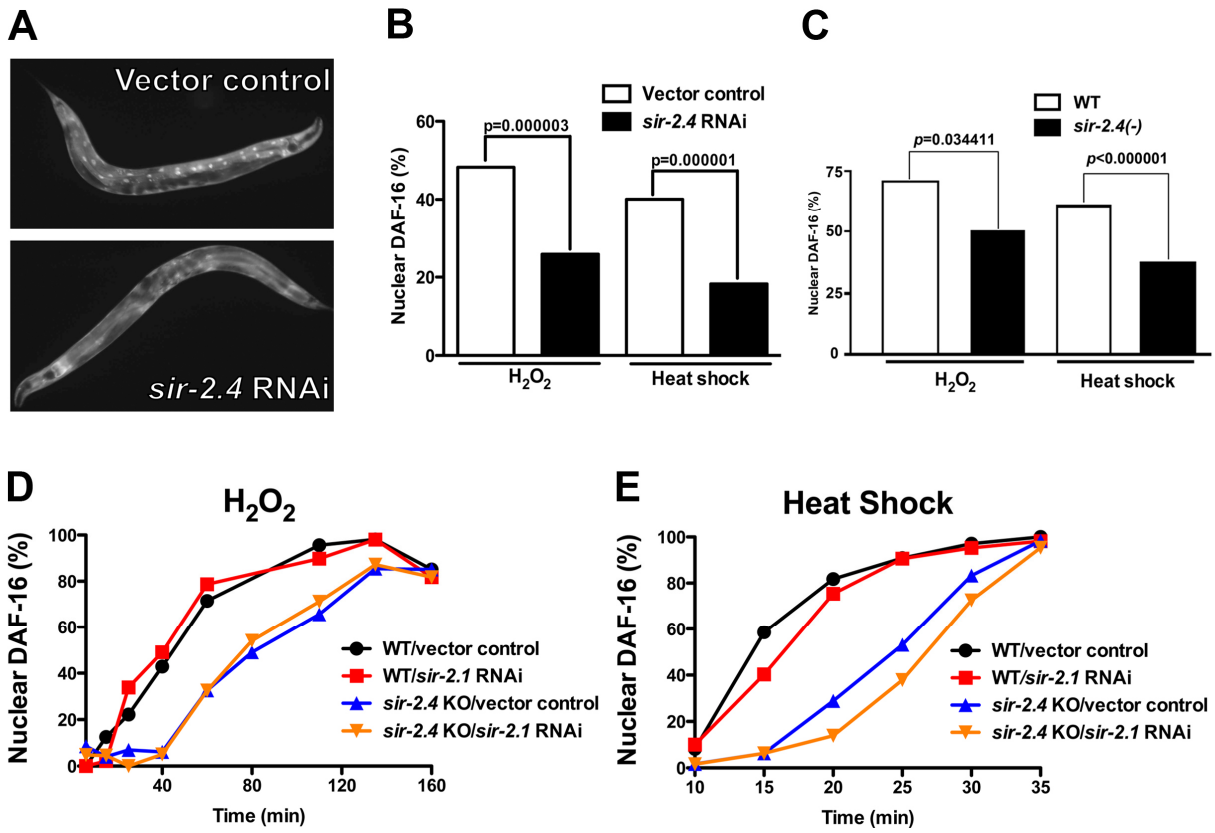

Figure 26. SIR-2.4 is required for proper onset of DAF-16 nuclear localization [1]
TJ356 animals carrying an integrated *daf-16::gfp* array were fed either vector control or *sir-2.4* RNAi bacteria for at least one generation before being subjected to heat-shock or oxidative stress. **(A)** Images of TJ356 animals grown on control or *sir-2.4* RNAi bacteria after 15 min heat-shock. **(B and C)** Quantification of DAF-16::GFP nuclear accumulation in response to oxidative stress (1.5 mM H_2O_2 for 1 hr) or heat-shock (35°C for 15 min.). Worms were scored for the presence or absence of GFP accumulation within the intestinal nuclei (n = 120 or greater for all treatments). An animal was scored as having nuclear GFP if one or more intestinal nuclei contained DAF-16-GFP. **(D and E)** Time course analysis of DAF-16::GFP nuclear accumulation in response to stress. TJ356 (*daf-16::gfp*) or EQ200 [*sir-2.4(n5137)*; *daf-16::gfp*] animals grown on either control or *sir-2.1* RNAi bacteria were subjected to (D) oxidative stress (1.5 mM H_2O_2) or (E) heat-shock (35°C) or. Worms were scored for GFP accumulation within the head hypodermic nuclei at day 1 of adulthood (n = 30~50) every 5–30 min.

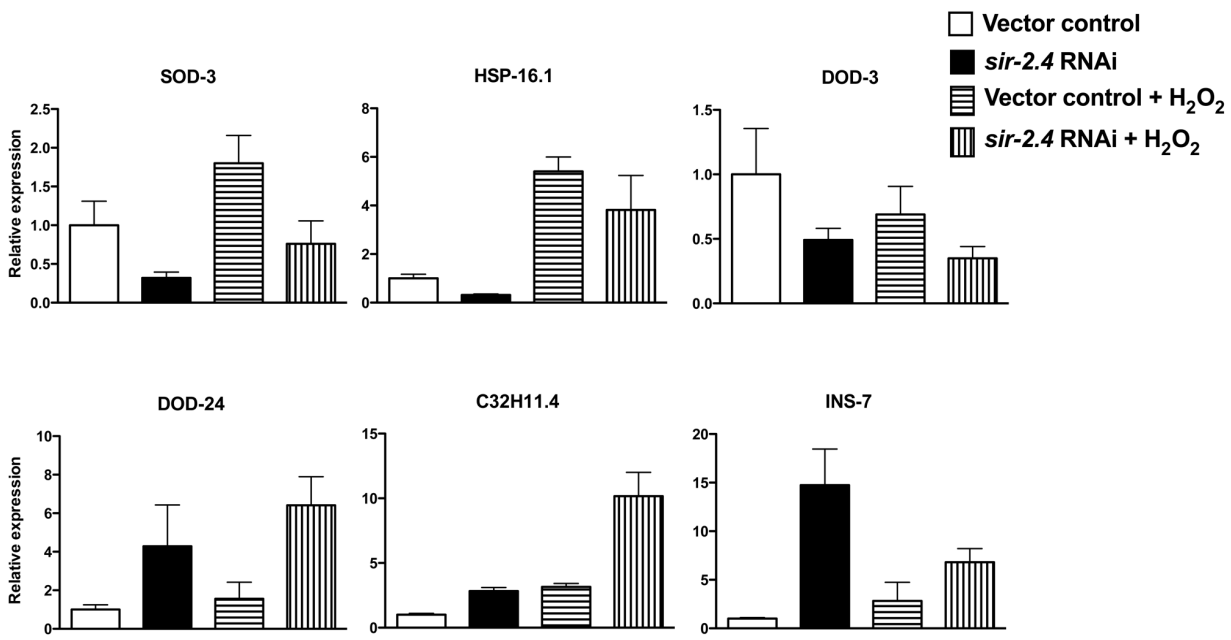

P values	*sod-3*	*hsp-16.1*	*dod-3*	*dod-24*	*C32H11.4*	*ins-7*
Vector control vs *sir-2.4* RNAi	**0.018**	**0.017**	**0.012**	**0.011**	**0.003**	**0.023**
Vector control vs Vector control + H_2O_2	**0.016**	**0.004**	0.280	0.377	**0.002**	0.243
Vector control + H_2O_2 vs *sir-2.4* RNAi + H_2O_2	**0.005**	**0.018**	0.096	**0.014**	**0.020**	**0.050**
sir-2.4 RNAi vs *sir-2.4* RNAi + H_2O_2	0.054	**0.050**	0.121	0.238	**0.018**	0.051

Figure 27. SIR-2.4 is required for optimal DAF-16–dependent gene expression [1]
Wild-type N2 animals fed on either vector control or *sir-2.4* RNAi bacteria from the time of hatching were exposed to 10 mM H_2O_2 for 80 min. Relative mRNA levels of s*od-3, hsp-16.1, dod-3, dod-24, C32H11.4,* and *ins-7* were measured by quantitative RT-PCR and the means of three different sample sets are shown. Relative mRNA levels were normalized against *act-1* (beta-actin). Error bars: ± STD. Statistical significance as determined by two-tailed t-test is shown in the table below; significant differences are represented in black font.

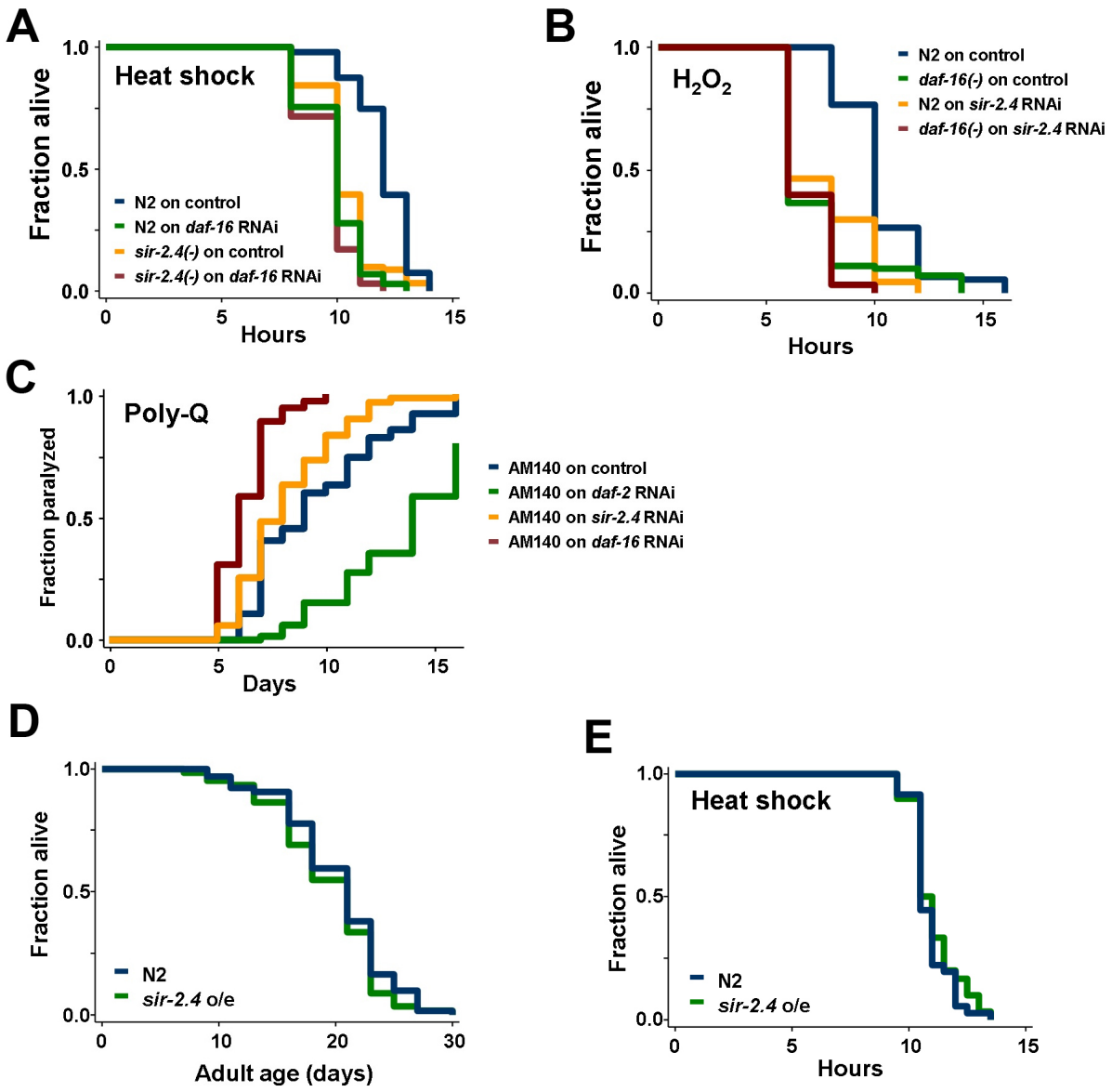

Figure 28. SIR-2.4 is required for stress resistance, but not longevity [1]
(A) Wild-type N2 or *sir-2.4(n5137)* worms grown on vector control or *daf-16* RNAi bacteria were subjected to heat-shock at 35°C and scored for viability every 1-2 hours. **(B)** Wild-type N2 or *daf-16(mu86)* worms grown on vector control or *sir-2.4* RNAi bacteria were treated with 1.5 mM H_2O_2 and scored for viability every 1–2 hours. **(C)** AM140 worms expressing polyQ-containing protein (Q35::YFP) were seeded on the RNAi bacteria indicated and scored for polyQ induced paralysis every other day. **(D and E)** Lifespan of wild-type (N2) animals or transgenic animals overexpressing native SIR-2.4 (EQ158) at 20°C. **(D)** Thermotolerance assay. N2 and EQ158 were exposed to 35°C heat stress. Viability was then scored at the time points indicated. See Table 4 for statistical analysis.

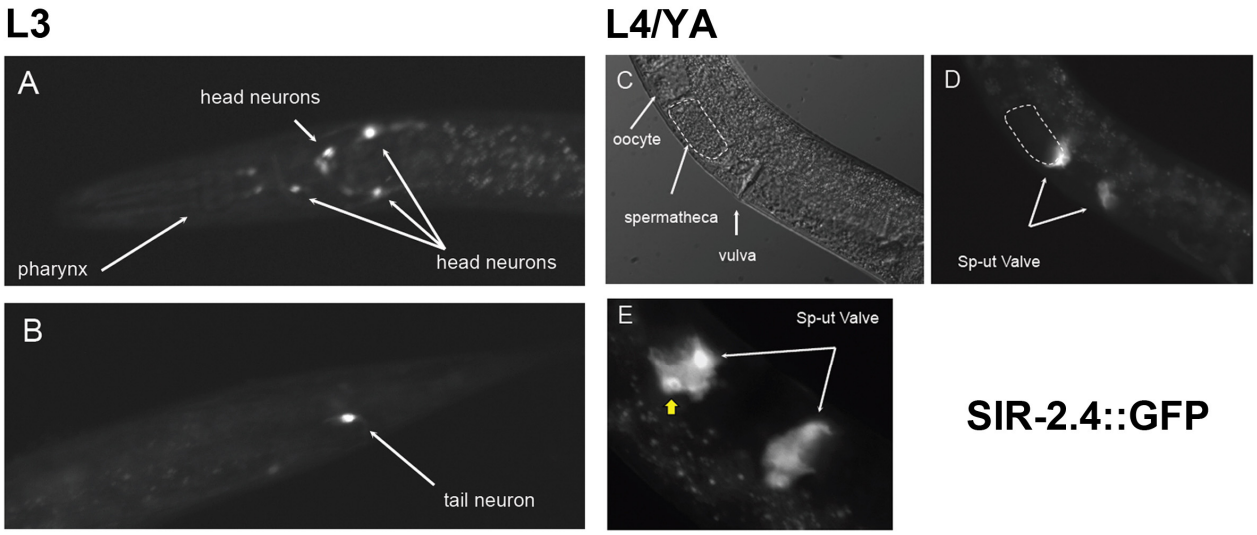

Figure 29. Expression pattern of *sir-2.4* in *C. elegans* [1]
Transgenic lines expressing a SIR-2.4 translational GFP fusion (*sir-2.4p::sir-2.4::gfp*) were utilized to analyze the expression pattern of *sir-2.4* in *C. elegans*. Images of L3 (A and B) or late L4/young adult (C–E) stage transgenic animals (EQ137) expressing GFP protein under control of the *sir-2.4* promoter. *sir-2.4* is highly expressed in a subset of head and tail neurons beginning at early larval stage, indicated by white arrows. High expression of *sir-2.4* is also found in spermathecal-uterine valve (sp-ut valve) cells beginning at L4 larval stage, indicated by white arrows. The yellow arrow indicates the nuclear accumulation of SIR-2.4::GFP fusions in these cells. It is worth noting that very weak expression of *sir-2.4* is found ubiquitously in most tissues, although it is difficult to capture in these images.

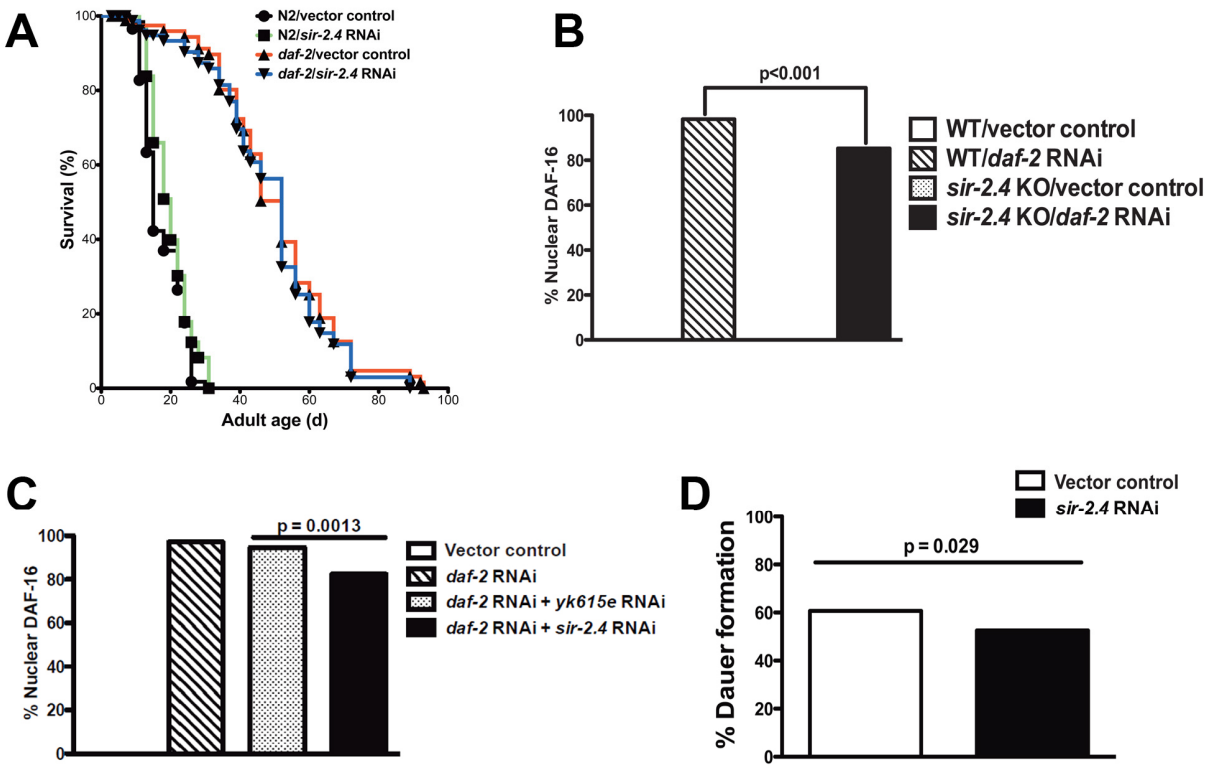

Figure 30. Minimal impact of SIR-2.4 on DAF-2 mediated longevity, DAF-16 nuclear localization, and dauer formation [1]

(A) Lifespan analysis of wild-type (N2) animals or *daf-2(e1370)* mutants grown on vector control bacteria (black or red) or *sir-2.4* RNAi bacteria (green or blue) at 20°C. **(B)** DAF-16 nuclear localization was assessed in TJ356 (*daf-16::gfp*) or EQ200 (*daf-16::gfp*; *sir-2.4(n5137)*) animals. Animals were fed with either vector control or *daf-2* RNAi from the time of hatching. Worms were scored for the presence or absence of GFP accumulation within the head hypodermic nuclei as day 1 adult (n = 116 or greater) under unstressed condition. *p*-values were calculated by Pearson's chi-square test. **(C)**TJ356 animals were fed with either vector control, *daf-2* RNAi, a 1:1 mix of *daf-2* and *sir-2.4* RNAi, or a 1:1 mix of *daf-2* and *yk615e* RNAi bacteria from the time of hatching. *yk615e* is a gene randomly selected as a negative control in double RNAi experiments. Animals (n = 125 or greater) were scored for DAF-16::GFP nuclear translocation. **(D)** *daf-2(e1370)* mutants (P_0) were fed with control or *sir-2.4* RNAi bacteria at 20°C. F_1 eggs were then moved to 22°C for 72 hours prior to being scored for dauer formation (n = 336 or greater). *p*-values were calculated by Pearson's chi-square test.

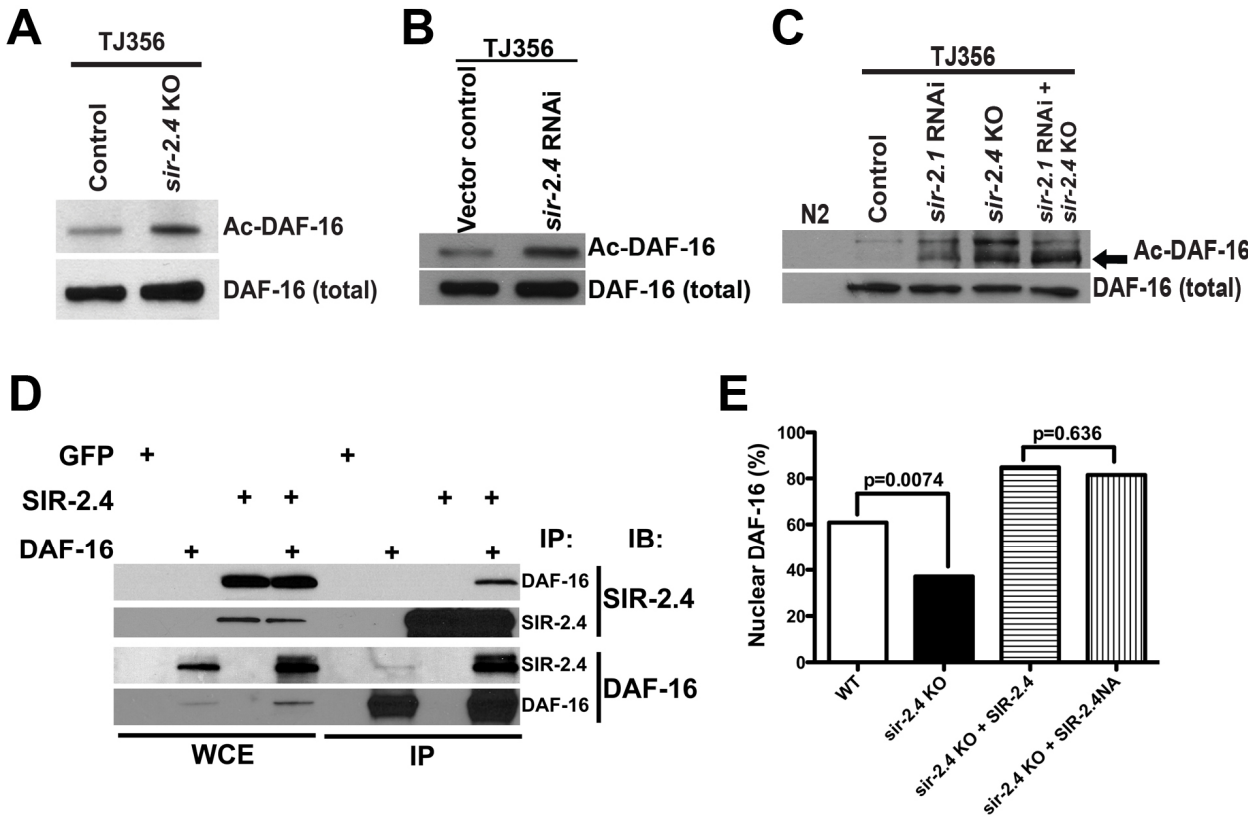

Figure 31. SIR-2.4 interacts with DAF-16 and promotes DAF-16 deacetylation and function independent of its catalytic activity [1]
(A and B) *sir-2.4* RNAi inactivation and deletion promote DAF-16 acetylation. DAF-16 acetylation was assessed in control, *sir-2.4* deletion (KO) or RNAi worms by acetyl-lysine immunoprecipitation followed by GFP western blot. **(C)** DAF-16 acetylation was assessed in *sir-2.4* deletion *sir-2.1* RNAi, or double loss-of function animals as indicated. **(D)** SIR-2.4 and DAF-16 are interacted. Plasmids encoding FLAG-tagged SIR-2.4 and HA-tagged DAF-16 were transfected into 293T cells as indicated (GFP, negative control). Immunoprecipitation and western blot were performed as shown. **(E)** Rescue of DAF-16 nuclear localization with a catalysis-defective *sir-2.4* mutant. Stable transgenic strains of *sir-2.4(n5137)* were generated expressing either wild-type SIR-2.4 or the *sir-2.4* N124A mutant. Worms were scored for GFP accumulation within the head hypodermic nuclei as day 1 adult (n = 50 or greater) after 20 min of heat-shock at 35°C. *p*-values were calculated by Pearson's chi-square test.

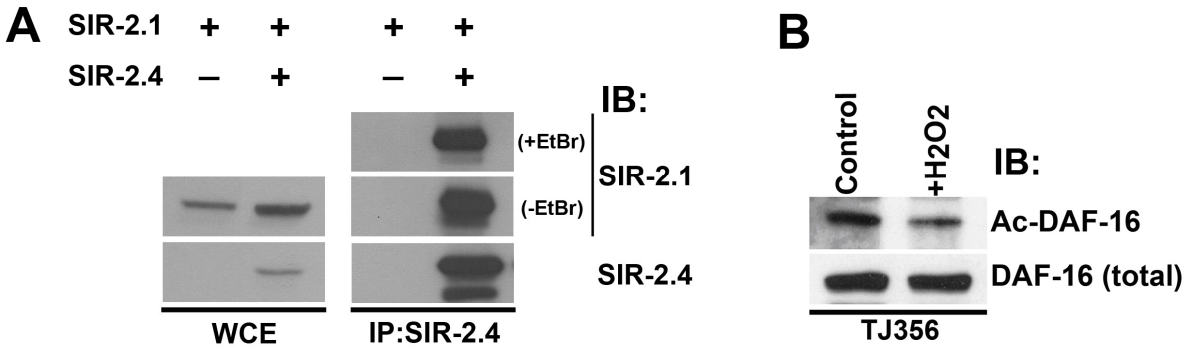

Figure 32.
(A) SIR-2.4 and SIR-2.1 are physically interacted. Plasmids encoding FLAG-tagged SIR-2.4 and Myc-tagged SIR-2.1 were transfected into 293T cells as indicated. WCE were immunoprecipitated with or without the presence of 1μg/ml ethedium bromide (+/-EtBr). Immunoblots were performed as shown. The presence of EtBr did not reduce the amount of co-immunoprecipitated SIR-2.1, suggesting that the interaction between SIR-2.1 and SIR-2.4 does not occur through chromatin association. **(B)** Elevated level of DAF-16 acetylation in response to oxidative stress. TJ356 (*daf-16::gfp*) worms were treated with 5 mM H_2O_2 for 20 minutes before harvest. DAF-16 acetylation was assessed by acetyl-lysine immunoprecipitation followed by GFP immunoblot.

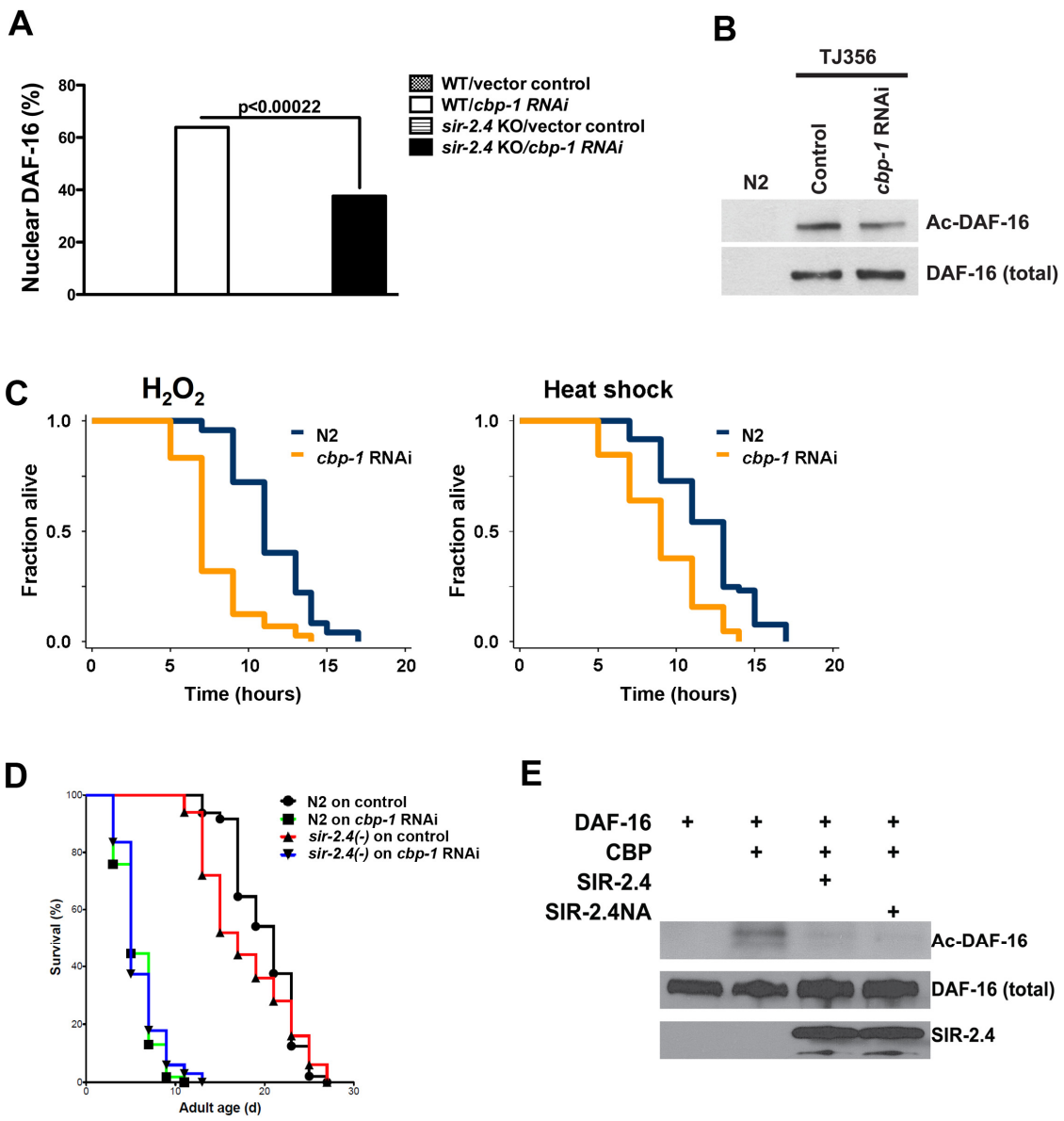

Figure 33. SIR-2.4 inhibits CBP1-mediated DAF-16 acetylation [1]
(A) DAF-16 nuclear localization was assessed in TJ356 (*daf-16::gfp*) or EQ200 (*daf-16::gfp; sir-2.4(n5137)*). Animals (n = 90 or greater) were scored for DAF-16::GFP nuclear translocation as described in Figure 30B. **(B)** *cbp-1* knockdown decreasesDAF-16 acetylation. DAF-16 acetylation was assessed in TJ356 worms grown on either control or *cbp-1* RNAi by acetyl-lysine immunoprecipitation followed by GFP western blot. **(C)** *cbp-1* inactivation confers stress sensitivity. Mean survival of *cbp-1* RNAi worms in response to peroxide stress (left) and heat shock (right). **(D)** *cbp-1* inactivation leads to shortened lifespan. Lifespan curves of wild-type or *sir-2.4* deletion animals in the presence of *cbp-1* or control RNAi bacteria. **(E)** SIR-2.4 blocks CBP1-dependent DAF-16 acetylation *in vitro*. Purified tagged DAF-16 was incubated with CBP-1 in the presence of WT SIR-2.4 or the SIR-2.4 NA mutant at 37°C. DAF-16 acetylation levels were assessed by using anti-epitope tag antibody.

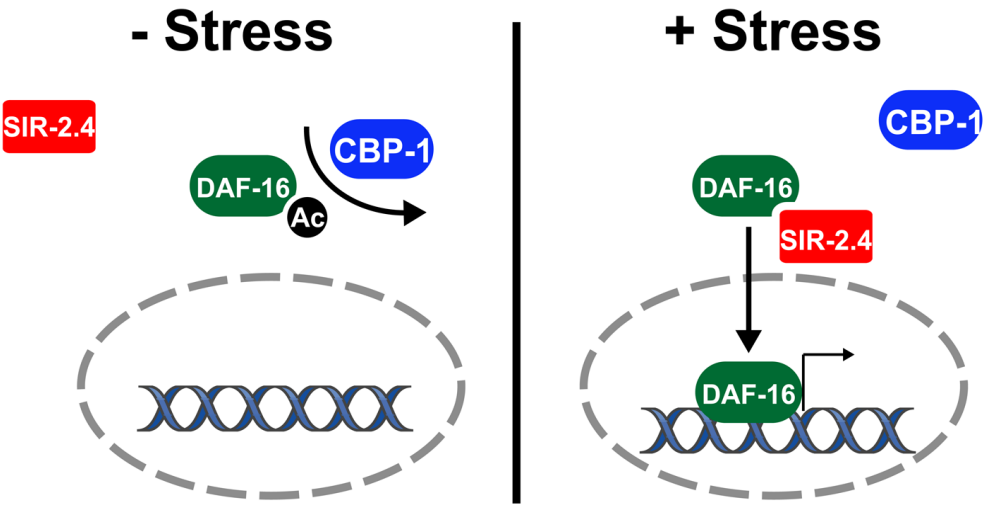

Figure 34. Hypothesized Model
We hypothesized that SIR-2.4 does not interact with DAF-16 under basal conditions. This allows CBP-1 to directly acetylate DAF-16 and prevent DAF-16 nuclear translocation and function. Upon stress conditions, SIR-2.4 binds to DAF-16, inhibits CBP-1-dependent acetylation, perhaps by blocking K248, K253, K375, and K379 and promotes DAF-16 nuclear accumulation and subsequent activation.

3-7 Tables

Table 4.

Strain	Stress	Mean Survival ± SEM (Hours)	75th Percentile (Hours)	*P* Value	n
N2, control *	Heat-shock	12.05 ± 0.05	13	–	94/102
N2, *daf-16(RNAi)* *	Heat-shock	9.89 ± 0.10	11	<0.0001[a]	101/102
sir-2.4(n5137), control *	Heat-shock	10.30 ± 0.11	11	<0.0001[a]	96/102
sir-2.4(n5137), *daf-16(RNAi)* *	Heat-shock	9.63 ± 0.09	10	<0.0001[a], 0.0611[b], 0.0001[c]	100/102
N2, control	Heat-shock	11.04 ± 0.08	12	–	102/120
N2, *daf-16(RNAi)*	Heat-shock	9.46 ± 0.09	11	<0.0001[a]	109/120
sir-2.4(n5137), control	Heat-shock	10.68 ± 0.06	11	<0.0228[a]	80/90
sir-2.4(n5137), *daf-16(RNAi)*	Heat-shock	9.81 ± 0.08	11	<0.0001[a], 0.0936[b], 0.0001[c]	87/90
N2, *control* *	H_2O_2	10.31 ± 0.21	12	–	86/90
N2, *sir-2.4(RNAi)* *	H_2O_2	7.30 ± 0.24	8	<0.0001[a]	88/90
daf-16(mu86), control *	H_2O_2	7.63 ± 0.21	10	<0.0001[a]	89/90
daf-16(mu86), sir-2.4(RNAi) *	H_2O_2	6.87 ± 0.12	8	<0.0001[a], 0.0004[b], 0.2423[c]	90/90
N2, *control*	H_2O_2	10.96 ± 0.23	12	–	90/90
N2, *sir-2.4(RNAi)*	H_2O_2	8.95 ± 0.33	10	<0.0001[a]	88/90
daf-16(mu86), control	H_2O_2	7.98 ± 0.23	10	<0.0001[a]	86/90
daf-16(mu86), sir-2.4(RNAi)	H_2O_2	8.59 ± 0.37	10	<0.0001[a], 0.1728[b], 0.6965[c]	84/90
N2	Heat-shock	16.07 ± 0.20	18	–	79/84
sir-2.4(n5137)	Heat-shock	14.71 ± 0.17	16	<0.0001	79/84
N2	H_2O_2	8.75 ± 0.09	8	–	72/72
sir-2.4(n5137)	H_2O_2	7.65 ± 0.11	8	<0.0001	72/72

N2 *	Heat-shock	12.84 ± 0.61	19	–	98/140
daf-16(RNAi) *	Heat-shock	9.81 ± 0.32	17	0.0001	102/140
sir-2.4(RNAi) *	Heat-shock	9.34 ± 0.19	17	<0.0001	143/176
N2	Heat-shock	15.52 ± 1.02	24	–	116/140
daf-16(RNAi)	Heat-shock	11.70 ± 0.32	20	<0.0001	134/140
sir-2.4(RNAi)	Heat-shock	11.07 ± 0.19	20	<0.0001	163/176
N2	Heat-shock	15.84 ± 0.74	22	–	103/160
daf-16(RNAi)	Heat-shock	11.70 ± 0.68	15	0.0004	118/160
sir-2.4(RNAi)	Heat-shock	10.53 ± 0.41	15	<0.0001	145/196
N2 *	H_2O_2	7.58 ± 0.06	8	–	140/160
daf-16(RNAi) *	H_2O_2	5.33 ± 0.08	5.5	<0.0001	156/160
sir-2.4(RNAi) *	H_2O_2	5.14 ± 0.08	5.5	<0.0001	191/196
N2	H_2O_2	11.68 ± 0.1	8	–	134/160
daf-16(RNAi)	H_2O_2	5.81 ± 0.06	5	<0.0001	152/160
sir-2.4(RNAi)	H_2O_2	5.68 ± 0.10	5	<0.0001	183/196
N2, control	Heat-shock	12.01 ± 0.26	13	–	65/72
N2, *cbp-1(RNAi)*	Heat-shock	9.09 ± 0.32	11	<0.0001	68/72
N2, control	H_2O_2	11.56 ± 0.22	13	–	72/72
N2, *cbp-1(RNAi)*	H_2O_2	7.72 ± 0.16	9	<0.0001	72/72
N2 *	Heat-shock	17.08 ± 0.25	19	–	81/90
EQ137 (*sir-2.4::gfp o/e*) *	Heat-shock	16.16 ± 0.24	19.2	0.1506	86/86
N2 *	Heat-shock	12.70 ± 0.18	13	–	65/65
EQ137 (*sir-2.4::gfp o/e*)	Heat-shock	12.16 ± 0.16	14	0.4989	54/72
N2 *	Heat-shock	10.90 ± 0.13	11		36/36
EQ158 (*sir-2.4 o/e*) *	Heat-shock	11.07 ± 0.16	11.5	0.4654	30/30

Table 4. Effects of *sir-2.4* expression on stress resistance
Animals grown on vector control, *daf-16* or *sir-2.4* RNAi bacteria were exposed to heat or oxidative stress. Mean survival ± SEM, in hours, observed in the stress analysis was shown in the table. 75th percentile is the time at which the fraction of animals alive reaches 0.25. 'n' indicates the number of animals scored in the each experiment. *P*-Values calculated by pair-wise comparisons to vector control of the same experiment. We used Stata 8 software for statistical analysis and to determine means and percentiles. The logrank (Mantel-Cox) test was used to test the hypothesis that the survival functions among groups were equal.

a *P*-Values calculated by pair-wise comparisons to N2 grown on vector control of the same experiment.
b Compared to N2 grown on the same RNAi bacteria.
c Compared to the same mutants grown on vector control.
'*' indicates the sets of experiments plotted and shown in Figures.

Table 5.

Strain	Mean Lifespan ± SEM (Days)	75th Percentile (Days)	*P* Value	n
N2; control	17.57 ± 0.24	24	–	57/60
N2; *sir-2.4(RNAi)*	18.87 ± 0.55	24	0.0638[a]	73/75
daf-2(e1370); control	50.23 ± 0.91	63	<0.0001[a]	64/90
daf-2(e1370); *sir-2.4(RNAi)*	48.43 ± 0.61	60	<0.0001[a], 0.5428[b]	68/90
N2; control	20.16 ± 1.03	23	–	48/59
N2; *cbp-1(RNAi)*	5.79 ± 0.42	7	<0.0001[a]	54/60
sir-2.4(n5137); control	18.15 ± 1.15	23	0.1988[a]	50/71
sir-2.4(n5137); *cbp-1(RNAi)*	6.16 ± 0.26	7	<0.0001[a], <0.0001[b], 0.3274[c]	67/76
N2	16.51 ± 0.72	20	–	63/72
EQ137 (*sir-2.4::gfp o.e.*)	17.85 ± 0.66	22	0.1318	53/72
N2	20.18 ± 0.62	23	–	61/72
EQ158 (*sir-2.4 o.e.*)	19.33 ± 0.63	23	0.2818	57/72

Table 5. Effects of *sir-2.4* expression on lifespan
Adult mean lifespan ± SEM, in days, observed in lifespan analyses. Lifespan experiments were carried out at 20°C. 75th percentile is the age at which the fraction of animals alive reaches 0.25. 'n' shows the number of observed deaths relative to total number of animals started at day 1. The difference between these numbers represents the number of animals censored during the experiment, and includes animals that exploded, bagged (*i.e.* exhibited internal progeny hatching), or crawled off the plates.

a *p*-Values calculated by pair-wise comparisons to N2 control of the same experiment.
b *p*-Values calculated by pair-wise comparisons to mutants fed with control bacteria of the same experiment.
c *p*- Values calculated by pair-wise comparisons to N2 fed with the same RNAi bacteria of the same experiment. We used Stata 8 software for statistical analysis and to determine means and percentiles. The logrank (Mantel-Cox) test was used to test the hypothesis that the survival functions among groups were equal.

3-8 Contributions

Figure 29: SIR-2.4::GFP translational fusion construct was made by Dr. Bo Yang in Dr. David Lombard's lab.

Figure 31D: DAF-16/SIR-2.4 co-immunoprecipitation was performed by Dr. Daniel Tishkoff in Dr. David Lombard's lab.

Figure 33 E: *in vitro* CBP-1 acetylation assay was performed by Dr. Daniel Tishkoff in Dr. David Lombard's lab.

Mass-spec identification of DAF-16 acetylation sites was performed by Dr. Joshua Wilson-Grady in Dr. Steven Gygi's lab.

Chapter 4. Conclusions

4-1 DDL-1 and DDL-2 as negative regulators of HSF-1

Heat-shock response is the universal and fundamental mechanism for cell protection against heat stress. The most important feature of the heat-shock response is the elevated expression of heat-shock proteins (HSPs), which is regulated by heat-shock factor (HSF). Multiple mechanisms have been shown to tightly control HSF activity to ensure fine-tuned expression of the heat-shock responsive genes. Multi-chaperone complex, a heat-sensitive protein complex, was previously known to inhibit HSF-1 activity through assembling HSF-1 into a heterocomplex, thereby preventing subsequent HSF-1 activation. In this study, we revealed that two novel HSF-1 regulators, DDL-1 and DDL-2, modulate longevity and stress response. Our data strongly suggested that DDL-1, DDL-2, HSB-1, and HSF-1 form a distinct heat-insensitive heterocomplex (DHIC) that negatively regulates the activation of HSF-1.

Although we found DDL-1 and DDL-2 as novel negative regulators of HSF-1, it is unclear whether DDL-1 and DDL-2 act in a tissue-specific manner to modulate HSF-1 activity. Future work will aim to create transgenic worms overexpressing DDL-1 or DDL-2 shRNA driven by tissue-specific promoter, and the requirement of DDL-1/2 in specific tissue will be examined by lifespan or stress resistance assays. The overlapping expression pattern among HSF-1, HSB-1, and DDL-1 supports the idea that these proteins interact in the same tissue. However, the expression pattern of DDL-2 does not entirely overlap

other DHIC components. It is not clear whether DDL-2 in those non-overlapping tissues plays a role in HSF-1 regulation. Thus, future work will also aim to elucidate whether DDL-2 acts in those non-overlapping tissues to specify longevity and stress resistance. Overall, in this study, we revealed crucial roles for two novel HSF-1 regulators, DDL-1 and DDL-2, in attenuation of HSF-1 activity and provided a novel mechanism by which HSF-1 activity is controlled.

4-2 Insulin/IGF-like signaling modulates HSF-1 activity though DHIC complex

HSF-1 has long been implicated as playing a critical role in the insulin/IGF-like signaling pathway, as the increased longevity observed in many of the DAF-2 pathway mutants requires *hsf-1*. Previous reports have shown that optimal expression of a subset of longevity genes downstream of insulin/IGF-like signaling requires both DAF-16 and HSF-1, indicating that HSF-1 may act in concert with DAF-16 to mediate the longevity of *daf-2* mutants. Although the role of HSF-1 in regulating longevity and stress response has been previously described, evidence of HSF-1 regulation by insulin/IGF-like signaling is incomplete. Our study has shown for the first time that HSF-1 is indeed subjected to direct regulation by the insulin/IGF-like signaling, and this regulation occurs through the modulation of DHIC formation.

DHIC links insulin/IGF-like signaling to HSF-1. Our data showed that the formation of DHIC is diminished when DAF-2 signaling is inactivated by RNAi (Figure 20D), strongly suggesting that the insulin/IGF-like signaling modulates the formation of DHIC. Moreover, we also found that the overall level of DDL-1 threonine phosphorylation appeared to be negatively regulated by DAF-2 activity (Figure 20C). The formation of DHIC is affected

by the phosphorylation status of DDL-1, as the threonine-to-alanine mutation at T182 of DDL-1 strongly enhanced the binding between HSF-1 and DDL-1 (Figure 20E). Together, these results suggested a model in which insulin/IGF-like signaling regulates HSF-1 activity through the modulation of DDL-1 phosphorylation, which in turn affects the formation of DHIC, resulting in a change in the level of heat-susceptible/inducible HSF-1. Together, our proposed model provides a novel mechanism by which DHIC links insulin/IGF-like signaling to heat-shock response (Figure 24).

Although our biochemical evidence have suggested a disruption of DHIC formation upon reduced insulin/IGF-like signaling (Figure 20D), the *in vivo* molecular detail of this process remains unclear and should be explored in the future. While the *in vivo* interaction between DDL-1 and HSB-1 has been confirmed by BiFC (Figure 19), other interactions among DHIC components are not verified *in vivo*. To further validate DHIC complex formation, we will create transgenic worms expressing all combinations of DDL-1, DDL-2, and HSB-1 proteins tagged with fluorescent protein (VN173/VC155) fragments, and examine protein-protein interactions by BiFC. However, an optimized fusion protein pair for BiFC should be carefully designed. The distance and sterical orientation of the interaction partners within the complex are not predictable and would greatly affect the chances for protein fragments to come together. Thus, in order to detect the interaction among DHIC components *in vivo*, it may be necessary to create all possible combinations of N- or C- terminal fusions and optimize the length of polypeptide linker between the protein and BiFC fragment.

As shown in Figure 22, DDL-1 T182A mutation minimally impacts DAF-2 longevity,

indicating that phosphorylation on T182 may only partially contribute to DAF-2-mediated HSF-1 regulation. The insulin/IGF-like signaling may modulate DHIC formation through parallel mechanisms. Thus, to determine whether DHIC formation may be regulated by other parallel pathways, an optimized DDL-1-HSF-1 BiFC system may also be used for a genetic screen to identify novel genes that modulate DHIC formation.

Our observation indicated that the phosphorylation of DDL-1 may play a key role in the regulation of DHIC formation; however, the identity of the protein(s) that modulate DDL-1 phosphorylation is unclear. Although DDL-1 is predicted to be phosphorylated by GSK3 kinase, inactivation of both GSK-3α and GSK-3β did not alter the phosphorylation status of DDL-1 (Figure 23). Thus, to identify potential DDL-1 kinase(s) or phosphatase(s), a genetic screen for genes that modulate DDL-1 phosphorylation may be performed. We may focus on putative kinase/phosphatase genes that have known genetic interactions with DHIC components or the insulin/IGF-like signaling pathways. This screen will provide insight into the upstream components that control the formation of DHIC.

4-3 The role of DHIC in regulating the level of heat-inducible HSF-1 activity

The binding of multi-chaperone complex to HSF-1 was shown to prevent HSF-1 oligomerization and inhibit its subsequent activation. It has been previously demonstrated that the assembly of multi-chaperone complexes can be disrupted by stress, allowing the oligomerization and activation of HSF-1. The disruption is known to play a critical role in the heat induction of HSF-1 activity. On the other hand, our data suggested the presence of a separate pool of HSF-1 that forms a complex with DDL-1, DDL-2 and HSB-1 (DHIC). This complex appears to be distinct from the multi-chaperone

complex, as the formation of DHIC cannot be disrupted by heat stress (Figure 21B). The lack of dissociation indicates that HSF-1 molecules present in DHIC may not be subjected to activation by heat stress. Thus, the formation of DHIC diminishes the overall level of heat-susceptible HSF-1, reduces the expression of stress-responsive genes, and consequently impairs the robustness of heat-shock response. We proposed that the formation of DHIC may play a crucial role in modifying heat-shock response through controlling the level of heat-inducible HSF-1.

Genetic studies in model organisms have indicated that the longevity is usually correlated with increased stress resistance against environmental stresses. A decrease heat-shock response results in a reduced level of stress-inducible HSPs, leading to an impaired protein homeostasis capacity to withstand the damage caused by cellular stress. This impairment has been shown to be associated with age-dependent mortality. Recent studies indicated that heat-shock response might play a crucial role in longevity regulation. Since HSF is a known central determinant of heat-shock response, molecular mechanisms that control the level of heat-inducible HSF may be crucial in determining the effectiveness of heat-shock response and thereby longevity. In this study, we proposed that insulin/IGF-like signaling controls the level of heat-inducible HSF-1 via the modulation of DHIC formation, revealing a novel mechanism by which heat-shock response may be fine-tuned by a longevity signaling pathway.

While the role of HSF-1 in the regulation of stress response, longevity, and protein homeostasis has been described, whether and how the activity of HSF-1 is modulated by hormonal cues is previously unknown. Our study presented here provides better

understanding of molecular mechanism underlying the regulation of HSF-1 by the insulin/IGF-like signaling pathway. This study could provide invaluable insights into the molecular mechanisms that control aging and aid the development of therapeutic strategies for age-related diseases.

4-4 SIR-2.4 plays a key role in stress resistance and stress-induced DAF-16 nuclear translocation

Sirtuins are important regulators of metabolism, longevity, and stress resistance in diverse species. It has been previously reported that sirtuins modulate FoxO activity through diverse means. In this work, we revealed a crucial role for *C. elegans* SIR-2.4, a mammalian SIRT6/7 homolog, in promoting stress resistance and the onset of DAF-16 nuclear translocation in response to stress. SIR-2.4 inactivation rendered animals sensitive to both oxidative and heat stress in a *daf-16*-dependent manner (Figure 28A and B). The deletion of *sir-2.4* led to a delayed onset of stress-induced DAF-16 nuclear accumulation (Figure 26D and E) but did not prevent DAF-16 nuclear recruitment after prolonged stress exposure, indicating that SIR-2.4 may play a critical role in the initiation or the kinetics of stress-induced DAF-16 nuclear recruitment.

Based on its tissue expression pattern, the expression level of SIR-2.4 appeared to be strong in a subset of neurons and somatic gonad cells (Figure 29). It is possible that SIR-2.4 regulates DAF-16 in neurons to affect the production of insulin-like peptides such as INS-7, thereby influencing systematic DAF-16 localization and function. However, we are not certain whether those tissues are key sites for SIR-2.4 to specify stress resistance or DAF-16 function, as SIR-2.4 is also expressed in other tissues at

lower levels. Thus, in the future, in order to examine whether SIR-2.4 regulates DAF-16 function in a cell-autonomous fashion, we plan to selectively inactivate SIR-2.4 in specific tissues by creating worms carrying *sir-2.4* shRNA transgene driven by tissue-specific promoter, and assess the effect of tissue-specific knockdown of SIR-2.4 on DAF-16 localization and function.

4-5 SIR-2.4 modulates DAF-16 acetylation status through the inhibition of CBP

As observed in our experiment, the inactivation of *sir-2.4* greatly delayed stress-induced nuclear translocation of DAF-16 and promoted acetylation of DAF-16, suggesting that DAF-16 could be the substrate of SIR-2.4 for deacetylation. However, our *in vitro* deacetylase assay suggested that SIR-2.4 may not deacetylate DAF-16. Indeed, *in viv*o rescue experiments showed that SIR-2.4 catalytic activity is dispensable for DAF-16 nuclear accumulation during stress (Figure 31E), indicating that SIR-2.4 does not directly regulate the localization and function of DAF-16 through its enzymatic activity. Our *in vitro* acetyltransferase assay revealed that SIR-2.4 blocks CBP-1-dependent DAF-16 acetylation in a catalytic-independent manner (Figure 33E), similar to the role of DEK in the inhibition of p300 and PCAF-mediated histone acetylation [131]. Since our biochemical assay showed that DAF-16 and SIR-2.4 interact (Figure 31D), we concluded that SIR-2.4 prevents CBP-mediated DAF-16 acetylation likely through protein-protein interaction. To test our model, future work will aim to examine whether SIR-2.4 inhibits DAF-16 acetylation on CBP-1-dependent sites, including K248, K253, K375 and K379, *in vivo* by quantitative mass spectrometry. We will also address whether the interaction between SIR-2.4 and DAF-16 is important for preventing CBP-1-dependent acetylation of DAF-16 by mapping the interacting domains between SIR-2.4 and DAF-16. The

requirement of SIR-2.4/DAF-16 interaction for inhibiting CBP-1-dependent DAF-16 acetylation can be assessed by creating deletion/truncation mutants of SIR-2.4 followed by *in vitro* acetylatransferase assay. Collectively, our data presented here suggested that the antagonistic function of SIR-2.4 and CBP-1 might play a crucial role in regulating DAF-16 localization, and non-catalytic functions of sirtuins may play a significant role in modulating cellular functions.

4-6 The role of acetylation in DAF-16 nuclear translocation and function

Despite the acetylation of mammalian FoxOs playing a potent role in modulating their localizations, function and other physiological outcomes, the role of DAF-16 acetylation in *C. elegans* was not clear. In this work, we demonstrated for the first time that DAF-16 is acetylated in worms, and the level of DAF-16 acetylation is modulated by CBP-1 and SIR-2.4 (Figure 31A-C and Figure 33B). Inactivation of SIR-2.4 promoted DAF-16 acetylation and dramatically affected stress-induced nuclear translocation of DAF-16 (Figure 26D and 21E), whereas *cbp-1* RNAi led to a decrease in DAF-16 acetylation level and constitutive DAF-16 nuclear accumulation (Figure 33A) These results suggested that DAF-16 acetylation may prevent its nuclear accumulation. Moreover, our biochemical evidence showed that DAF-16 can be directly acetylated by CBP-1 *in vitro* at four lysine residues: K248, K253, K375, and K379. Thus, modulation of DAF-16 acetylation status may be crucial for proper DAF-16 localization, target gene expression, and organismal survival upon stress. To understand whether the acetylation of these lysine residues plays a key role in DAF-16 localization and function, we plan to perform site-directed mutagenesis on acetylated lysine residues to assess the functional impact of acetylation on DAF-16 localization and function. We will create transgenic animals

carrying DAF-16::GFP array on which these lysine residues are mutated to arginine (K to R) or glutamate (K to Q) to mimic deacetylation or acetylation, respectively. These transgenic lines will be analyzed for stress-dependent DAF-16 nuclear translocation, DAF-16-dependent gene expression, stress resistance, and longevity.

While our data suggested that the modulation of DAF-16 acetylation by CBP-1 and SIR-2.4 may play a crucial role in regulating DAF-16 localization and function, it is likely that other acetyltransferases and deacetylases may also participate in this regulation. As shown previously, the inactivation of CBP-1 led to a modest decrease in the level of acetylated DAF-16 but did not completely eliminate DAF-16 acetylation, indicating that DAF-16 is a target of other acetyltransferases. On the other hand, according to our model, if SIR-2.4 prevents CBP-1-dependent DAF-16 acetylation in a deacetylase activity-independent fashion, another protein(s) has to be present in order to deacetylate DAF-16. Thus, future plans will aim to characterize other DAF-16 deacetylases and acetyltransferases and examine their functions in DAF-16 regulation. There are at least nine potential protein acetyltransferases (including *cbp-1*, *pcaf-1*, *mys-1,-2* and *-4*) and twelve protein deacetylases (including *sir-2.1* to *sir-2.4*) encoded in *C. elegans* genome. To fully characterize DAF-16 deacetylases and acetyltransferases, we will test whether the inactivation of these candidate genes affects DAF-16 acetylation and examine functional impact of these genes on DAF-16 nuclear translocation and function, under basal and stress conditions. Once the DAF-16 deacetylases and acetyltransferases are characterized, we will also attempt to identify the acetylation sites on DAF-16 by mass spectrometry analysis.

4-7 Final remark: Cross-talk between the insulin/IGF-like signaling and stress response pathways

Regulation of the insulin/IGF-like signaling and stress response pathways plays a crucial role in aging and longevity assurance. Stress resistance is found to be a general feature of many long-lived mutant animals, while the expression of many stress-responsive genes has been shown to promote longevity [2,40,132]. These observations imply that the insulin/IGF-like signaling and stress response pathways are closely linked, and cross-talks between these pathways are very likely to coordinate the physiological process that control longevity in many systems.

Stress has a known role in influencing the activity of the insulin/IGF-like signaling pathway. In worms, it has been shown that environmental stress (e.g. starvation or elevated temperature) leads to a reduction in DAF-2 signaling and alters many physiological pathways through modulating DAF-16. In mammals, stress signals are known to modulate the activity of several components of insulin signaling. For instance, it has been shown that endogenous redox levels play both positive and negative roles in modulating insulin receptor autophosphorylation [133]. Moreover, PTEN is shown to be inactivated by oxidative conditions through altering disulfide bond formation within its catalytic site [134]. These data indicate that stress signals can alter the activity of the insulin/IGF-like signaling pathway.

Moreover, multiple types of stressors, including heat-shock, oxidative stress, and heavy metals are known to modulate FoxO/DAF-16 activity in parallel to the insulin/IGF-like signaling. For instance, c-Jun N-terminal kinase (JNK), Ste20-like protein kinase MST1,

and B55α regulatory subunit of protein phosphatase 2A (PP2A) are reported to promote nuclear translocation and activation of DAF-16/FoxO in response to stress. [47,49,93]. DAF-16/FoxO can also be modulated by other stress-induced PTMs including acetylation [42-45], mono-ubiquitylation [46], and methylation [51]. In this study, we proposed that SIR-2.4 promotes stress-induced DAF-16 nuclear translocation and function via preventing CBP-1-dependent DAF-16 acetylation (Figure 34), providing a unique, novel mechanism by which sirtuins regulate DAF-16/FoxO.

On the other hand, insulin/IGF-like signaling regulates stress response through modulating certain components of stress signaling pathways. In worms, SKN-1, an ortholog of mammalin Nrf transcription factor that drives the expression of Phase 2 detoxification genes in response to stress [135], is known to be regulated by the p38 MAPK pathway [136]. SKN-1 was considered to be an integral part of stress signaling; however, it has been recently found that SKN-1 can also be directly regulated by insulin/IGF-like signaling. It was shown that DAF-2 inhibits nuclear accumulation and downstream gene expression of SKN-1 through *AKT-1*/2- and SGK-1-dependent phosphorylation [137]. Similarly, our work here showed that HSF-1, a transcription factor previously known to function primarily in stress response, is also subject to regulation by insulin/IGF-like signaling. The regulation of HSF-1 by insulin/IGF-like signaling occurs through the modulation of the formation of DHIC, a protein complex that contains HSF-1, DDL-1, DDL-2, and HSB-1. This study revealed a potential mechanism by which insulin/IGF-like signaling modulates heat shock response through fine-tuning the level of heat-susceptible/inducible HSF-1, and provides a new link between insulin/IGF-like signaling and heat shock response pathway.

The insulin/IGF-like signaling and stress response pathways are distinct but functionally intertwined biological processes; however, our understanding with regard to the interactions between these pathways is still incomplete. The studies presented in this thesis have provided potential mechanisms at the molecular level that link these pathways together. Since most of the components of insulin/IGF-like signaling and stress response pathways are largely homologous, the cross-talk between these pathways could be important for specifying optimum longevity and stress resistance in higher organisms, including humans. As a model organism, *C. elegans* is unique, inexpensive, and powerful for studying systemic regulation of longevity and stress response, as similar studies in mammals can be laborious and extremely expensive. Findings obtained in worms will provide important insights into how these pathways are regulated in organismal level. Therefore, future studies focusing on cross-talks between insulin/IGF-like signaling and stress response pathways in worms will shed light on the mechanisms by which the aging process and stress response are controlled, and provide new insights for developing future pharmacological interventions to promote longevity and health span in human populations.

References

1. Chiang WC, Tishkoff DX, Yang B, Wilson-Grady J, Yu X, et al. (2012) C. elegans SIRT6/7 homolog SIR-2.4 promotes DAF-16 relocalization and function during stress. PLoS Genet 8: e1002948.
2. Hsu A-L, Murphy C, Kenyon C (2003) Regulation of aging and age-related disease by DAF-16 and heat-shock factor. Science (New York, NY) 300: 1142-1145.
3. Chiang W-C, Ching T-T, Lee H, Mousigian C, Hsu A-L (2012) HSF-1 regulators DDL-1/2 link insulin-like signaling to heat-shock responses and modulation of longevity. Cell 148: 322-334.
4. Frye RA (2000) Phylogenetic classification of prokaryotic and eukaryotic Sir2-like proteins. Biochemical and Biophysical Research Communications 273: 793-798.
5. Corsi AK (2006) A biochemist's guide to Caenorhabditis elegans. Anal Biochem 359: 1-17.
6. Hulme SE, Whitesides GM (2011) Chemistry and the worm: Caenorhabditis elegans as a platform for integrating chemical and biological research. Angew Chem Int Ed Engl 50: 4774-4807.
7. Garigan D, Hsu AL, Fraser AG, Kamath RS, Ahringer J, et al. (2002) Genetic analysis of tissue aging in Caenorhabditis elegans: A role for heat-shock factor and bacterial proliferation. Genetics 161: 1101-1112.
8. Herndon LA, Schmeissner PJ, Dudaronek JM, Brown PA, Listner KM, et al. (2002) Stochastic and genetic factors influence tissue-specific decline in ageing C-elegans. Nature 419: 808-814.
9. Strehler BL, Mark DD, Mildvan AS, Gee MV (1959) Rate and Magnitude of Age Pigment Accumulation in the Human Myocardium. Journals of Gerontology 14: 430-439.
10. Tatar M, Kopelman A, Epstein D, Tu MP, Yin CM, et al. (2001) A mutant Drosophila insulin receptor homolog that extends life-span and impairs neuroendocrine function. Science 292: 107-110.
11. Kenyon C, Chang J, Gensch E, Rudner A, Tabtiang R (1993) A C-Elegans Mutant That Lives Twice as Long as Wild-Type. Nature 366: 461-464.
12. Kimura KD, Tissenbaum HA, Liu YX, Ruvkun G (1997) daf-2, an insulin receptor-like gene that regulates longevity and diapause in Caenorhabditis elegans. Science

277: 942-946.
13. Clancy DJ, Gems D, Harshman LG, Oldham S, Stocker H, et al. (2001) Extension of life-span by loss of CHICO, a Drosophila insulin receptor substrate protein. Science 292: 104-106.
14. Tu MP, Epstein D, Tatar M (2002) The demography of slow aging in male and female Drosophila mutant for the insulin-receptor substrate homologue chico. Aging Cell 1: 75-80.
15. Bluher M, Kahn BB, Kahn CR (2003) Extended longevity in mice lacking the insulin receptor in adipose tissue. Science 299: 572-574.
16. Holzenberger M, Dupont J, Ducos B, Leneuve P, Geloen A, et al. (2003) IGF-1 receptor regulates lifespan and resistance to oxidative stress in mice. Nature 421: 182-187.
17. Brown-Borg HM, Borg KE, Meliska CJ, Bartke A (1996) Dwarf mice and the ageing process. Nature 384: 33.
18. Coschigano KT, Holland AN, Riders ME, List EO, Flyvbjerg A, et al. (2003) Deletion, but not antagonism, of the mouse growth hormone receptor results in severely decreased body weights, insulin, and insulin-like growth factor I levels and increased life span. Endocrinology 144: 3799-3810.
19. Suh Y, Atzmon G, Cho MO, Hwang D, Liu B, et al. (2008) Functionally significant insulin-like growth factor I receptor mutations in centenarians. Proc Natl Acad Sci U S A 105: 3438-3442.
20. Guevara-Aguirre J, Balasubramanian P, Guevara-Aguirre M, Wei M, Madia F, et al. (2011) Growth Hormone Receptor Deficiency Is Associated with a Major Reduction in Pro-Aging Signaling, Cancer, and Diabetes in Humans. Science Translational Medicine 3.
21. Pierce SB, Costa M, Wisotzkey R, Devadhar S, Homburger SA, et al. (2001) Regulation of DAF-2 receptor signaling by human insulin and ins-1, a member of the unusually large and diverse C. elegans insulin gene family. Genes Dev 15: 672-686.
22. Li W, Kennedy SG, Ruvkun G (2003) daf-28 encodes a C. elegans insulin superfamily member that is regulated by environmental cues and acts in the DAF-2 signaling pathway. Genes Dev 17: 844-858.
23. Murphy CT, McCarroll SA, Bargmann CI, Fraser A, Kamath RS, et al. (2003) Genes that act downstream of DAF-16 to influence the lifespan of Caenorhabditis elegans. Nature 424: 277-283.
24. Murphy CT, Lee SJ, Kenyon C (2007) Tissue entrainment by feedback regulation of

insulin gene expression in the endoderm of Caenorhabditis elegans. Proc Natl Acad Sci U S A 104: 19046-19050.
25. Hertweck M, Gobel C, Baumeister R (2004) C. elegans SGK-1 is the critical component in the Akt/PKB kinase complex to control stress response and life span. Developmental Cell 6: 577-588.
26. Morris JZ, Tissenbaum HA, Ruvkun G (1996) A phosphatidylinositol-3-OH kinase family member regulating longevity and diapause in Caenorhabditis elegans. Nature 382: 536-539.
27. Paradis S, Ailion M, Toker A, Thomas JH, Ruvkun G (1999) A PDK1 homolog is necessary and sufficient to transduce AGE-1 PI3 kinase signals that regulate diapause in Caenorhabditis elegans. Genes & Development 13: 1438-1452.
28. Paradis S, Ruvkun G (1998) Caenorhabditis elegans Akt/PKB transduces insulin receptor-like signals from AGE-1 PI3 kinase to the DAF-16 transcription factor. Genes & Development 12: 2488-2498.
29. Wolkow CA, Munoz MJ, Riddle DL, Ruvkun G (2002) Insulin receptor substrate and p55 orthologous adaptor proteins function in the Caenorhabditis elegans daf-2/insulin-like signaling pathway. J Biol Chem 277: 49591-49597.
30. Lin K, Dorman JB, Rodan A, Kenyon C (1997) daf-16: An HNF-3/forkhead family member that can function to double the life-span of Caenorhabditis elegans. Science 278: 1319-1322.
31. Ogg S, Paradis S, Gottlieb S, Patterson GI, Lee L, et al. (1997) The Fork head transcription factor DAF-16 transduces insulin-like metabolic and longevity signals in C-elegans. Nature 389: 994-999.
32. Arden KC (2008) FOXO animal models reveal a variety of diverse roles for FOXO transcription factors. Oncogene 27: 2345-2350.
33. Jacobs FM, van der Heide LP, Wijchers PJ, Burbach JP, Hoekman MF, et al. (2003) FoxO6, a novel member of the FoxO class of transcription factors with distinct shuttling dynamics. J Biol Chem 278: 35959-35967.
34. Furuyama T, Nakazawa T, Nakano I, Mori N (2000) Identification of the differential distribution patterns of mRNAs and consensus binding sequences for mouse DAF-16 homologues. Biochem J 349: 629-634.
35. Biggs WH, 3rd, Cavenee WK, Arden KC (2001) Identification and characterization of members of the FKHR (FOX O) subclass of winged-helix transcription factors in the mouse. Mamm Genome 12: 416-425.
36. Hoekman MF, Jacobs FM, Smidt MP, Burbach JP (2006) Spatial and temporal expression of FoxO transcription factors in the developing and adult murine brain.

Gene Expr Patterns 6: 134-140.
37. Su AI, Cooke MP, Ching KA, Hakak Y, Walker JR, et al. (2002) Large-scale analysis of the human and mouse transcriptomes. Proc Natl Acad Sci U S A 99: 4465-4470.
38. Yen K, Narasimhan SD, Tissenbaum HA (2011) DAF-16/Forkhead box O transcription factor: many paths to a single Fork(head) in the road. Antioxid Redox Signal 14: 623-634.
39. McElwee J, Bubb K, Thomas JH (2003) Transcriptional outputs of the Caenorhabditis elegans forkhead protein DAF-16. Aging Cell 2: 111-121.
40. Murphy CT, McCarroll SA, Bargmann CI, Fraser A, Kamath RS, et al. (2003) Genes that act downstream of DAF-16 to influence the lifespan of Caenorhabditis elegans. Nature 424: 277-284.
41. Nemoto S, Finkel T (2002) Redox regulation of forkhead proteins through a p66shc-dependent signaling pathway. Science 295: 2450-2452.
42. Brunet A, Sweeney LB, Sturgill JF, Chua KF, Greer PL, et al. (2004) Stress-dependent regulation of FOXO transcription factors by the SIRT1 deacetylase. Science 303: 2011-2015.
43. Frescas D, Valenti L, Accili D (2005) Nuclear trapping of the forkhead transcription factor FoxO1 via Sirt-dependent deacetylation promotes expression of glucogenetic genes. J Biol Chem 280: 20589-20595.
44. van der Horst A, Tertoolen LGJ, de Vries-Smits LMM, Frye RA, Medema RH, et al. (2004) FOXO4 is acetylated upon peroxide stress and deacetylated by the longevity protein hSir2(SIRT1). Journal of Biological Chemistry 279: 28873-28879.
45. Kitamura YI, Kitamura T, Kruse JP, Raum JC, Stein R, et al. (2005) FoxO1 protects against pancreatic beta cell failure through NeuroD and MafA induction. Cell Metabolism 2: 153-163.
46. van der Horst A, de Vries-Smits AMM, Brenkman AB, van Triest MH, van den Broek N, et al. (2006) FOXO4 transcriptional activity is regulated by monoubiquitination and USP7/HAUSP. Nature Cell Biology 8: 1064-U1040.
47. Lehtinen MK, Yuan Z, Boag PR, Yang Y, Villen J, et al. (2006) A conserved MST-FOXO signaling pathway mediates oxidative-stress responses and extends life span. Cell 125: 987-1001.
48. Essers MA, Weijzen S, de Vries-Smits AM, Saarloos I, de Ruiter ND, et al. (2004) FOXO transcription factor activation by oxidative stress mediated by the small GTPase Ral and JNK. EMBO J 23: 4802-4812.

49. Oh SW, Mukhopadhyay A, Svrzikapa N, Jiang F, Davis RJ, et al. (2005) JNK regulates lifespan in Caenorhabditis elegans by modulating nuclear translocation of forkhead transcription factor/DAF-16. Proc Natl Acad Sci U S A 102: 4494-4499.
50. Sunayama J, Tsuruta F, Masuyama N, Gotoh Y (2005) JNK antagonizes Akt-mediated survival signals by phosphorylating 14-3-3. J Cell Biol 170: 295-304.
51. Yamagata K, Daitoku H, Takahashi Y, Namiki K, Hisatake K, et al. (2008) Arginine Methylation of FOXO Transcription Factors Inhibits Their Phosphorylation by Akt. Molecular Cell 32: 221-231.
52. Spange S, Wagner T, Heinzel T, Kramer OH (2009) Acetylation of non-histone proteins modulates cellular signalling at multiple levels. International Journal of Biochemistry & Cell Biology 41: 185-198.
53. Lin SJ, Ford E, Haigis M, Liszt G, Guarente L (2004) Calorie restriction extends yeast life span by lowering the level of NADH. Genes & Development 18: 12-16.
54. Finkel T, Deng CX, Mostoslavsky R (2009) Recent progress in the biology and physiology of sirtuins. Nature 460: 587-591.
55. Tissenbaum HA, Guarente L (2001) Increased dosage of a sir-2 gene extends lifespan in Caenorhabditis elegans. Nature 410: 227-230.
56. Rogina B, Helfand SL (2004) Sir2 mediates longevity in the fly through a pathway related to calorie restriction. Proc Natl Acad Sci U S A 101: 15998-16003.
57. Herranz D, Munoz-Martin M, Canamero M, Mulero F, Martinez-Pastor B, et al. (2010) Sirt1 improves healthy ageing and protects from metabolic syndrome-associated cancer. Nat Commun 1: 3.
58. Kanfi Y, Naiman S, Amir G, Peshti V, Zinman G, et al. (2012) The sirtuin SIRT6 regulates lifespan in male mice. Nature 483: 218-221.
59. Burnett C, Valentini S, Cabreiro F, Goss M, Somogyvari M, et al. (2011) Absence of effects of Sir2 overexpression on lifespan in C. elegans and Drosophila. Nature 477: 482-485.
60. Kobayashi Y, Furukawa-Hibi Y, Chen C, Horio Y, Isobe K, et al. (2005) SIRT1 is critical regulator of FOXO-mediated transcription in response to oxidative stress. International Journal of Molecular Medicine 16: 237-243.
61. Jing EX, Gesta S, Kahn CR (2007) SIRT2 regulates adipocyte differentiation through FoxO1 acetylation/deacetylation. Cell Metabolism 6: 105-114.
62. Wang F, Tong Q (2009) SIRT2 suppresses adipocyte differentiation by deacetylating FOXO1 and enhancing FOXO1's repressive interaction with PPARgamma. Mol Biol Cell 20: 801-808.

63. Matsuzaki H, Daitoku H, Hatta M, Aoyama H, Yoshimochi K, et al. (2005) Acetylation of Foxo1 alters its DNA-binding ability and sensitivity to phosphorylation. Proc Natl Acad Sci U S A 102: 11278-11283.
64. Jacobs KM, Pennington JD, Bisht KS, Aykin-Burns N, Kim HS, et al. (2008) SIRT3 interacts with the daf-16 homolog FOXO3a in the mitochondria, as well as increases FOXO3a dependent gene expression. Int J Biol Sci 4: 291-299.
65. Sundaresan NR, Gupta M, Kim G, Rajamohan SB, Isbatan A, et al. (2009) Sirt3 blocks the cardiac hypertrophic response by augmenting Foxo3a-dependent antioxidant defense mechanisms in mice. J Clin Invest 119: 2758-2771.
66. Sarge KD, Murphy SP, Morimoto RI (1993) Activation of heat shock gene transcription by heat shock factor 1 involves oligomerization, acquisition of DNA-binding activity, and nuclear localization and can occur in the absence of stress. Mol Cell Biol 13: 1392-1407.
67. Walker GA, Thompson FJ, Brawley A, Scanlon T, Devaney E (2003) Heat shock factor functions at the convergence of the stress response and developmental pathways in Caenorhabditis elegans. Faseb Journal 17: 1960-+.
68. Morley J, Morimoto R (2004) Regulation of longevity in Caenorhabditis elegans by heat shock factor and molecular chaperones. Mol Biol Cell 15: 657-664.
69. Morimoto RI (1998) Regulation of the heat shock transcriptional response: cross talk between a family of heat shock factors, molecular chaperones, and negative regulators. Genes & Development 12: 3788-3796.
70. Harrison CJ, Bohm AA, Nelson HC (1994) Crystal structure of the DNA binding domain of the heat shock transcription factor. Science 263: 224-227.
71. Vuister GW, Kim SJ, Wu C, Bax A (1994) Nmr Evidence for Similarities between the DNA-Binding Regions of Drosophila-Melanogaster Heat-Shock Factor and the Helix-Turn-Helix and Hnf-3/Forkhead Families of Transcription Factors. Biochemistry 33: 10-16.
72. Schultheiss J, Kunert O, Gase U, Scharf KD, Nover L, et al. (1996) Solution structure of the DNA-binding domain of the tomato heat-stress transcription factor HSF24. European Journal of Biochemistry 236: 911-921.
73. Sorger PK, Nelson HCM (1989) Trimerization of a Yeast Transcriptional Activator Via a Coiled-Coil Motif. Cell 59: 807-813.
74. Clos J, Westwood JT, Becker PB, Wilson S, Lambert K, et al. (1990) Molecular-Cloning and Expression of a Hexameric Drosophila Heat-Shock Factor Subject to Negative Regulation. Cell 63: 1085-1097.
75. Peteranderl R, Nelson HCM (1992) Trimerization of the Heat-Shock Transcription

Factor by a Triple-Stranded Alpha-Helical Coiled-Coil. Biochemistry 31: 12272-12276.
76. Chen YQ, Barlev NA, Westergaard O, Jakobsen BK (1993) Identification of the C-Terminal Activator Domain in Yeast Heat-Shock Factor - Independent Control of Transient and Sustained Transcriptional Activity. Embo Journal 12: 5007-5018.
77. Green M, Schuetz TJ, Sullivan EK, Kingston RE (1995) A Heat Shock-Responsive Domain of Human Hsf1 That Regulates Transcription Activation Domain Function. Mol Cell Biol 15: 3354-3362.
78. Shi YH, Kroeger PE, Morimoto RI (1995) The Carboxyl-Terminal Transactivation Domain of Heat-Shock Factor-1 Is Negatively Regulated and Stress-Responsive. Mol Cell Biol 15: 4309-4318.
79. Wisniewski J, Orosz A, Allada R, Wu C (1996) The C-terminal region of Drosophila heat shock factor (HSF) contains a constitutively functional transactivation domain. Nucleic Acids Research 24: 367-374.
80. Rabindran SK, Haroun RI, Clos J, Wisniewski J, Wu C (1993) Regulation of heat shock factor trimer formation: role of a conserved leucine zipper. Science 259: 230-234.
81. Shamovsky I, Ivannikov M, Kandel ES, Gershon D, Nudler E (2006) RNA-mediated response to heat shock in mammalian cells. Nature 440: 556-560.
82. Boellmann F, Guettouche T, Guo Y, Fenna M, Mnayer L, et al. (2004) DAXX interacts with heat shock factor 1 during stress activation and enhances its transcriptional activity. Proc Natl Acad Sci U S A 101: 4100-4105.
83. Dai Q, Zhang C, Wu Y, McDonough H, Whaley RA, et al. (2003) CHIP activates HSF1 and confers protection against apoptosis and cellular stress. EMBO J 22: 5446-5458.
84. Satyal SH, Chen D, Fox SG, Kramer JM, Morimoto RI (1998) Negative regulation of the heat shock transcriptional response by HSBP1. Genes Dev 12: 1962-1974.
85. Guettouche T, Boellmann F, Lane WS, Voellmy R (2005) Analysis of phosphorylation of human heat shock factor 1 in cells experiencing a stress. BMC Biochem 6: 4.
86. Xia W, Guo Y, Vilaboa N, Zuo J, Voellmy R (1998) Transcriptional activation of heat shock factor HSF1 probed by phosphopeptide analysis of factor 32P-labeled in vivo. J Biol Chem 273: 8749-8755.
87. Wang X, Grammatikakis N, Siganou A, Calderwood SK (2003) Regulation of molecular chaperone gene transcription involves the serine phosphorylation, 14-3-3 epsilon binding, and cytoplasmic sequestration of heat shock factor 1. Mol Cell Biol 23: 6013-6026.

88. Holmberg CI, Hietakangas V, Mikhailov A, Rantanen JO, Kallio M, et al. (2001) Phosphorylation of serine 230 promotes inducible transcriptional activity of heat shock factor 1. EMBO J 20: 3800-3810.
89. Wang X, Khaleque MA, Zhao MJ, Zhong R, Gaestel M, et al. (2006) Phosphorylation of HSF1 by MAPK-activated protein kinase 2 on serine 121, inhibits transcriptional activity and promotes HSP90 binding. J Biol Chem 281: 782-791.
90. Soncin F, Zhang X, Chu B, Wang X, Asea A, et al. (2003) Transcriptional activity and DNA binding of heat shock factor-1 involve phosphorylation on threonine 142 by CK2. Biochem Biophys Res Commun 303: 700-706.
91. Westerheide SD, Anckar J, Stevens SM, Jr., Sistonen L, Morimoto RI (2009) Stress-inducible regulation of heat shock factor 1 by the deacetylase SIRT1. Science 323: 1063-1066.
92. Hong Y, Rogers R, Matunis MJ, Mayhew CN, Goodson ML, et al. (2001) Regulation of heat shock transcription factor 1 by stress-induced SUMO-1 modification. J Biol Chem 276: 40263-40267.
93. Yan L, Guo S, Brault M, Harmon J, Robertson RP, et al. (2012) The B55alpha-containing PP2A holoenzyme dephosphorylates FOXO1 in islet beta-cells under oxidative stress. Biochem J 444: 239-247.
94. Calnan DR, Webb AE, White JL, Stowe TR, Goswami T, et al. (2012) Methylation by Set9 modulates FoxO3 stability and transcriptional activity. Aging (Albany NY) 4: 462-479.
95. Morimoto RI (1998) Regulation of the heat shock transcriptional response: cross talk between a family of heat shock factors, molecular chaperones, and negative regulators. Genes Dev 12: 3788-3796.
96. Voellmy R (2004) On mechanisms that control heat shock transcription factor activity in metazoan cells. Cell Stress Chaperones 9: 122-133.
97. http://www.phosphosite.org.
98. Hajdu-Cronin YM, Chen WJ, Sternberg PW (2004) The L-type cyclin CYL-1 and the heat-shock-factor HSF-1 are required for heat-shock-induced protein expression in Caenorhabditis elegans. Genetics 168: 1937-1949.
99. Li S, Armstrong CM, Bertin N, Ge H, Milstein S, et al. (2004) A map of the interactome network of the metazoan C. elegans. Science 303: 540-543.
100. Kenyon C, Chang J, Gensch E, Rudner A, Tabtiang R (1993) A C. elegans mutant that lives twice as long as wild type. Nature 366: 461-464.
101. Hansen M, Hsu AL, Dillin A, Kenyon C (2005) New genes tied to endocrine, metabolic, and dietary regulation of lifespan from a Caenorhabditis elegans

genomic RNAi screen. PLoS Genet 1: 119-128.
102. Hiatt SM, Shyu YJ, Duren HM, Hu CD (2008) Bimolecular fluorescence complementation (BiFC) analysis of protein interactions in Caenorhabditis elegans. Methods 45: 185-191.
103. Shyu YJ, Hiatt SM, Duren HM, Ellis RE, Kerppola TK, et al. (2008) Visualization of protein interactions in living Caenorhabditis elegans using bimolecular fluorescence complementation analysis. Nat Protoc 3: 588-596.
104. Derivery E, Sousa C, Gautier JJ, Lombard B, Loew D, et al. (2009) The Arp2/3 activator WASH controls the fission of endosomes through a large multiprotein complex. Developmental Cell 17: 712-723.
105. Rual JF, Venkatesan K, Hao T, Hirozane-Kishikawa T, Dricot A, et al. (2005) Towards a proteome-scale map of the human protein-protein interaction network. Nature 437: 1173-1178.
106. Fan JY, Cui ZQ, Wei HP, Zhang ZP, Zhou YF, et al. (2008) Split mCherry as a new red bimolecular fluorescence complementation system for visualizing protein-protein interactions in living cells. Biochem Biophys Res Commun 367: 47-53.
107. Hunt-Newbury R, Viveiros R, Johnsen R, Mah A, Anastas D, et al. (2007) High-throughput in vivo analysis of gene expression in Caenorhabditis elegans. PLoS Biol 5: e237.
108. Cohen E, Bieschke J, Perciavalle RM, Kelly JW, Dillin A (2006) Opposing activities protect against age-onset proteotoxicity. Science 313: 1604-1610.
109. Haigis MC, Sinclair DA (2010) Mammalian sirtuins: biological insights and disease relevance. Annu Rev Pathol 5: 253-295.
110. Viswanathan M, Guarente L (2011) Regulation of Caenorhabditis elegans lifespan by sir-2.1 transgenes. Nature 477: E1-2.
111. Lin SJ, Defossez PA, Guarente L (2000) Requirement of NAD and SIR2 for life-span extension by calorie restriction in Saccharomyces cerevisiae. Science 289: 2126-2128.
112. Wang Y, Tissenbaum HA (2006) Overlapping and distinct functions for a Caenorhabditis elegans SIR2 and DAF-16/FOXO. Mech Ageing Dev 127: 48-56.
113. Rogina B, Helfand SL (2004) Sir2 mediates longevity in the fly through a pathway related to calorie restriction. Proc Natl Acad Sci U S A 101: 15998-16003.
114. Mostoslavsky R, Chua KF, Lombard DB, Pang WW, Fischer MR, et al. (2006) Genomic instability and aging-like phenotype in the absence of mammalian SIRT6. Cell 124: 315-329.

115. Brenner S (1974) The genetics of Caenorhabditis elegans. Genetics 77: 71-94.
116. Apfeld J, Kenyon C (1999) Regulation of lifespan by sensory perception in Caenorhabditis elegans. Nature 402: 804-809.
117. Kenyon C (2005) The plasticity of aging: insights from long-lived mutants. Cell 120: 449-460.
118. Honda Y, Honda S (1999) The daf-2 gene network for longevity regulates oxidative stress resistance and Mn-superoxide dismutase gene expression in Caenorhabditis elegans. Faseb Journal 13: 1385-1393.
119. Yanase S, Yasuda K, Ishii N (2002) Adaptive responses to oxidative damage in three mutants of Caenorhabditis elegans (age-1, mev-1 and daf-16) that affect life span. Mech Ageing Dev 123: 1579-1587.
120. Daitoku H, Hatta M, Matsuzaki H, Aratani S, Ohshima T, et al. (2004) Silent information regulator 2 potentiates Foxo1-mediated transcription through its deacetylase activity. Proc Natl Acad Sci U S A 101: 10042-10047.
121. Motta MC, Divecha N, Lemieux M, Kamel C, Chen D, et al. (2004) Mammalian SIRT1 represses forkhead transcription factors. Cell 116: 551-563.
122. Wang Y, Oh SW, Deplancke B, Luo J, Walhout AJ, et al. (2006) C. elegans 14-3-3 proteins regulate life span and interact with SIR-2.1 and DAF-16/FOXO. Mech Ageing Dev 127: 741-747.
123. Heidler T, Hartwig K, Daniel H, Wenzel U (2010) Caenorhabditis elegans lifespan extension caused by treatment with an orally active ROS-generator is dependent on DAF-16 and SIR-2.1. Biogerontology 11: 183-195.
124. Senf SM, Sandesara PB, Reed SA, Judge AR (2011) p300 Acetyltransferase activity differentially regulates the localization and activity of the FOXO homologues in skeletal muscle. Am J Physiol Cell Physiol 300: C1490-1501.
125. Zhang M, Poplawski M, Yen K, Cheng H, Bloss E, et al. (2009) Role of CBP and SATB-1 in aging, dietary restriction, and insulin-like signaling. PLoS Biol 7: e1000245.
126. Pfister JA, Ma C, Morrison BE, D'Mello SR (2008) Opposing effects of sirtuins on neuronal survival: SIRT1-mediated neuroprotection is independent of its deacetylase activity. PLoS One 3: e4090.
127. Fukuoka M, Daitoku H, Hatta M, Matsuzaki H, Umemura S, et al. (2003) Negative regulation of forkhead transcription factor AFX (Foxo4) by CBP-induced acetylation. International Journal of Molecular Medicine 12: 503-508.
128. Henderson ST, Johnson TE (2001) daf-16 integrates developmental and environmental inputs to mediate aging in the nematode Caenorhabditis elegans.

Curr Biol 11: 1975-1980.
129. Lee RY, Hench J, Ruvkun G (2001) Regulation of C. elegans DAF-16 and its human ortholog FKHRL1 by the daf-2 insulin-like signaling pathway. Curr Biol 11: 1950-1957.
130. Lin K, Hsin H, Libina N, Kenyon C (2001) Regulation of the Caenorhabditis elegans longevity protein DAF-16 by insulin/IGF-1 and germline signaling. Nat Genet 28: 139-145.
131. Ko SI, Lee IS, Kim JY, Kim SM, Kim DW, et al. (2006) Regulation of histone acetyltransferase activity of p300 and PCAF by proto-oncogene protein DEK. FEBS Lett 580: 3217-3222.
132. Lee SS, Kennedy S, Tolonen AC, Ruvkun G (2003) DAF-16 target genes that control C. elegans life-span and metabolism. Science 300: 644-647.
133. Papaconstantinou J (2009) Insulin/IGF-1 and ROS signaling pathway cross-talk in aging and longevity determination. Mol Cell Endocrinol 299: 89-100.
134. Lee SR, Yang KS, Kwon J, Lee C, Jeong W, et al. (2002) Reversible inactivation of the tumor suppressor PTEN by H2O2. J Biol Chem 277: 20336-20342.
135. Oliveira RP, Abate JP, Dilks K, Landis J, Ashraf J, et al. (2009) Condition-adapted stress and longevity gene regulation by Caenorhabditis elegans SKN-1/Nrf. Aging Cell 8: 524-541.
136. Inoue H, Hisamoto N, An JH, Oliveira RP, Nishida E, et al. (2005) The C. elegans p38 MAPK pathway regulates nuclear localization of the transcription factor SKN-1 in oxidative stress response. Genes Dev 19: 2278-2283.
137. Tullet JM, Hertweck M, An JH, Baker J, Hwang JY, et al. (2008) Direct inhibition of the longevity-promoting factor SKN-1 by insulin-like signaling in C. elegans. Cell 132: 1025-1038.